A mathematical analysis of the hydro-mechanics associated with the Vitros Immunodiagnostic System.

Al-Tuwairqi, Salma Mohammad Aboras

A Mathematical Analysis Of The Hydro-Mechanics Associated With The Vitros Immunodiagnostic System

by

Salma Mohammad Aboras Al-Tuwairqi

A dissertation submitted in candidature for the degree of Philosophiae Doctor in the University of Wales, Swansea

2000

To the two dearer to me than my soul
My Father & My Mother

SUMMARY

Ortho-Clinical Diagnostics, a Johnson & Johnson company, has developed a new machine called 'Vitros Immunodiagnostic System' which can be used for the diagnosis of a wide range of auto-immune diseases. The design and manufacture of the Vitros Instrument has neither been directed nor supported by mathematical analysis. The aim and purpose of the present dissertation is to set up a working mathematical model of the hydro-mechanics within the instrumentation cycle of the Vitros System.

A description of the Vitros Immunodiagnostic System is given in Chapter 1. In Chapter 2, a mathematical model is developed to describe the structure of the mixture within the well.

In Chapter 3, dynamical equations are formulated with respect to a moving frame of reference at rest relative to the well. In particular, with reference to two especial states of motion: that of a 'sweep' at constant angular velocity of the outer carousel ring, and that of a 'jiggle' at rapidly fluctuating angular velocity. In the former the equations admit a solution in which the fluid moves as if it were rigid. Whereas, in the latter the equations admit an axially symmetric motion of the mixture.

In Chapter 4, the equations describing the primary flow and the (incipient) secondary flow are solved *exactly* for a hemispherical shaped well. This analytic solution gives a powerful description of the flow, being valid for the whole spectrum of values of the Reynolds number. The analysis shows that for large values of the Reynolds number the flow varies rapidly in the region immediately adjacent to the boundary wall, but elsewhere the flow is approximately a rigid body rotation.

In Chapter 5, a similar type analysis is carried out for a cylindrical shaped well. The results obtained run much in parallel (and support) the findings of the previous chapter.

Chapter 6 is concerned with the problem of determining the way in which the suspended reagents drift through the patient sample, and of ascertaining the pattern they create when becoming entrapped on the boundary wall. The results are interesting: the reagents have preferred orientation within the flow and result in a preferred coverage of the well boundary wall, and are not uniformly placed as previously anticipated.

Finally, some relevant remarks are added in Chapter 7 together with an outline of a (possible) programme of further research.

Declaration

This work has not previously been accepted in substance for any degree and is not being concurrently submitted in candidature for any degree.

S. M. Aboras Al-Tuwairqi (Candidate)

Signed .....

Date .....18/7/2000.....

Statement 1

This dissertation is the result of my own investigations except where otherwise stated. Other sources are acknowledged by citations giving explicit references. A bibliography is appended.

S. M. Aboras Al-Tuwairqi (Candidate)

Signed .....

Date .....18/7/2000.....

Statement 2

I hereby give consent for this dissertation, if accepted, to be available for photocopying and for interlibrary loan, and for the title and summary to be made available to outside organisations.

S. M. Aboras Al-Tuwairqi (Candidate)

Signed .....

Date .....18/7/2000.....

PREFACE

A new machine called 'Vitros Immunodiagnostic System' has become firmly established in the commercial field, and is now extensively used in most large hospitals for the speedy and reliable diagnosis of a wide range of auto-immune diseases. Despite its extensive use, comprehension of the mathematical theory that underlies and describes the many and varied workings of the machine is lacking. It is the aim of this dissertation to develop such a theoretical framework and to throw light on what can be expected of the system. It has to be understood that the study is an exploratory one, though deemed self consistent and rigorous in mathematical parlance. Within these terms, one attempts at a presentation and development that will be readily understood (in its entirety) by readers not specifically trained in the field that is mathematics, in particular, by the engineers and physicists attached to Ortho-Clinical Diagnostics Ltd., Cardiff.

So far as is known, no part of the dissertation has been anticipated by other writers. The results derived within the dissertation break new ground. Specific references to the work of other writers are made in the text and are listed at the end of the individual chapters.

As I arrive at the completion of this dissertation, I cannot help but express my appreciation to those who made it possible. First, all my gratitude is due to God the Almighty who guided and aided me to complete this dissertation. It is a pleasure to express my deep gratitude to Dr. I. M. Davies for his supervision, advice and especially his valuable suggestions with the work involving Mathematica. I am enor-

mously indebted to Dr. J. R. Jones, a generous scientist, from whom I have learned a great deal mathematically and who not only directed me during the elaboration of the present work but was a constant source of encouragement. My sincere appreciation is extended to Prof. A. Truman who suggested this problem and has taken the time to read this dissertation and to share his comments.

Deep thanks are due to the staff and secretaries of the Mathematics Department in Swansea. I also wish to thank King Abdul Aziz University for granting me a scholarship to continue my postgraduate studies in the UK.

As for my family, words do not exist to express my gratitude to them: my father for leaving his whole world behind him in Saudi Arabia to be with me and my sister in Swansea to lend us moral support and create that homely atmosphere which was vital; my mother for her love and concern, for bearing everything with a smile; my sister Hanan for going out of her way to make life easy for me; my sister Reem, my companion on this journey, for never being bored with my endless discussions; my brothers Rami, Bandar & Bassem for doing tasks that no man likes to do just to give me more time for my studies; and lastly, but not least, my friend Afia for making Swansea a wondrous place to live in, a second home.

Miss Salma Mohammad Aboras Al-Tuwairqi
University of Wales, Swansea
July 2000

CONTENTS

CHAPTER 1
INTRODUCTION

Ortho-Clinical Diagnostics, a Johnson & Johnson company based in Cardiff, specialises in the production of diagnostic test equipment. They have in recent times developed a new machine called 'Vitros Immunodiagnostic System' which can be used for the speedy and reliable diagnosis of a wide range of auto-immune diseases such as thyroid diseases. The design and manufacture of the Vitros Instrument has neither been directed nor supported by mathematical analysis. The aim and purpose of the present dissertation is to set up a working mathematical model of the hydro-mechanics within the instrumentation cycle of the Vitros System.

1.1 Vitros - An Overview

The Vitros Instrument (see Fig. 1.1.1) is a compact, self contained, easily transportable assemblage which works on a patient's blood sample. It is made up, in the main, of two coaxial rings - an outer ring of radius 105mm and an inner ring - mounted on a carousel whose rotational motions are co-related (Fig. 1.1.2). The blood sample is delivered in a thimble shaped well onto the outer carousel ring. This outer ring can accommodate many such wells and its (rotational) motion both agitates the content of each well and transports them within the body of the machine. The wells are initially empty, being ejected from a pack onto the ring, their surfaces coated with biological reagents specific for the immuno-assay to be performed. After

delivering the patient sample under examination, biological reagents are added and the whole is incubated whilst in motion on the outer ring for some 10 - 15 minutes, the time deemed necessary for the reagents to become entrapped on the wall. At the end of this period (which differs for different samples), the well is transferred onto the inner ring. It is then taken up, washed, and a signal generating reagent added that makes the residuum of the mixture (entrapped on the wall) emit light in much the same way as a firefly. By amplifying and measuring the light using a photon multiplier the patient's dysfunction can be diagnosed.

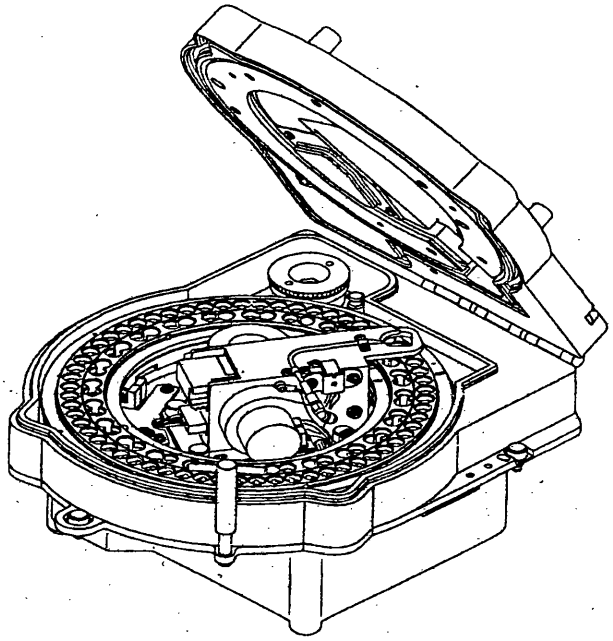

Fig.1.1.1 Vitros Immunodiagnostic System.

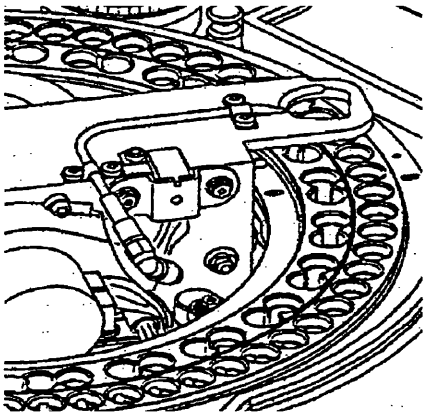

Fig. 1.1.2 The outer and inner rings of the carousel.

The accurate functioning of the machine depends critically upon how completely the blood sample has mixed with the reagents. It is important that the carousel motion not only does this efficiently, but that it also gives the best possible distribution of the reagents on the well boundary wall. Such issues are addressed in the present dissertation.

Ortho-Clinical Diagnostic Ltd. propound on several matters, matters which they deem important to the overall running of the Vitros Instrument. Of these one lists what are seen as the four critical phases affecting the instrumentation cycle.

I. The delivery of the patient sample and reagents to the well (with characteristic time of seconds).
II. The motion of the mixture within the well as it is transported round the outer ring (with characteristic (or incubation) time of minutes).
III. The drift of the reagents through the blood sample whilst in motion and the area of their entrapment on the boundary wall.

IV. The spillage of the well content, that occurs from time to time, resulting in instrument contamination and a serious breakdown of the testing programme.

No quantitative assessment of phase I is attempted. This represents a robust rheological process, with delivery into a stationary well, an advantage that should not be lost. Neither is any attempt made to analyse phase IV, other than to comment that spillage is likely to be due to the well vibrating within its seating in the circumferential direction and to the well section departing (slightly) from the circular.

The main body of the dissertation is taken up with a broad, but in depth, analysis of phases II and III, the aim being to ascertain the basic features of the motion within the well (i.e. of the motion as measured relative to the well when in transportation on the outer ring), together with that of the geometry of the entrapment area on the boundary wall. No experimental results are on view and the complexity of the instrumentation cycle suggests that such results may be long in coming. Hence, the present (theoretical) analysis is seen to hold a special place in the development of the Vitros Instrument.

1.2 Plan of Research

The dissertation is concerned with the hydro-mechanics associated with the Vitros Immunodiagnostic System, viz. that of the motion of the mixture within the well and of the (particulate) reagents suspended within the mixture itself. On observing the instrument in action, it is clear that such motions are complicated and that

certain simplifying assumptions need to be made. It is claimed that these are self consistent and appropriate (in a broad sense) to the scale of the happenings within the instrumentation cycle.

In Chapter 2, a simple mathematical model is developed to describe the structure of the mixture within the well. This owes a great deal to the earlier work of Fröhlich & Sack (1946) and Oldroyd (1950, 1953).

In Chapter 3, dynamical equations (i.e. those comprising the equation of continuity, the stress equations of motion and the rheological equations) are formulated with respect to a moving frame of reference at rest relative to the well. In particular, with reference to two especial states of motion: that of a 'sweep' at constant angular velocity of the outer carousel ring, and that of a 'jiggle' at rapidly fluctuating angular velocity. In the former (steady) state, the equations admit a solution in which the velocity as measured relative to the well is identically zero, i.e. in which the fluid moves as if it were rigid. Whereas, in the latter (oscillatory) state, the equations admit an axially symmetric motion of the mixture.

In Chapter 4, the equations describing the primary flow and the (incipient) secondary flow are solved *exactly* for a hemispherical shaped well. This analytic solution gives a powerful description of the flow, being valid for the whole spectrum of values of the Reynolds number, small to large. The analysis shows that for large values of the Reynolds number (based on the angular frequency of the carousel ring), indicative of the 'jiggle'-mode of oscillation, the flow varies rapidly in the region immediately adjacent to the boundary wall, but elsewhere, in the main body of the well, the flow is approximately a rigid body rotation.

In Chapter 5, a similar type of analysis is carried out for a cylindrical shaped well. Although an exact analytic solution is presented for the primary flow, one has to rely on an approximate formulation of the secondary flow. The results obtained run much in parallel (and support) the findings of the previous chapter.

Chapter 6 is concerned with the problem of determining the way in which the suspended (particulate) reagents drift through the patient sample, and of ascertaining the pattern they create when becoming entrapped on the boundary wall. The results are interesting: the reagents have preferred orientation within the flow and result in a preferred coverage of the well boundary wall, and are not uniformly placed as previously anticipated.

Finally, some relevant remarks are added in Chapter 7 together with an outline of a (possible) programme of further research.

CHAPTER 2

DEVELOPMENT OF A MATHEMATICAL MODEL

Many (and various) physical and mechanical factors affect the Vitros Immunodiagnostic System, and some of these have already been highlighted in the previous chapter. For obvious reasons, not all factors can be looked at and investigated in the present study. In a first attempt at a theoretical analysis of the system attention is naturally confined to what is seen as the main problem, that of ascertaining the general features of the motion of the mixture - the reagents and the patient sample - within the well whilst travelling on the (outer) carousel ring. There is no hard evidence of any practical measurements made in relation to the structure and motion of the mixture; and this is understandable, the Vitros Instrument being in the competitive commercial field. Thus, in developing a mathematical model, one has to be guided by, and to rely on, observations of the instrumentation cycle[1]. Although close attention has to be paid to the correspondence between 'rough' observation and precise mathematical description, the model should be sufficiently broad in scope to allow for features that may yet come to light with more detailed and prolonged observations. Such a development is the purpose and aim of the present chapter.

[1] Johnson & Johnson Clinical Diagnostics Ltd. have allowed access to observe the Vitros Immunodiagnostic System in action.

2.1 Flow Kinematics

The bodily motion of the well, supposedly rigidly mounted in the carousel ring housing, is comprised of an alternating sequence of two basic, but simple, motions. The first is one in which the carousel rotates with constant angular velocity and the second is one in which the carousel oscillates rapidly with small angular amplitude. These two motions are interspersed with short periods of rest when one of the wells comes down onto the carousel to be filled with the 'mixture' and when a well is taken up and transferred to the inner carousel ring in preparation for photo-electric analysis. The complication of the process is the seemingly haphazard way in which these basic motions are interwoven over a 10 - 15 minute period. After scrutiny of the Vitros Instrument (when in action) no progress can be reported on the finding of a 'natural time' for the operation, if indeed there is one, the sequence of motions being in some way dependent on how many wells are queuing-up to come onto the carousel, on how many wells are on the carousel and, of these, how many are queuing-up to be taken off the carousel[2]. It is thus observed that the motion of the mixture within the well during its incubation period on the carousel is governed by rather complicated time-variant boundary conditions, conditions that are likely to prove difficult to accommodate in any mathematical analysis of the problem. However, it must be made clear that the present study is an exploratory one in which it is hoped to throw light on the main, general, features of the motion of the mixture within the well. Such a programme may appear to be modest, but if it can be achieved, even

[2] Different samples are associated with different incubation times on the carousel.

if only in some restricted sense, then it represents a major step forward, for be it understood that, although the Vitros Immunodiagnostic System is established within the commercial market, there appear to be no theoretical considerations - one way or another - which may help to improve the design and efficiency of the instrument. Moreover, no such results seem forthcoming, and so the way forward has to rely on, and be guided by, the present mathematical analysis.

To make progress on the theoretical front, the basic motions imposed on the boundary walls of the well by the carousel ring housing are supposed separate and apart. In reality, there will be transient motions induced in the mixture in passing from one state of motion to another, but it is deemed that these will decay rapidly and play minor roles in comparison with those motions generated by forcing agents. A study of the literature lends support to this supposition: free oscillating systems, in which forcing agents are notable in their absence, have not proved too attractive to the experimentalist for this very reason (see, for example, Roscoe 1958, Roscoe & Bainbridge 1958, and Jones & Walters 1965, 1966). It seems reasonable therefore, in the first instance, to suppose the states of motion to be non-interactive.

The angular velocity $\boldsymbol{\Omega}(t)$ of the carousel ring is made up of 'sweeps' at constant values $\boldsymbol{\Omega}(t) = \boldsymbol{\Omega}_0$ and of 'jiggles' at rapidly fluctuating values of $\boldsymbol{\Omega}(t)$. The step function $\boldsymbol{\Omega}(t)$ during any one 'sweep' and 'jiggle' is exhibited in Fig. 2.1.1: $\Omega_0 \simeq 2\pi/8$ and the time scale is measured in seconds. Although this is not the result of detailed measurement, but of broad scale observation, it is nevertheless deemed near to actuality. It is reasonable to assume that one can proceed analytically without incurring serious disadvantages by smoothing this step function. Thus the 'jiggle'

is supposed to be described by a harmonic oscillatory function of angular amplitude $\Omega_0 \simeq 2\pi/8$ and angular frequency $n \simeq 3$ cycles per second as exhibited in Fig. 2.1.2.

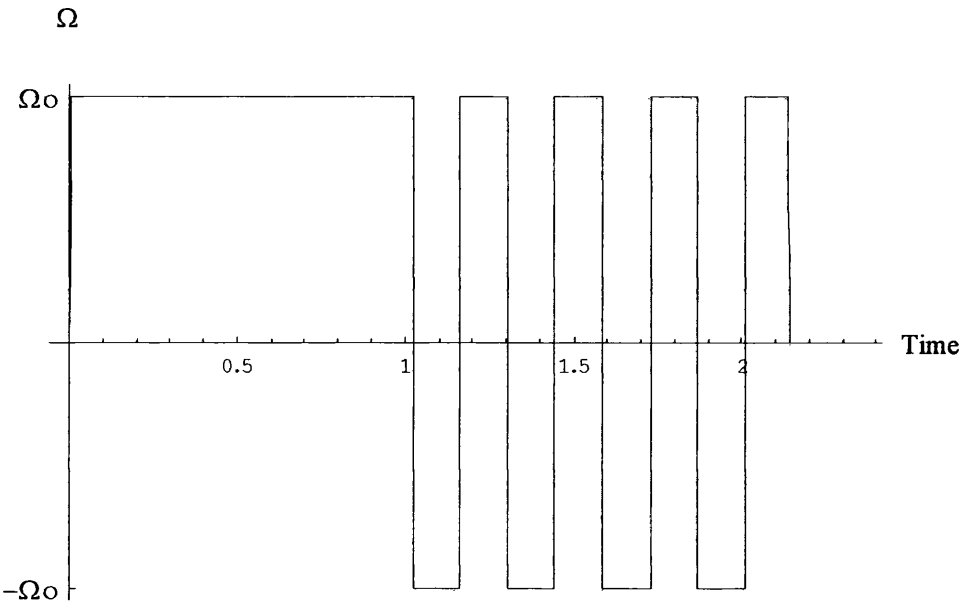

Fig. 2.1.1 The step function $\Omega(t)$ describing both the 'sweep' and the 'jiggle'.

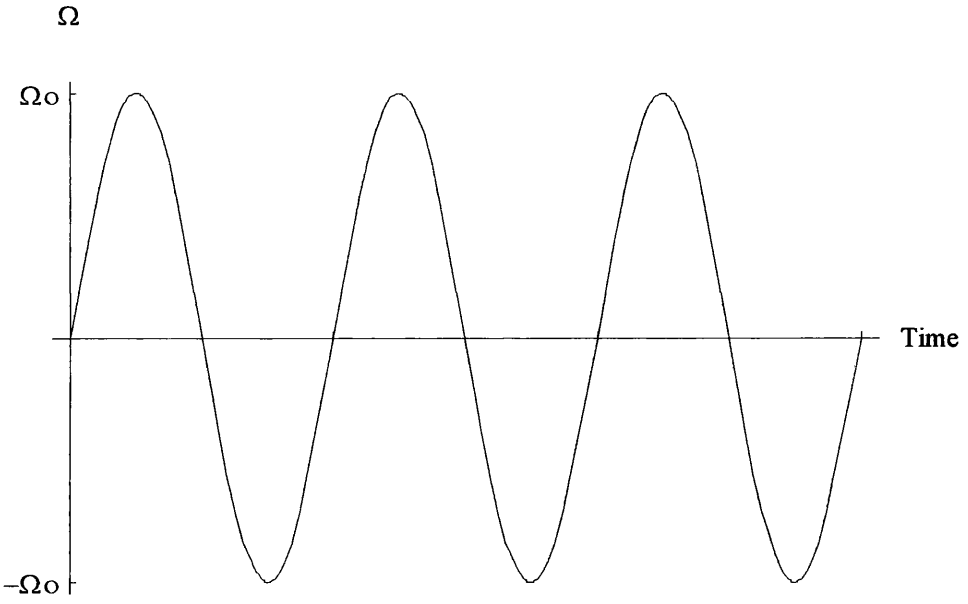

Fig. 2.1.2 The 'jiggle' described by a harmonic oscillatory function of amplitude Ω_0 and angular frequency n.

2.2 Structure of the Mixture

The delivery of the patient sample and reagents to the well (with a characteristic time of seconds) is seen as a finely controlled and well monitored phase of the instrumentation cycle. The resulting mixture consists of one material, the reagents, in the form of small particles, either solid or liquid, dispersed randomly through another (host) fluid, the patient sample[3]. If the characteristic length scale of the suspension (or mixture) is large in comparison with the average distance between particles, one may regard the suspension (or mixture) as a homogeneous fluid, but with mechanical properties different from those of the sample in which the particles are suspended. Further, one may suppose that a random distribution of *spherical particles* confers no preferred directional properties on the homogeneous whole. One of the answers sought by the Immuno Diagnostic Group is on how the motion of the carousel affects the mixing of the two phases within the well and on how it affects the drift (or diffusion) of the reagents through the sample. However, they give information neither on the concentration of reagents within a given sample (i.e. the fraction of the whole volume occupied by the reagents) nor on how the actually deposited amount has been deemed appropriate. Moreover, they are not prepared to release information on the nature of the reagents. To do so would give advantage to their competitors. It is anticipated that the concentration be such as to allow the reagents to drift through the sample by centrifugal action without in anyway affecting the motion and the structural nature of the sample. However, the concentration has to be sufficiently

[3] When the particles are liquid droplets, the mixture then being an emulsion, their disparate identity is supposed maintained by interfacial tension.

large not only to give a measurable interaction, but also to give an interaction which is characteristic of the sample. On the other hand, if the concentration is too large, then it will affect the structural nature of the sample, in which case the reagents play an intrinsic part in determining the flow. Thus there appears to be a need to place bounds on the reagent concentration, and it would be helpful if one could give some indication on how this might be done.

Two-phase systems have long been the case of serious investigation. The first is by Einstein (1906), who considered a highly idealized system, a suspension of rigid spherical particles dispersed in a purely viscous fluid of viscosity η. On the assumption that the particles are small, uniform in size, and widely dispersed, so that their concentration c is small, Einstein has shown that the mixture behaves macroscopically like a viscous fluid of constant viscosity η^*, where

$$\eta^* = \eta(1 + \frac{5}{2}c) + O(c^2).$$

Again, Taylor (1932) has investigated the behavior of a suspension of small spherical drops of one incompressible viscous fluid in another, the suspended fluid drops being maintained spherical by *large* interfacial tension. It is found that the macroscopic behavior of the system - an emulsion - is that of a purely viscous fluid, characterized by a viscosity η^*, where

$$\eta^* = \eta[1 + \frac{(\eta + \frac{5}{2}\eta')c}{\eta + \eta'} + O(c^2)],$$

η and η' being the viscosities of the continuous and disperse phases and c the concentration of the dispersed phase[4].

[4] It is seen that Einstein's formula follows on a special case of Taylor's in the limit $\frac{\eta'}{\eta} \to \infty$.

The above two systems are seen to be purely viscous, exhibiting no elasticity of shape. There is little, if any, information on the nature and type of the reagents employed in the Vitros. They may be rigid or they may be elastic. There is advantage, at this juncture, in supposing the reagents to have some 'springiness' of shape, allowing them to be deformed on the application of applied stress. The storage of elastic energy in such reagents will not be instantaneous but will take some time due to the reaction of the sample. Likewise, on removal of external stress, such reagents will take time to return to their former shape, giving rise to elastic recovery. It is clear therefore that a more sophisticated model is required to describe the mixture. Two such models have been developed, one by Fröhlich & Sack (1946) and one by Oldroyd (1953), models which may be considered natural extensions of those of Einstein and of Taylor.

Fröhlich and Sack discussed the flow properties of a suspension of elastic particles S in a viscous fluid L, the assumption being made that the suspended particles are solid spheres obeying Hooke's law. Oldroyd, on the other hand, looked at an idealized emulsion in which the elastic solid spheres of the Fröhlich & Sack model are replaced by liquid droplets L', with elasticity of shape as a consequence only of a *finite* interfacial tension between the continuous and disperse phases (L and L'). The methods used by Fröhlich & Sack and by Oldroyd to determine the macroscopic elastic and viscous properties of a disperse system from the properties of its components are not dissimilar: a fictitious, homogeneous liquid L^* is envizaged to have the same macroscopic rheological properties as the disperse system, the flow

properties of L^* being such that if a small part of the macroscopic element of L^* is replaced by the actual components of the disperse system, the macroscopic behavior remains unchanged[5]. The investigations of Fröhlich & Sack and of Oldroyd are well documented. Nevertheless, within this important area of analysis, it is deemed appropriate to discuss briefly, without recourse to any detailed mathematical computation, the method for ascertaining the rheological description of the homogeneous liquid L^* taken to represent the mixture. For illustration purposes, there is no advantage in choosing the one model rather than the other, although it would seem that the emulsion model of Oldroyd may hold sway in a description of the Assay System.

To fix ideas, attention is confined to the Fröhlich & Sack model. The element is considered in an arbitrary state of flow in which the rates of shear are so small that all non-linear terms can be neglected. Also, the suspension is assumed incompressible and isotropic, so that any convenient system of external stresses and any convenient shape may be chosen to investigate its flow properties.

The equations of state relating the stress tensor p_{ik} and the rate-of-strain tensor $e_{ik}^{(1)}$ in the continuous liquid phase L of constant viscosity η are

$$\begin{aligned} p_{ik} &= p'_{ik} - pg_{ik}, \\ p'_{ik} &= 2\eta e_{ik}^{(1)}, \end{aligned}$$

where g_{ik} is the metric tensor and p is an arbitrary isotropic pressure which can be superimposed without affecting the rate of strain[6]. The corresponding equations of

[5] A macroscopic element of the material is taken to mean an element whose linear dimensions are large compared with those of the elastic particles / liquid droplets and to the distance between neighbouring particles / droplets.

[6] The notation is clarified in §2.4.

state in the disperse elastic solid phase S, of rigidity modulus μ, are of the same mathematical form (for small rates of strain) but with η replaced by a viscosity operator[7]

$$\eta_s = \frac{\mu}{\triangle} \qquad (\triangle \equiv \frac{\partial}{\partial t}).$$

Again, when the rates of strain are small, the equation of state for L^*- a homogeneous liquid with the same macroscopic properties as the suspension of S in L - may be assumed to involve p'_{ik}, $e^{(1)}_{ik}$ and their derivatives linearly, and may be written in the above form with η replaced by a viscosity operator

$$\eta^* = \eta_0 \frac{1 + \lambda_2 \triangle + v_2 \triangle^2 + ...}{1 + \lambda_1 \triangle + v_1 \triangle^2 + ...} \qquad (\triangle \equiv \frac{\partial}{\partial t}),$$

where $\eta_0, \lambda_1, \lambda_2, v_1, v_2, ...$ are constants to be determined by the properties of L and S.

The rheological properties of a macroscopic element of L^* ($r < R$, referred to suitably chosen spherical polar coordinates r, θ, ϕ) are determined by the requirement that they are unchanged by a perturbation in which the portion $r < b$ ($b << R$) is replaced by the actual components S (in $r < a$) and L (in $a < r < b$), where a is the radius of an elastic solid, and b is defined in terms of the volume concentration c of the disperse phase by $b^3 c = a^3$. The scheme is illustrated diagrammatically in Fig. 2.2.1.

---

[7] The notation is standard: $p'_{ik} = 2\eta_s e^{(1)}_{ik}$ is understood to mean $\triangle p'_{ik} = 2\mu e^{(1)}_{ik}$.

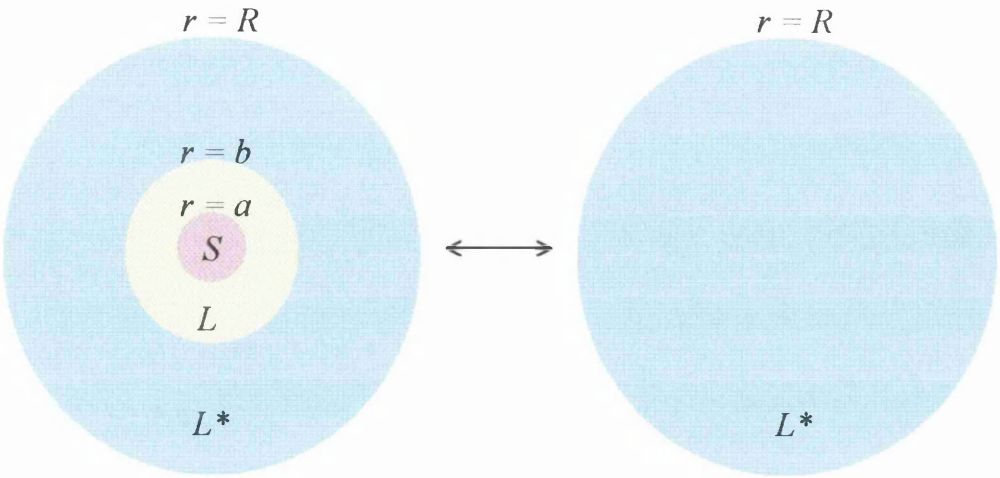

Fig. 2.2.1 Fröhlich & Sack model

The homogeneous element and the composite element are now considered separately when each is subjected over the surface $r = R$ to the same axially symmetric stress system

$$\begin{aligned} p_{(rr)} &= T(3\cos^2\theta - 1), \quad p_{(\theta\theta)} = T(2 - 3\cos^2\theta), \quad p_{(\phi\phi)} = -T, \\ p_{(\theta\phi)} &= 0, \quad p_{(\phi r)} = 0, \quad p_{(r\theta)} = -3T\cos\theta\sin\theta, \end{aligned} \tag{2.2.1}$$

where T is a small arbitrary function of the time t. The parameters $\eta_0, \lambda_1, \lambda_2, \upsilon_1, \upsilon_2, \ldots$ are then determined by identifying the velocity distribution on $r = R$ in the two systems.

For an axially symmetric flow, whether within the homogeneous or composite element, the components of velocity referred to spherical polar coordinates r, θ, ϕ may be written, consistently with the equation of continuity ($e_i^{(1)i} = 0$), in the form

$$\left(-\frac{1}{r^2\sin\theta}\frac{\partial\psi}{\partial\theta}, \frac{1}{r\sin\theta}\frac{\partial\psi}{\partial r}, 0\right),$$

where the stream function $\psi = \psi(r, \theta, t)$. It is a simple matter to express the

(physical) stress components $p_{(ik)}$ $(i,k = r,\theta,\phi)$ in terms of ψ and its derivatives, and to substitute them into the (linearized) equations of motion. The pressure p is easily eliminated and an equation derived for ψ.

Within the homogeneous element L^* the values of ψ and p, finite at the origin $(r = 0)$ and satisfying the given imposed stress distribution (2.2.1) on $r = R$, are

$$\psi = -\frac{T}{2\eta^*} r^3 \sin^2\theta\cos\theta, \quad p = 0. \tag{2.2.2}$$

Within the composite element the appropriate solutions in L are

$$\psi = -\frac{1}{2}\left(\frac{1}{7}Ar^5 + \frac{1}{2}B + 2Cr^3 - 3Dr^{-2}\right)\sin^2\theta\cos\theta, \tag{2.2.3a}$$

$$p = \frac{1}{2}\eta(Ar^2 + Br^{-3})(3\cos^2\theta - 1) + p_0, \tag{2.2.3b}$$

where A, B, C, D and p_0 are functions of the time t only. The associated, non-vanishing components of stress are

$$p_{(rr)} = \frac{1}{2}\eta(-\frac{1}{7}Ar^2 - 3Br^{-3} + 4C + 24Dr^{-5})(3\cos^2\theta - 1) - p_0, \tag{2.2.4a}$$

$$p_{(\theta\theta)} = \eta[(\frac{5}{14}Ar^2 + 3Dr^{-5})(3 - 7\cos^2\theta) + C(4 - 6\cos^2\theta)] - p_0, \tag{2.2.4b}$$

$$p_{(\phi\phi)} = \eta[(\frac{5}{14}Ar^2 + 3Dr^{-5})(1 - 5\cos^2\theta) - 2C] - p_0, \tag{2.2.4c}$$

$$p_{(r\theta)} = -\eta(\frac{8}{7}Ar^2 + \frac{3}{2}Br^{-3} + 6C - 24Dr^{-5})\cos\theta\sin\theta. \tag{2.2.4d}$$

The velocity and stress distribution in S $(r < a)$ and L^* $(r > b)$ are given by expressions of exactly the same form as (2.2.3a,b), (2.2.4a-d) above but with the symbols A, B, C, D, p_0, η replaced by A', B', C', D', p_0', η_s and by A^*, B^*, C^*, D^*, p_0^*, η^* respectively. There are sixteen unknowns involved, the operator η^* and the fifteen functions of time $A, A', A^*, B, B', B^*, C, C', C^*, D, D', D^*$, p_0, p_0', p_0^*. These are simply determined by the conditions of continuity of velocity and of stress in

the composite element across $r = a, b$, and by identifying these with those of the homogeneous element (as given by (2.2.1), (2.2.2)) on $r = R$.

It is found that the flow conditions on $r = R$ in the homogeneous and composite element cannot be matched exactly, but for sufficiently large values of R the differences are very small. Eventually, it emerges that

$$\frac{\eta^*}{\eta_0} = \frac{1 + \lambda_2 \triangle}{1 + \lambda_1 \triangle}, \tag{2.2.5}$$

where

$$\begin{aligned} \eta_0 &= \eta[1 + \frac{5}{2}c + O(c^2)], \\ \lambda_1 &= \frac{3\eta}{2\mu}[1 + \frac{5}{3}c + O(c^2)], \\ \lambda_2 &= \frac{3\eta}{2\mu}[1 - \frac{5}{2}c + O(c^2)]. \end{aligned}$$

.

Thus the rheological behavior of a dilute suspension at small rates of shear is governed by the equations

$$p_{ik} = p'_{ik} - p g_{ik}, \tag{2.2.6a}$$

$$(1 + \lambda_1 \frac{\partial}{\partial t}) p'_{ik} = 2\eta_0 (1 + \lambda_2 \frac{\partial}{\partial t}) e^{(1)}_{ik}. \tag{2.2.6b}$$

It is observed that

(i) the constants $\eta_0, \lambda_1, \lambda_2$ are independent of the actual size of the solid particles, depending only on the volume concentration c,

(ii) the intrinsic viscosity η_0 is independent of the rigidity of the suspended particles and has the same value as given by Einstein, and

(iii) the relaxation times λ_1, λ_2 vary directly with the viscosity η of the continuous phase and inversely with the rigidity modulus of the disperse phase.

The form of η^* appropriate to the Oldroyd model is easily computed. The above analysis goes over unchanged except that the operator η_s is replaced by a constant η' (the viscosity of the dispersed liquid phase). Also, due to the constant interfacial tension γ everywhere between L and L', there is now in the composite element a discontinuity in the normal stress $p_{(rr)}$ across $r = a$. The resulting formula for η^* is found to be of the same form as (2.2.5) with

$$\begin{aligned}
\eta_0 &= \eta[1 + \frac{(\eta + \frac{5}{2}\eta')}{\eta + \eta'}c + O(c^2)], \\
\lambda_1 &= \frac{a(16\eta + 19\eta')}{40(\eta + \eta')\gamma}[3\eta + 2\eta' + \frac{\eta(16\eta + 19\eta')}{5(\eta + \eta')}c + O(\eta c^2)], \\
\lambda_2 &= \frac{a(16\eta + 19\eta')}{40(\eta + \eta')\gamma}[3\eta + 2\eta' - \frac{3\eta(16\eta + 19\eta')}{10(\eta + \eta')}c + O(\eta c^2)].
\end{aligned}$$

It is thus seen that macroscopic elastic and viscous properties of a dilute emulsion are qualitatively the same as for a suspension of elastic solid spheres. Again, the intrinsic viscosity is seen to be independent of the drop size and of the interfacial tension between the two liquids, and has the value given for η^* by Taylor's formula. In contrast, parameters λ_1, λ_2 are seen to vary directly as the drop radius a and inversely as the interfacial tension[8].

It is observed that in the two models the relaxation times λ_1, λ_2 are such that $\lambda_1 \geq \lambda_2 \geq 0$, the models representing a purely viscous liquid when $\lambda_1 = \lambda_2$. The parameters λ_1, λ_2 are seen to have direct physical significance: when the motion is stopped ($e_{ik}^{(1)} = 0$) the stress p'_{ik} decays to zero as $\exp(-t/\lambda_1)$ and when the stress is removed ($p'_{ik} = 0$) the rate-of-strain $e_{ik}^{(1)}$ decays to zero as $\exp(-t/\lambda_2)$.

[8] Although the analysis in this section is restricted to one or other of two disperse systems, one may expect the resulting stress-rate-of-strain relations (2.2.6a,b) to be applicable to other materials which exhibit some degree of elasticity of shape.

Again, the sample itself, a patient's blood or plasma, is a suspension of solid particles in a viscous liquid. These particles deform under the application of stress and become preferentially orientated to facilitate the flow. Several studies have been made on the viscous and elastic properties of non-Newtonian fluids with a view of determining how closely they simulate the flow of human blood (see, for example, Liepsch *et al* (1991) and Gijsen *et al* (1999)). In the present work the sample is supposed represented by the Fröhlich & Sack model, so that, under sufficiently small rates of strain, its rheological behavior is characterized by three parameters, a viscosity coefficient and two relaxation times. The model does not exhibit all aspects of blood flow in that it does not accommodate 'shear thinning' but blood is only one of many body fluids investigated by Ortho-Clinical Diagnostics Group, fluids whose rheological properties are yet to be ascertained.

It remains for the experimentalist to determine the values of the three parameters characteristic of the mixture (sample and reagents) and of the sample itself so as to resolve, in part, the question posed at the beginning of this section. This should not prove difficult as there are many rheometers available in the commercial field to measure the three material parameters $\eta_0, \lambda_1, \lambda_2$ (see, for example, Oldroyd, Strawbridge and Toms 1951, Broadbent & Walters 1971, and Brindley & Keene 1974). Whatever the outcome, whether one has to consider the motion of the mixture or of the sample, one has to proceed with the rheological description represented by equation (2.2.6a,b) when the rates of shear are sufficiently small.

2.3 Rheological Equations at Finite Rates of Shear

So far one has supposed the rates of shear to be small, allowing one to neglect all non-linear terms, in which case the (general) rheological behavior can be represented by linear equations. Next, one needs to recast these equations in a such a form that they are applicable under all states of stress and of motion. Oldroyd (1950) has looked at this problem in some detail. The generalized equations of state, which describe the rheological behavior of an arbitrary material element moving as part of a continuum, have to satisfy the following three conditions:

I. **The equations must describe behaviour which is independent of the position and the motion of the element as a whole in space.**

II. **The equations must describe behaviour which may depend on the previous rheological history of the element but not in any way on the history of neighbouring elements.**

III. **The equations of state must describe behaviour which is consistent with the known linear behaviour when the rates of strain are small, corresponding here to the linear representation**

$$p_{ik} = p'_{ik} - pg_{ik},$$

$$(1 + \lambda_1 \frac{\partial}{\partial t}) p'_{ik} = 2\eta_0 (1 + \lambda_2 \frac{\partial}{\partial t}) e^{(1)}_{ik}.$$

It has been demonstrated by Oldroyd that such generalization cannot be carried through without ambiguity. For example, possible valid generalization of equations

(2.2.6a,b) are

$$(1+\lambda_1\frac{\mathfrak{D}}{\mathfrak{D}t})p'_{ik}=2\eta_0(1+\lambda_2\frac{\mathfrak{D}}{\mathfrak{D}t})e^{(1)}_{ik} \qquad \text{(Oldroyd A)}$$

and

$$(1+\lambda_1\frac{\mathfrak{D}}{\mathfrak{D}t})p'^{\,ik}=2\eta_0(1+\lambda_2\frac{\mathfrak{D}}{\mathfrak{D}t})e^{(1)ik}, \qquad \text{(Oldroyd B)}$$

where for any *absolute* tensor $b^{\cdot\cdot k\cdot\cdot}_{\cdot\cdot i\cdot\cdot}(\mathbf{x},t)$

$$\frac{\mathfrak{D}}{\mathfrak{D}t}b^{\cdot\cdot k\cdot\cdot}_{\cdot\cdot i\cdot\cdot}=\frac{\partial}{\partial t}b^{\cdot\cdot k\cdot\cdot}_{\cdot\cdot i\cdot\cdot}+v^m\frac{\partial b^{\cdot\cdot k\cdot\cdot}_{\cdot\cdot i\cdot\cdot}}{\partial x^m}+\sum\frac{\partial v^m}{\partial x^i}b^{\cdot\cdot k\cdot\cdot}_{\cdot\cdot m\cdot\cdot}-\sum{}'\frac{\partial v^k}{\partial x^m}b^{\cdot\cdot m\cdot\cdot}_{\cdot\cdot i\cdot\cdot}$$

$\sum(\sum')$ denoting a sum of all similar terms, one for each covariant (contravariant) suffix. But other generalizations are equally acceptable[9]. The physical significance of the convected derivative $\mathfrak{D}/\mathfrak{D}t$ is that it is a total time derivative in relation to a convected system of reference which at time t has the same velocity v_i, the same spin (or vorticity), and is being deformed at the same rate $e^{(1)}_{ik}$ as the material element at x^i that is being followed. When applied to a tensor intrinsically associated with the material element of a moving continuum at position x^i at time t , it introduces no (irrelevant) dependence on the fixed frame of reference or on the motion of the element as a whole in space.

The liquid defined by equation (B) - referred to by Oldroyd as liquid B - can boast to be able to describe most (but not all) of the well known large scale flow behavior of real materials[10]. For example, it is capable of describing the positive Weissenberg

[9] What would appear at first sight to be another possible generalization is the equation

$$g^{mi}(1+\lambda_1\frac{\mathfrak{D}}{\mathfrak{D}t})p'^{\,k}_m=2\eta_0(1+\lambda_2\frac{\mathfrak{D}}{\mathfrak{D}t})e^{(1)ik}$$

but on closer examination the left hand side is not symmetric in the free suffix and is therefore not valid.

[10] Liquid B fails to exhibit shear thinning which is observed in many real elastic fluids.

(1948) climbing effect when confined between coaxial rotating cylinders, and of describing the normal stress differences observed by Robert (1953) in real liquids, equivalent to equal normal stresses in all directions normal to the streamlines, in steady flow between rotating coaxial cones, and an extra tension along the streamlines. For such reasons, and for simplicity of mathematical form, it seems safe, at an exploratory stage, to proceed with the analysis on the assumption that the flow in the well, whether it be that of the mixture or of the sample, is described by equations of state representative of liquid B.

2.4 Convention and Notation

The notation used throughout the text is the usual one, but may be less familiar to those readers who approach the work with a view to its application rather than to its (wider) theoretical value. A word on the convention and notation adopted may therefore be appropriate at this stage.

In the above, $x^i\,(i = 1, 2, 3)$ represents a fixed system of curvilinear coordinates for which the line element is defined in terms of the metric tensor $g_{ik}(\mathbf{x})$[11] by the equation

$$ds^2 = g_{ik}dx^i dx^k.$$

Here the scheme adopted is that covariant suffixes are written below, contravariant suffixes above and the usual convention of summation over the values 1,2,3 applies to repeated suffixes.

[11] x is used as an abbreviation for x^1, x^2, x^3.

Referred to such a system x^i, $p_{ik}(\mathbf{x},t)$ denotes the stress tensor, and $e^{(1)}_{ik}(\mathbf{x},t)$ the (first) rate-of-strain tensor, defined in terms of the velocity vector $v_i(\mathbf{x},t)$ by

$$e^{(1)}_{ik} = \frac{1}{2}(v_{i,k} + v_{k,i}),$$

a suffix i following a comma indicating a covariant derivative with respect to a space coordinate x^i.

In the solution of the flow problem undertaken in the next chapter, it is found convenient (so as to accommodate the conditions on the boundary of the mixture) to work in orthogonal curvilinear coordinates $x^i\,(i = 1,2,3)$[12]. For such systems

$$\begin{aligned} g_{ik} &= g^{ik} = 0 \quad (i \neq j), \\ g_{ii} &= (g^{ii})^{-1} = h_i^2 \quad (i \text{ not summed}). \end{aligned}$$

Again, in order that the results obtained bear the physical dimensions of the tensor field to which they relate, and so to be capable of immediate physical interpretation, it is appropriate to introduce physical components of tensors, namely the Cartesian components in directions coinciding with the curvilinear coordinate directions $x^i\,(i = 1,2,3)$ locally at any particular point under consideration. If $b^{k\ldots}_{i\ldots}$ are the components of an absolute tensor in a general curvilinear system $x^i (i = 1,2,3)$, then its physical components, written $b_{(ik\ldots.)}$ (i.e. with brackets placed round suffixes), are defined by

$$b_{(ik\ldots.)} = \frac{\Pi'(h_k)}{\Pi(h_i)} b^{k\ldots}_{i\ldots} \qquad (i,k \text{ not summed}),$$

[12] In particular, in cylindrical polar coordinates $(x^1 = r, x^2 = \phi, x^3 = z)$ and in spherical polar coordinates $(x^1 = R, x^2 = \theta, x^3 = \phi)$.

where $\Pi(\Pi')$ denotes a product of all similar terms, one for each covariant (contravariant) suffix[13]. For example, the physical components of the contravariant stress tensor p^{ik} are defined by

$$p_{(ik)} = p_{(ki)} = h_i h_k p^{ik} \qquad (i, k \text{ not summed}),$$

or, equally, by

$$p^{ik} = p^{ki} = \frac{p_{(ik)}}{h_i h_k} \qquad (i, k \text{ not summed}).$$

Again, the physical components of the velocity vector v^i are defined by

$$v_{(i)} = h_i v^i \qquad (i \text{ not summed}).$$

2.5 References

Brindley, G., and Keene, D. E., "On using a Weissenberg rheogoniometer for oscillatory testing of stiff materials", 1974, *Journal of Physics E: Scientific Instruments*, **7**, 934.

Broadbent, J. M., and Walters, K., "Some suggestions for new rheometer designs II. Interpretation of experimental results", 1971, *Journal of Physics D: Applied Physics*, **4**, 1863.

Einstein, A., 1906, *Ann. Phys. Lpz.*, **19**, 289.

Fröhlich, H. and Sack, R., "Theory of the rheological properties of dispersions",1946, *Proc. Roy. Soc.* **A**, **185**, 415.

[13] The physical components of a tensor differ from its ordinary covariant and contravariant components in that they do not obey the tensor transformation laws.

Gijsen, F. J. H., Allanic, E., van de Vosse, F. N. and Janssen, J. D., "The influence of the non-Newtonian properties of blood on the flow in large arteries: unsteady flow in a 90 degrees curved tube", 1999, *Journal of Biomechanics,* **32** (7), 705.

Jones, J. R., and Walters, T. S., "Oscillatory motion of an elastico-viscous liquid contained between two coaxial cylinders", 1965, *Mathematika,* **12,** 246.

Jones, J. R., and Walters, T. S., "Oscillatory motion of an elastico-viscous liquid contained in a cylindrical cup I. Theoretical", 1966, *Brit. J. Appl. Phys.,* **17**, 937.

Liepsch, D., Thurston, G. and Lee, M., "Studies of fluids simulating blood-like rheological properties and applications in models of arterial branches", 1991, *Biorheology,* **28** (1-2), 39.

Oldroyd, J. G., "On the formulation of rheological equations of state", 1950, *Proc. Roy. Soc.* **A, 200,** 523.

Oldroyd, J. G., "The elastic and viscous properties of emulsions and suspensions", 1953, *Proc. Roy. Soc.* **A, 218,** 122.

Oldroyd, J. G., Strawbridge, D. J., and Toms, B. A., "A coaxial-cylinder elastoviscometer", 1951, *Proc. Phys. Soc.* **B, 64,** 44.

Roberts, J. E., "Pressure distribution in liquids in laminar shearing motion and comparison with predictions from various theories", 1953, *Proc. II Int. Congr. Rheo. Oxford,* 93.

Roscoe, R., "Viscosity determination by the oscillating vessel method I", 1958, *Proc. Phys. Soc.*, **72,** 576.

Roscoe, R. and Bainbridge, W., "Viscosity determination by the oscillating vessel method II", 1958, *Proc. Phys. Soc.*, **72,** 585.

Taylor, G. I., "The viscosity of a fluid containing small drops of another fluid", 1932, *Proc. Roy. Soc.* **A, 138,** 41.

Weissenberg, K., "Abnormal substances and abnormal phenomena of flow", 1948, *Proc. Int. Rheological Congr. Holland,* **I**, 29.

CHAPTER 3

EQUATIONS GOVERNING THE MOTION OF THE MIXTURE

The main body of the dissertation is taken up with a broad analysis of the critical phase in which the mixture within the well is transported on the outer carousel ring (with characteristic (or incubation) time of minutes), the aim being to ascertain the basic features of the motion within the well. The aim and purpose of the present chapter is to derive, and to exhibit, precise mathematical equations which describe this large scale motion, and to develop an analytic process that allows for their solution.

3.1 Basic Flow Equations

The motion that is of primary interest in the present study is that of the mixture, supposed homogeneous and incompressible of density ρ, as measured relative to the well when in transportation on the outer carousel ring. It is therefore appropriate to measure all relevant kinematic and dynamic variables relative to a (moving) frame $Oxyz$ rigidly attached to the well, with Oz drawn vertically upwards and coinciding with the axis of the well. Thus relative to this frame the boundary wall of the well is stationary. The scheme is illustrated diagrammatically in Fig. 3.1.1: the height measure is 12mm and the rim diameter measure is 8mm. Henceforth, unless otherwise explicitly stated, it is to be understood that all variables within the text are

as measured with respect to this moving frame $Oxyz$.

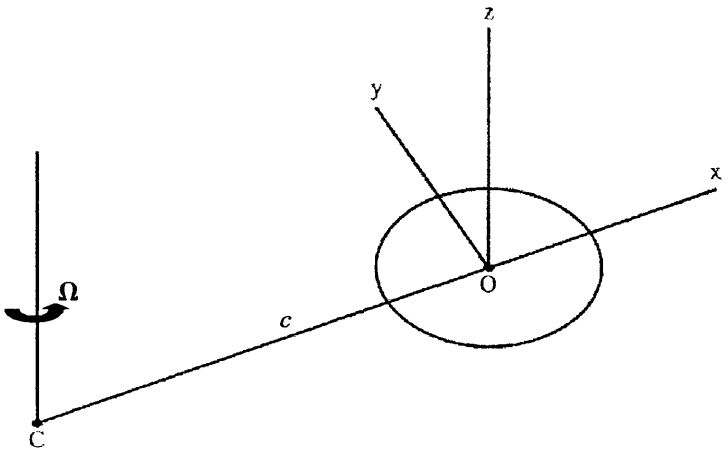

Fig. 3.1.1 The moving frame of reference $Oxyz$, rigidly attached to the well. C denotes the centre of the carousel ring and $c = CO$ its radius.

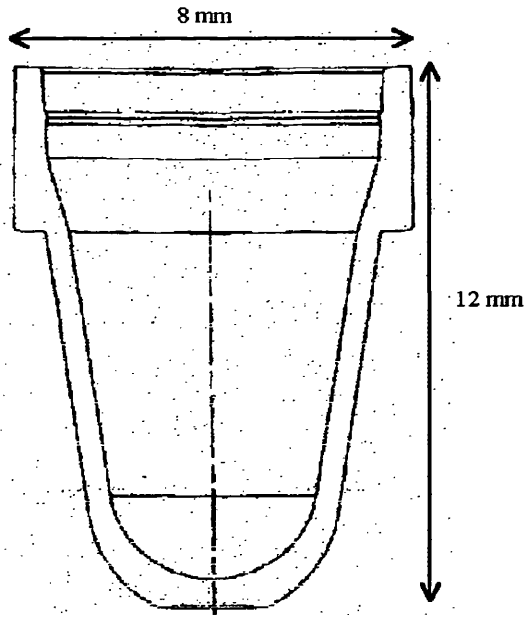

Fig. 3.1.2 Geometrical shape and dimensions of the well.

The equation of continuity expresses the principle of conservation of mass while the stress equations of motion are derived from Newton's laws of motion, and they may be written in the general tensorial form

$$v^i{}_{,i} = 0 \qquad \text{(equation of continuity)}, \tag{3.1.1}$$

$$\rho f^i = p^{ik}{}_{,k} + \rho F^i \qquad \text{(stress equations of motion)}, \tag{3.1.2}$$

independently of the flow properties of the mixture. When referred to the Cartesian frame $Oxyz$ (in which case x^1, x^2, x^3 are identified with x, y, z) the equations of continuity and of motion (exhibited in general by (3.1.1) and (3.1.2)) take on the more familiar form[14]

$$\frac{\partial v^i}{\partial x^i} = 0, \tag{3.1.3}$$

$$\rho f^i_{abs} = -\frac{\partial p}{\partial x^i} + \frac{\partial p'^{ik}}{\partial x^k} + \rho F^i, \tag{3.1.4}$$

F^i denoting the body force field per unit mass. Here, the acceleration f^i_{abs}, in contrast to the velocity v^i, represents the 'absolute' acceleration of the fluid element and not as measured relative to the moving frame $Oxyz$[15]. It is appropriate to write

$$\mathbf{f}_{abs} = \mathbf{f}_0 + \mathbf{f}',$$

where $\mathbf{f}_0$ is the acceleration of the origin O and $\mathbf{f}'$ is the acceleration of the fluid element relative to O. If in a Lagrangian representation of the flow relative to the

[14] In a Cartesian representation there is no need to distinguish between covariant and contravariant components and so it is convenient to place all suffixes in the upper position.

[15] It is noted that $v^i{}_{,i} (= e^{(1)i}{}_{,i})$ is a flow invariant so that the equation of continuity for an incompressible fluid takes on the same mathematical form in all frames of reference.

frame $Oxyz$, a frame rotating with angular velocity $\boldsymbol{\Omega}(t) = (0, 0, \Omega(t))$, $\mathbf{x} = \mathbf{x}(\mathbf{x}_0, t)$ represents the position of the fluid element at time t which at prior time t_0 is in position $\mathbf{x}_0$, then the velocity $\mathbf{v}'(\mathbf{x}_0, t)$ and the acceleration $\mathbf{f}'(\mathbf{x}_0, t)$ as measured relative to O are given by the formulae

$$\begin{aligned}
\mathbf{v}'(\mathbf{x}_0, t) &= \left(\frac{d\mathbf{x}}{dt}\right)_{\mathbf{x}_0} + \boldsymbol{\Omega} \times \mathbf{x}, \\
\mathbf{f}'(\mathbf{x}_0, t) &= \left(\frac{d\mathbf{v}'}{dt}\right)_{\mathbf{x}_0} + \boldsymbol{\Omega} \times \mathbf{v}' \\
&= \left(\frac{d^2\mathbf{x}}{dt^2}\right)_{\mathbf{x}_0} + 2\boldsymbol{\Omega} \times \left(\frac{d\mathbf{x}}{dt}\right)_{\mathbf{x}_0} + \dot{\boldsymbol{\Omega}} \times \mathbf{x} + \boldsymbol{\Omega} \times (\boldsymbol{\Omega} \times \mathbf{x}).
\end{aligned}$$

Now, $(d\mathbf{x}/dt)_{\mathbf{x}_0}$ and $(d^2\mathbf{x}/dt^2)_{\mathbf{x}_0}$ are recognized as the velocity $\mathbf{v}(\mathbf{x}, t)$ and the acceleration $D\mathbf{v}(\mathbf{x}, t)/Dt$ in an Eulerian representation as measured relative to the rotating frame $Oxyz$. Thus

$$\mathbf{f}_{abs} = \mathbf{f}_0 + \frac{D\mathbf{v}}{Dt} + 2(\boldsymbol{\Omega} \times \mathbf{v}) + (\dot{\boldsymbol{\Omega}} \times \mathbf{x}) + \boldsymbol{\Omega} \times (\boldsymbol{\Omega} \times \mathbf{x}),$$

and may be rewritten in the form

$$\mathbf{f}_{abs} = \frac{D\mathbf{v}}{Dt} + 2(\boldsymbol{\Omega} \times \mathbf{v}) + (\dot{\boldsymbol{\Omega}} \times \mathbf{x}) + \boldsymbol{\Omega} \times (\boldsymbol{\Omega} \times \mathbf{x}) + \nabla(\mathbf{f}_0 \cdot \mathbf{x}),$$

which in the present regime reduces to

$$\mathbf{f}_{abs} = \frac{D\mathbf{v}}{Dt} + 2(\boldsymbol{\Omega} \times \mathbf{v}) + (\dot{\boldsymbol{\Omega}} \times \mathbf{x}) + \boldsymbol{\Omega} \times (\boldsymbol{\Omega} \times \mathbf{x}) + \nabla(c(-\Omega^2 x + \dot{\Omega}\, y)).$$

Here, it is recalled that $c = CO$. It is thus seen that the stress equations of motion can be rewritten in the modified form

$$\rho\left(\frac{D\mathbf{v}}{Dt} + 2(\boldsymbol{\Omega} \times \mathbf{v}) + (\dot{\boldsymbol{\Omega}} \times \mathbf{x}) + \boldsymbol{\Omega} \times (\boldsymbol{\Omega} \times \mathbf{x})\right)^i = -\frac{\partial p}{\partial x^i} + \frac{\partial p'^{ik}}{\partial x^k} + \rho F^i, \quad (3.1.5)$$

where the term

$$\rho c(-\Omega^2 x + \dot{\Omega}\, y)$$

has been incorporated in the isotropic pressure p.

The instantaneous state of stress for an incompressible fluid is expressible as the superposition of two stress systems, viz.

$$p_{ik} = p'_{ik} - pg_{ik},$$

where the (partial) stress system p'_{ik} is related to the rate-of-strain components $e^{(1)}_{ik}$ by a set of differential equations involving the convected derivatives $\mathfrak{D}p'_{ik}/\mathfrak{D}t$ and $\mathfrak{D}e^{(1)}_{ik}/\mathfrak{D}t$ together with scalar physical parameters $\eta_0, \lambda_1, \lambda_2$ characteristic of the fluid, and p represents an isotropic pressure whose variation with $\mathbf{x}$ and t is determined by the equations of motion[16].

Now the components of stress are real physical agents and as such are not a subjective property of the frame of reference, the components $e^{(1)}_{ik}$ define the rates at which distances between neighbouring points of a fluid element are changing with respect to time and, hence, are independent of both the translational and rotational motion of the element, and the convected derivative $\mathfrak{D}/\mathfrak{D}t$, as emphasized in the previous chapter, is an operator that introduces no dependence on the frame of reference. Thus the equations of state (2.2.6a,b) remain unchanged in mathematical form when referred to the moving frame $Oxyz$, it then being understood that all kinematic variables are as measured relative to this frame. Thus in the frame $Oxyz$

[16] For an incompressible fluid, an added, arbitrary, isotropic state of stress has no effect on the kinematics.

the equation of state for liquid Oldroyd B may be written as previously[17], viz.

$$p^{ik} = p'^{ik} - pg^{ik}, \tag{3.1.6a}$$

$$(1 + \lambda_1 \frac{\mathfrak{D}}{\mathfrak{D}t}) p'^{ik} = 2\eta_0 (1 + \lambda_2 \frac{\mathfrak{D}}{\mathfrak{D}t}) e^{(1)\,ik}. \tag{3.1.6b}$$

3.2 Axially Symmetric Flow

It is convenient to introduce cylindrical polar coordinates r, ϕ, z defined by

$$x = r\cos\phi, \quad y = r\sin\phi, \quad z = z,$$

in which scheme the boundary wall of the well may be represented by the equation $f(r, z) = 0$. An axially symmetric flow is assumed in which the physical components of the velocity vector, $v_{(r)}, v_{(\phi)}, v_{(z)}$, when referred to the coordinates r, ϕ, z, are functions of r, z and t only. The equation of continuity (3.1.1) reduces to

$$\frac{\partial}{\partial r}(rv_{(r)}) + \frac{\partial}{\partial z}(rv_{(z)}) = 0, \tag{3.2.1}$$

and is the condition for the existence of a stream function $\psi(r, z, t)$ such that

$$v_{(r)} = \frac{1}{r}\frac{\partial \psi}{\partial z}, \quad v_{(z)} = -\frac{1}{r}\frac{\partial \psi}{\partial r}.$$

Hence, consistent with the incompressibility condition, the velocity field is written in the form

$$v_{(r)} = \frac{1}{r}\frac{\partial \psi}{\partial z}, \quad v_{(\phi)} = r[\omega(r, z, t) - \Omega(t)], \quad v_{(z)} = -\frac{1}{r}\frac{\partial \psi}{\partial r}. \tag{3.2.2}$$

[17] It is noted that, *even when working within a Cartesian frame*, one has to make a distinction between associated covariant and contravariant tensors when evaluating their convected derivatives.

The physical components of the modified acceleration field as depicted by the left-hand side of equation (3.1.5) are now easily computed, these being

$$\frac{\partial v_{(r)}}{\partial t} + v_{(r)}\frac{\partial v_{(r)}}{\partial r} - r\omega^2 + v_{(z)}\frac{\partial v_{(r)}}{\partial z},$$
$$\frac{\partial \omega}{\partial t} + v_{(z)}\frac{\partial \omega}{\partial z} + \frac{2\omega v_{(r)}}{r} + v_{(r)}\frac{\partial \omega}{\partial r},$$
$$\frac{\partial v_{(z)}}{\partial t} + v_{(z)}\frac{\partial v_{(z)}}{\partial z} + v_{(r)}\frac{\partial v_{(z)}}{\partial r},$$

and are seen to be independent of the parameter $\Omega(t)$. These expressions have to be equated with the right-hand side of equation (3.1.5). For any contravariant tensor T^{ik}

$$T^{ik}{}_{,j} = \frac{\partial T^{ik}}{\partial x^j} + \Gamma^i_{ej}T^{ek} + \Gamma^k_{ej}T^{ie},$$

where Γ^j_{ik} is the Christoffel three-index symbol defined in terms of the metric g_{ik} by

$$\Gamma^j_{ik} = \frac{1}{2}g^{mj}(g_{im,k} + g_{mk,i} - g_{ki,m}).$$

In the polar coordinate description r, ϕ, z,

$$g_{rr} = 1, \quad g_{\phi\phi} = r, \quad g_{zz} = 1, \quad g_{\phi z} = g_{zr} = g_{r\phi} = 0,$$

in which case it is easily shown that the only non vanishing components of Γ^j_{ik} are

$$\Gamma^\phi_{r\phi} = \frac{1}{r}, \quad \Gamma^r_{\phi\phi} = -r.$$

It follows that

$$p^{rr}{}_{,r} = \frac{\partial p_{(rr)}}{\partial r}, \quad p^{r\phi}{}_{,\phi} = \frac{1}{r}(p_{(rr)} - p_{(\phi\phi)}), \quad p^{rz}{}_{,z} = \frac{\partial p_{(rz)}}{\partial z},$$
$$p^{\phi r}{}_{,r} = \frac{1}{r}\frac{\partial p_{(r\phi)}}{\partial r}, \quad p^{\phi\phi}{}_{,\phi} = \frac{2}{r^2}p_{(r\phi)}, \quad p^{\phi z}{}_{,z} = \frac{1}{r}\frac{\partial p_{(\phi z)}}{\partial z},$$
$$p^{zr}{}_{,r} = \frac{\partial p_{(rz)}}{\partial r}, \quad p^{z\phi}{}_{,\phi} = \frac{1}{r}p_{(rz)}, \quad p^{zz}{}_{,z} = \frac{\partial p_{(zz)}}{\partial z}.$$

Hence, the stress equations of motion reduce to[18]

$$\begin{aligned} & \rho\left(\frac{\partial v_{(r)}}{\partial t} + v_{(r)}\frac{\partial v_{(r)}}{\partial r} - r\omega^2 + v_{(z)}\frac{\partial v_{(r)}}{\partial z}\right) \\ = \; & \frac{\partial p_{(rr)}}{\partial r} + \frac{\partial p_{(rz)}}{\partial z} + \frac{1}{r}(p_{(rr)} - p_{(\phi\phi)}) + \rho F_{(r)}, \qquad (3.2.3a) \\ & \rho r\left(\frac{\partial \omega}{\partial t} + v_{(z)}\frac{\partial \omega}{\partial z} + \frac{2\omega v_{(r)}}{r} + v_{(r)}\frac{\partial \omega}{\partial r}\right) \\ = \; & \frac{\partial p_{(r\phi)}}{\partial r} + \frac{\partial p_{(\phi z)}}{\partial z} + \frac{2}{r}p_{(r\phi)} + \rho F_{(\phi)}, \qquad (3.2.3b) \\ & \rho\left(\frac{\partial v_{(z)}}{\partial t} + v_{(z)}\frac{\partial v_{(z)}}{\partial z} + v_{(r)}\frac{\partial v_{(z)}}{\partial r}\right) \\ = \; & \frac{\partial p_{(rz)}}{\partial r} + \frac{\partial p_{(zz)}}{\partial z} + \frac{1}{r}p_{(rz)} + \rho F_{(z)}, \qquad (3.2.3c) \end{aligned}$$

where $F_{(r)}, F_{(\phi)}, F_{(z)}$ denote the physical components of the body force field.

Finally, the equations of state representing a liquid of type Oldroyd B need to be cast in terms of the appropriate physical components. Given the formulae

$$\frac{\mathfrak{D}}{\mathfrak{D}t}p'^{\,ik} = \frac{\partial p'^{\,ik}}{\partial t} + v^m p'^{\,ik}{}_{,m} - v^i{}_{,m}p'^{\,mk} - v^k{}_{,m}p'^{\,im},$$

$$\frac{\mathfrak{D}}{\mathfrak{D}t}e^{(1)\,ik} = \frac{\partial e^{(1)\,ik}}{\partial t} + v^m e^{(1)\,ik}{}_{,m} - v^i{}_{,m}e^{(1)\,mk} - v^k{}_{,m}e^{(1)\,im},$$

this represents a simple, but tedious, process. The results are

$$\begin{aligned} & p'_{(rr)} + \lambda_1\left[\left(\frac{\partial}{\partial t} + v_{(r)}\frac{\partial}{\partial r} + v_{(z)}\frac{\partial}{\partial z}\right)p'_{(rr)} - 2\frac{\partial v_{(r)}}{\partial r}p'_{(rr)} - 2\frac{\partial v_{(r)}}{\partial z}p'_{(rz)}\right] \\ = \; & 2\eta_0\frac{\partial v_{(r)}}{\partial r} + 2\eta_0\lambda_2\left[\left(\frac{\partial}{\partial t} + v_{(r)}\frac{\partial}{\partial r} + v_{(z)}\frac{\partial}{\partial z}\right)\frac{\partial v_{(r)}}{\partial r}\right. \\ & \left. -2\left(\frac{\partial v_{(r)}}{\partial r}\right)^2 - \frac{\partial v_{(z)}}{\partial z}\left(\frac{\partial v_{(r)}}{\partial z} + \frac{\partial v_{(z)}}{\partial r}\right)\right], \qquad (3.2.4a) \end{aligned}$$

[18] Here the conservative gravitational body force $(0, 0, -g)$ has been incorporated in the pressure field $p : p \to p + \rho\,\mathbf{g}\cdot\mathbf{x}$.

$$\frac{1}{r}p'_{(r\phi)} + \lambda_1[(\frac{\partial}{\partial t} + v_{(r)}\frac{\partial}{\partial r} + v_{(z)}\frac{\partial}{\partial z})\frac{p'_{(r\phi)}}{r}$$
$$-\frac{\partial v_{(r)}}{\partial r}\frac{p'_{(r\phi)}}{r} - \frac{\partial v_{(r)}}{\partial z}\frac{p'_{(\phi z)}}{r} - \frac{\partial \omega}{\partial r}p'_{(rr)} - \frac{\partial \omega}{\partial z}p'_{(rz)}]$$

$$= \eta_0\frac{\partial \omega}{\partial r} + \eta_0\lambda_2[(\frac{\partial}{\partial t} + v_{(r)}\frac{\partial}{\partial r} + v_{(z)}\frac{\partial}{\partial z})\frac{\partial \omega}{\partial r} - \frac{\partial v_{(r)}}{\partial r}\frac{\partial \omega}{\partial r}$$
$$-\frac{\partial v_{(r)}}{\partial z}\frac{\partial \omega}{\partial z} - 2\frac{\partial \omega}{\partial r}\frac{\partial v_{(r)}}{\partial r} - \frac{\partial \omega}{\partial z}(\frac{\partial v_{(r)}}{\partial z} + \frac{\partial v_{(z)}}{\partial r})], \qquad (3.2.4b)$$

$$p'_{(rz)} + \lambda_1[(\frac{\partial}{\partial t} + v_{(r)}\frac{\partial}{\partial r} + v_{(z)}\frac{\partial}{\partial z})p'_{(rz)} - (\frac{\partial v_{(r)}}{\partial r} + \frac{\partial v_{(z)}}{\partial z})p'_{(rz)}$$
$$-\frac{\partial v_{(r)}}{\partial z}p'_{(zz)} - \frac{\partial v_{(z)}}{\partial r}p'_{(rr)}]$$

$$= \eta_0(\frac{\partial v_{(r)}}{\partial z} + \frac{\partial v_{(z)}}{\partial r}) + \eta_0\lambda_2[(\frac{\partial}{\partial t} + v_{(r)}\frac{\partial}{\partial r} + v_{(z)}\frac{\partial}{\partial z})$$
$$(\frac{\partial v_{(r)}}{\partial z} + \frac{\partial v_{(z)}}{\partial r}) - (\frac{\partial v_{(r)}}{\partial z} + \frac{\partial v_{(z)}}{\partial r})(\frac{\partial v_{(r)}}{\partial r} + \frac{\partial v_{(z)}}{\partial z})$$
$$-\frac{\partial v_{(r)}}{\partial z}\frac{\partial v_{(z)}}{\partial z} - \frac{\partial v_{(r)}}{\partial r}\frac{\partial v_{(z)}}{\partial r}], \qquad (3.2.4c)$$

$$\frac{p'_{(\phi\phi)}}{r^2} + \lambda_1[(\frac{\partial}{\partial t} + v_{(r)}\frac{\partial}{\partial r} + v_{(z)}\frac{\partial}{\partial z})\frac{p'_{(\phi\phi)}}{r^2} - \frac{2}{r}\frac{\partial \omega}{\partial r}p'_{(r\phi)} - 2\frac{\partial \omega}{\partial z}\frac{p'_{(\phi z)}}{r}]$$

$$= 2\eta_0\frac{v_{(r)}}{r^3} + 2\eta_0\lambda_2[(\frac{\partial}{\partial t} + v_{(r)}\frac{\partial}{\partial r} + v_{(z)}\frac{\partial}{\partial z})\frac{v_{(r)}}{r^3}$$
$$-(\frac{\partial \omega}{\partial r})^2 - (\frac{\partial \omega}{\partial z})^2], \qquad (3.2.4d)$$

$$\frac{p'_{(\phi z)}}{r} + \lambda_1[(\frac{\partial}{\partial t} + v_{(r)}\frac{\partial}{\partial r} + v_{(z)}\frac{\partial}{\partial z})\frac{p'_{(\phi z)}}{r} - \frac{\partial \omega}{\partial r}p'_{(rz)} - \frac{\partial \omega}{\partial z}p'_{(zz)}$$
$$-\frac{\partial v_{(z)}}{\partial r}\frac{p'_{(\phi r)}}{r} - \frac{\partial v_{(z)}}{\partial z}\frac{p'_{(\phi z)}}{r}]$$

$$= \eta_0\frac{\partial \omega}{\partial z} + \eta_0\lambda_2[(\frac{\partial}{\partial t} + v_{(r)}\frac{\partial}{\partial r} + v_{(z)}\frac{\partial}{\partial z})\frac{\partial \omega}{\partial z} - 3\frac{\partial v_{(z)}}{\partial z}\frac{\partial \omega}{\partial z}$$
$$-\frac{\partial \omega}{\partial r}(\frac{\partial v_{(r)}}{\partial z} + \frac{\partial v_{(z)}}{\partial r}) - \frac{\partial v_{(z)}}{\partial r}\frac{\partial \omega}{\partial r}], \qquad (3.2.4e)$$

$$p'_{(zz)} + \lambda_1[(\frac{\partial}{\partial t} + v_{(r)}\frac{\partial}{\partial r} + v_{(z)}\frac{\partial}{\partial z})p'_{(zz)} - 2\frac{\partial v_{(z)}}{\partial r}p'_{(rz)} - 2\frac{\partial v_{(z)}}{\partial z}p'_{(zz)}]$$

$$= 2\eta_0\frac{\partial v_{(z)}}{\partial z} + 2\eta_0\lambda_2[(\frac{\partial}{\partial t} + v_{(r)}\frac{\partial}{\partial r} + v_{(z)}\frac{\partial}{\partial z})\frac{\partial v_{(z)}}{\partial z}$$

$$-\frac{\partial v_{(z)}}{\partial r}\frac{\partial v_{(r)}}{\partial z} - 3(\frac{\partial v_{(z)}}{\partial r})^2], \qquad (3.2.4f)$$

and are again seen to be independent of the parameter $\Omega(t)$.

It is observed that if the 'absolute' pressure does not occur in the boundary conditions, the flow within the well is not only axially symmetric, but can also be simulated in an arrangement independent of the Vitros instrumentation.

The wells on the carousel are almost completely filled and, although subject (throughout the incubation period) to vigorous accelerating and decelerating motions, there is no spillage of mixture, surface tension being sufficiently large to prevent this[19]. (Any spillage would cause contamination and result in serious disruption of the testing programme). It is reasonable to proceed on the assumption that surface tension is such as to prevent the growth of oscillations on the free surface, and for the free surface to be represented approximately by a (horizontal) plane $z = b$. The boundary conditions associated with equations (3.2.3a-c) then reduce to

$$\nabla\psi = 0, \quad \omega = \Omega(t) \quad \text{on the wall } f(r,z) = 0,$$

$$\psi = 0, \quad p_{(rz)} = p_{(z\phi)} = 0 \quad \text{on the free surface } z = b[20].$$

[19] Serious spillage occurs from time to time. This may well be due to the well vibrating within its seating in the circumferential direction and to the well section departing (slightly) from the circular. But such considerations and investigations are outside the scope of the present study.

[20] No information is sought from considerations of the normal stress at the free surface, it being supposed that any discontinuity in the normal stress there is balanced by surface tension acting at a slightly deformed free surface.

In this event as the 'absolute' pressure (together with the gravitational force potential) does not play an active role, both the velocity $(v_{(r)}, v_{(\phi)}, v_{(z)})$ and the normal stress differences $(p'_{(rr)} - p'_{(\phi\phi)}, p'_{(\phi\phi)} - p'_{(zz)}, p'_{(zz)} - p'_{(rr)})$ can be identified with those in a well in a fixed location rotating about its axis with (variable) angular velocity $\Omega(t)$.

3.2.1 'Sweep' at Constant Values of Ω

Inspection of the flow equations (3.2.3a-c) with $\omega = \Omega_0$ (a constant) on the wall $f(r,z) = 0$ confirms that the appropriate solution is

$$\psi = 0, \quad \omega = \Omega_0, \quad p'_{(ik)} = 0 \quad (i,k = r,\phi,z),$$

in which case the fluid moves with the well as if it were rigid. Thus the driving mechanism which causes 'mixing' to occur within the well is the single inertial term $\rho\, \dot{\mathbf{\Omega}} \times \mathbf{x}$ in the basic stress equations of motion (3.1.5). When $\dot{\mathbf{\Omega}} = 0$ (i.e. $\Omega =$ a constant $= \Omega_0$) $v_{(r)} = v_{(\phi)} = v_{(z)} = 0$. It is only when $\dot{\mathbf{\Omega}} \neq 0$, corresponding to the 'jiggle' arrangement, that there is (relative) motion of fluid within the well. This is the judgement of Johnson & Johnson Clinical Diagnostics Ltd. and in this they are proved correct.

3.2.2 'Jiggle' at Rapidly Oscillating Values of Ω

In this regime the carousel ring oscillates with angular amplitude Ω_0 and frequency $n/2\pi$:

$$\Omega = \mathrm{Re}(\Omega_0 e^{int}).$$

The governing equations are much too complicated for a direct analytical approach to be feasible. At this stage of the analysis there is no great advantage in seeking an

exact solution. What is desirable is to have some idea of the structure of the flow and on how it reacts to changes in external conditions. It is deemed that some strides can be made with the analysis of the governing equations by employing a method adopted by Jones (1970) in investigating oscillatory flows between coaxial surfaces of revolution. Such a method- one which allows for theoretical manoeuver only- has had a good measure of success when applied to steady regimes (Jones (1973), Griffiths *et al* (1969)), but somewhat less so when applied to unsteady regimes (Jones (1970), Lyne (1970), Zalosh & Nelson (1973), James (1975), (1975)[21]). However, for the oscillatory boundary driven motions investigated in the present work, it is anticipated that the approach allows not only for a reasonable qualitative description of the flow field, but that the information that results hold true over the entire range of values of the Reynolds number, more especially for large (as well as small) values. The method, in broad outline, is the following. The mixture is first constrained by a virtual body-force vector to flow steadily in paths which are circles with centres on, and planes perpendicular to, the well axis. The body-force vector is then, at some time $t = t_0$, suddenly removed and the initial (or acceleration) motion of the liquid calculated. The argument is that this incipient flow can give useful information about the nature of the fully developed flow: if the incipient flow consists of a cell pattern, it is reasonable to expect, from continuity consideration, the cell pattern to persist until the fully developed flow is attained.

[21] The results of Lyne (1970) and Zalosh & Nelson (1973) apply to a purely viscous regime, whereas those of James (1975), (1975) apply to a more general elastico-viscous regime.

I. Primary Flow

The mixture is first, for times $t < t_0$, constrained by a virtual body-force with components $F_{(r)}(r,z,t), F_{(\phi)}(r,z,t), F_{(z)}(r,z,t)$ (whose values are as yet unspecified) to flow in horizontal circles with centres on the axis of rotation. For this constrained regime (consistent with the incompressibility condition $v^i{}_{,i}=0$)

$$v_{(r)} = 0, \quad v_{(\phi)} = r[\omega(r,z,t) - \Omega(t)], \quad v_{(z)} = 0.$$

For this basic simple flow, the stress equations of motion reduce to give

$$\rho F_{(r)} = -\rho r\omega^2 - \frac{\partial p_{(rr)}}{\partial r} - \frac{\partial p_{(rz)}}{\partial z} - \frac{1}{r}(p_{(rr)} - p_{(\phi\phi)}), \tag{3.2.5a}$$

$$\rho F_{(\phi)} = 0, \tag{3.2.5b}$$

$$\rho F_{(z)} = -\frac{\partial p_{(rz)}}{\partial r} - \frac{\partial p_{(zz)}}{\partial z} - \frac{1}{r}p_{(rz)}, \tag{3.2.5c}$$

and

$$\rho r\frac{\partial \omega}{\partial t} = \frac{\partial p_{(r\phi)}}{\partial r} + \frac{\partial p_{(\phi z)}}{\partial z} + \frac{2}{r}p_{(r\phi)}; \tag{3.2.5d}$$

whilst the rheological equations of state reduce to give

$$p'_{(rr)} + \lambda_1\frac{\partial p'_{(rr)}}{\partial t} = 0, \tag{3.2.6a}$$

$$\frac{1}{r}p'_{(r\phi)} + \lambda_1(\frac{1}{r}\frac{\partial p'_{(r\phi)}}{\partial t} - \frac{\partial \omega}{\partial r}p'_{(rr)} - \frac{\partial \omega}{\partial z}p'_{(rz)}) = \eta_0(\frac{\partial \omega}{\partial r} + \lambda_2\frac{\partial^2\omega}{\partial t\partial r}), \tag{3.2.6b}$$

$$p'_{(rz)} + \lambda_1\frac{\partial p'_{(rz)}}{\partial t} = 0, \tag{3.2.6c}$$

$$\frac{p'_{(\phi\phi)}}{r^2} + \lambda_1(\frac{1}{r^2}\frac{\partial p'_{(\phi\phi)}}{\partial t} - \frac{2}{r}\frac{\partial \omega}{\partial r}p'_{(r\phi)} - \frac{2}{r}\frac{\partial \omega}{\partial z}p'_{(\phi z)}) = -2\eta_0\lambda_2[(\frac{\partial \omega}{\partial r})^2 + (\frac{\partial \omega}{\partial z})^2], \tag{3.2.6d}$$

$$\frac{1}{r}p'_{(\phi z)} + \lambda_1(\frac{1}{r}\frac{\partial p'_{(\phi z)}}{\partial t} - \frac{\partial \omega}{\partial r}p'_{(rz)} - \frac{\partial \omega}{\partial z}p'_{(zz)}) = \eta_0(\frac{\partial \omega}{\partial z} + \lambda_2\frac{\partial^2\omega}{\partial t\partial z}), \tag{3.2.6e}$$

$$p'_{(zz)} + \lambda_1\frac{\partial p'_{(zz)}}{\partial t} = 0. \tag{3.2.6f}$$

Inspection of equations (3.2.6a-f) show that

$$p'_{(rr)} = p'_{(rz)} = p'_{(zz)} = 0, \tag{3.2.7}$$

resulting in the simplified stress-rate-of-strain relations

$$\frac{1}{r}p'_{(r\phi)} + \lambda_1 \frac{1}{r}\frac{\partial p'_{(r\phi)}}{\partial t} = \eta_0(\frac{\partial \omega}{\partial r} + \lambda_2 \frac{\partial^2 \omega}{\partial t \partial r}), \tag{3.2.8}$$

$$\frac{1}{r}p'_{(\phi z)} + \lambda_1 \frac{1}{r}\frac{\partial p'_{(\phi z)}}{\partial t} = \eta_0(\frac{\partial \omega}{\partial z} + \lambda_2 \frac{\partial^2 \omega}{\partial t \partial z}), \tag{3.2.9}$$

$$\frac{p'_{(\phi\phi)}}{r^2} + \lambda_1(\frac{1}{r^2}\frac{\partial p'_{(\phi\phi)}}{\partial t} - \frac{2}{r}\frac{\partial \omega}{\partial r}p'_{(r\phi)} - \frac{2}{r}\frac{\partial \omega}{\partial z}p'_{(\phi z)}) = -2\eta_0\lambda_2[(\frac{\partial \omega}{\partial r})^2 + (\frac{\partial \omega}{\partial z})^2]. \tag{3.2.10}$$

Equations (3.2.5d), (3.2.8), (3.2.9), and (3.2.10) are to be associated with the boundary conditions

$$\omega(r, z, t) = \Omega(t) \text{ on the wall } f(r, z) = 0, \tag{3.2.11a}$$

$$p_{(\phi z)} = 0 \text{ ,i.e., } \frac{\partial \omega(r, z, t)}{\partial z} = 0, \text{ on the free surface } z = b, \tag{3.2.11b}$$

together with the understood condition that $\omega(r, z, t)$ is finite throughout the region of flow.

The motion under investigation is one in which the forcing agent is the oscillatory rotation of the well wall, a rotation of angular amplitude Ω_0 and of frequency $n/2\pi$. It is thus appropriate to look for a solution of the form

$$\omega(r, z, t) = \mathrm{Re}(\overline{\omega}(r, z)e^{int}), \tag{3.2.12}$$

the notation being that Re denotes the real part.

Inspection of equations (3.2.8), (3.2.9) and (3.2.10) suggests that the partial stresses $p'_{(r\phi)}, p'_{(\phi z)}$ can be written in the form

$$p'_{(r\phi)}(r, z, t) = \mathrm{Re}(\bar{p}'_{(r\phi)}(r, z)e^{int}),$$

$$p'_{(\phi z)}(r, z, t) = \mathrm{Re}(\bar{p}'_{(\phi z)}(r, z)e^{int}),$$

whilst $p'_{(\phi\phi)}$ can be written in the more complex form[22]

$$p'_{(\phi\phi)}(r,z,t) = \mathrm{Re}(\bar{p}'_{0(\phi\phi)}(r,z) + \bar{p}'_{2(\phi\phi)}(r,z)e^{2int}).$$

(It is observed that associated with a purely oscillatory motion the shear stresses $p'_{(r\phi)}, p'_{(\phi z)}$ are periodic with the same frequency as that of the forcing agent, but that the normal stress $p'_{(\phi\phi)}$ is not purely periodic but has a steady component as well as a periodic component with twice the frequency of the forcing agent.)

It is then not difficult to show that equations (3.2.8), (3.2.9) and (3.2.10) allow the solutions

$$p'_{(r\phi)}(r,z,t) = r\,\mathrm{Re}(\frac{\eta_0(1+in\lambda_2)}{1+in\lambda_1}\frac{\partial\overline{\omega}}{\partial r}e^{int}), \tag{3.2.13}$$

$$p'_{(\phi z)}(r,z,t) = r\,\mathrm{Re}(\frac{\eta_0(1+in\lambda_2)}{1+in\lambda_1}\frac{\partial\overline{\omega}}{\partial z}e^{int}), \tag{3.2.14}$$

$$\begin{aligned} p'_{(\phi\phi)}(r,z,t) &= r^2\,\mathrm{Re}\{\frac{\eta_0(\lambda_1-\lambda_2)}{1+in\lambda_1}(\frac{\partial\overline{\omega}}{\partial r}\frac{\partial\overline{\omega}^*}{\partial r}+\frac{\partial\overline{\omega}}{\partial z}\frac{\partial\overline{\omega}^*}{\partial z} \\ &\quad +\frac{1}{1+2in\lambda_1}[(\frac{\partial\overline{\omega}}{\partial r})^2+(\frac{\partial\overline{\omega}}{\partial z})^2]e^{2int})\}. \end{aligned} \tag{3.2.15}$$

Hence, on substituting these values of (3.2.13), (3.2.14) and (3.2.15) into equation (3.2.5d), it is found that the constrained, or *primary flow,* is governed by the equation

$$\frac{\partial^2\overline{\omega}}{\partial r^2}+\frac{3}{r}\frac{\partial\overline{\omega}}{\partial r}+\frac{\partial^2\overline{\omega}}{\partial z^2}+k^2\overline{\omega}=0, \tag{3.2.16}$$

where

$$k^2 = -in\rho(1+in\lambda_1)/\eta_0(1+in\lambda_2),$$

[22] It is observed that if C_1 and C_2 are any two complex numbers

$$\mathrm{Re}\,C_1\,\mathrm{Re}\,C_2 = \frac{1}{2}(\mathrm{Re}(C_1C_2)+\mathrm{Re}(C_1C_2^*)),$$

where the asterisk denotes complex conjugate.

and is to be associated with the boundary conditions

$$\overline{\omega}(r,z) = \Omega_0 \text{ on the wall } f(r,z) = 0, \tag{3.2.17a}$$

$$\frac{\partial\overline{\omega}(r,z)}{\partial z} = 0 \text{ on the free surface } z = b, \tag{3.2.17b}$$

together with the understood condition that $\overline{\omega}(r,z)$ is finite throughout the region of flow. Here it is observed that:

(i) the *primary flow* can be interpreted as that of a viscous fluid but of complex viscosity

$$\overline{\eta} = \eta' - i\frac{\mu'}{n},$$

where η' and μ', identified with

$$\eta' = \frac{\eta_0(1+n^2\lambda_1\lambda_2)}{(1+n^2\lambda_2^2)},$$

and

$$\mu' = \frac{\eta_0 n^2(\lambda_1-\lambda_2)}{(1+n^2\lambda_2^2)},$$

are known as the dynamic viscosity and dynamic rigidity, functions of the frequency $n/2\pi$ [23];

(ii) the Reynolds number is only a particular parameter of the flow and not a defining parameter, additional (dimensionless) parameters $\Lambda_1 = n\lambda_1$ and $\Lambda_2 = n\lambda_2$ arise from the elastic properties of the fluid.

II. Secondary Flow

To proceed with the investigation, it is supposed that at time $t = t_0$ the body-force vector $(F_{(r)}, F_{(\phi)}, F_{(z)})$, as defined by equations (3.2.5a-c), is suddenly removed,

[23] This representation is one of the popular ways of interpreting (linear) behaviour of elastico-viscous fluids, and several rheometers are available for the measurement of η' and μ'.

and, *within the mixture*[24], the velocity and stress components are represented as (ascending) power series of the parameter $t - t_0$, viz.

$$\omega = \omega^{(0)}(r,z,t_0) + \omega^{(1)}(r,z,t_0)(t-t_0) + \omega^{(2)}(r,z,t_0)(t-t_0)^2 + ..., \quad (3.2.18a)$$

$$\psi = \psi^{(0)}(r,z,t_0) + \psi^{(1)}(r,z,t_0)(t-t_0) + \psi^{(2)}(r,z,t_0)(t-t_0)^2 + ..., \quad (3.2.18b)$$

$$p'_{(ik)} = p'^{(0)}_{(ik)}(r,z,t_0) + p'^{(1)}_{(ik)}(r,z,t_0)(t-t_0) + p'^{(2)}_{(ik)}(r,z,t_0)(t-t_0)^2 + ... \quad (i,k = r,\phi,z). \quad (3.2.18c)$$

Here $\omega^{(0)}, \psi^{(0)}$ and $p'^{(0)}_{(ik)}$ denote the values of ω, ψ and $p'_{(ik)}$ prior to the release of the body-force field and so correspond to their values associated with the primary flow at time $t = t_0$. Substituting equations (3.2.18a-c) into the equations of motion (3.2.3a-c) and equating the coefficients independent of $(t - t_0)$, the following equations result

$$\rho\left(\frac{1}{r}\frac{\partial \psi^{(1)}}{\partial z} - r(\omega^{(0)})^2\right) = -\frac{\partial p^{(0)}}{\partial r} - \frac{p'^{(0)}_{(\phi\phi)}}{r}, \quad (3.2.19a)$$

$$\rho(r\omega^{(1)}) = \frac{\partial p'^{(0)}_{(r\phi)}}{\partial r} + \frac{\partial p'^{(0)}_{(\phi z)}}{\partial z} + \frac{2}{r}p'^{(0)}_{(r\phi)}, \quad (3.2.19b)$$

$$\rho\frac{1}{r}\frac{\partial \psi^{(1)}}{\partial r} = \frac{\partial p^{(0)}}{\partial z}, \quad (3.2.19c)$$

where $p^{(0)}(r,z,t_0)$ is an isotropic pressure. These equations are to be associated with the boundary conditions

$$\psi^{(1)}(r,z,t_0) = 0, \quad \omega^{(1)}(r,z,t_0) = \dot{\Omega}(t_0) \text{ on the wall } f(r,z) = 0, \quad (3.2.20a)$$

[24] There can be no discontinuity (either temporal or spatial) in the velocity of the mixture due to its inertia. In turn, there can be discontinuity neither in the rate-of-strain components nor in the stress components. At the boundary wall $f(r,z) = 0$, however, the possibility of a spatial discontinuity does arise. Such a discontinuity has to be interpreted in terms of the boundary conditions, requiring the boundary wall to be a streamline.

$$\psi^{(1)}(r,z,t_0) \;=\; 0, \quad \frac{\partial\omega^{(1)}(r,z,t_0)}{\partial z} = 0 \text{ on the free surface } z = b, \tag{3.2.20b}$$

together with the understood condition that $\psi^{(1)}(r,z,t_0)$ and $\omega^{(1)}(r,z,t_0)$ are finite throughout the region of flow.

Comparing equations (3.2.5d) and (3.2.11a,b) defining $\omega(r,z,t)$ with equations (3.2.19b) and (3.2.20a,b), it is seen that $\omega^{(1)}$ can be identified with $(\partial\omega/\partial t)_{t=t_0}$. Hence, equations (3.2.19b) and (3.2.20a,b) merely state that $\partial\omega/\partial t$ is continuous at $t = t_0$. One writes, therefore,

$$\omega^{(1)}(r,z,t_0) = \left(\frac{\partial\omega(r,z,t)}{\partial t}\right)_{t=t_0}.$$

The remaining two equations, viz.

$$\rho\left(\frac{1}{r}\frac{\partial\psi^{(1)}}{\partial z} - r\omega^2\right) \;=\; -\frac{\partial p^{(0)}}{\partial r} - \frac{p'^{(0)}_{(\phi\phi)}}{r}, \tag{3.2.21a}$$

$$\rho\frac{1}{r}\frac{\partial\psi^{(1)}}{\partial r} \;=\; \frac{\partial p^{(0)}}{\partial z}, \tag{3.2.21b}$$

together with the boundary conditions (3.2.20a,b), serve to define $\psi^{(1)}$ and $p^{(0)}$. Eliminating $p^{(0)}$ gives the equation

$$\frac{\partial^2\psi^{(1)}}{\partial r^2} - \frac{1}{r}\frac{\partial\psi^{(1)}}{\partial r} + \frac{\partial^2\psi^{(1)}}{\partial z^2} = \frac{\partial}{\partial z}\left(r^2\omega^2 - \frac{p'^{(0)}_{(\phi\phi)}}{\rho}\right). \tag{3.2.22}$$

Now, from equation (3.2.12) and (3.2.15),

$$\omega^2(r,z,t_0) = \frac{1}{2}\,\mathrm{Re}(\bar{\omega}\bar{\omega}^* + \bar{\omega}^2 e^{2int_0}),$$

and

$$\begin{aligned} p'^{(0)}_{(\phi\phi)}(r,z,t_0) \;=\; & \eta_0 r^2\,\mathrm{Re}\Big\{\frac{(1-in\lambda_1)(\lambda_1-\lambda_2)}{(1+n^2\lambda_1^2)}\Big(\frac{\partial\overline{\omega}}{\partial r}\frac{\partial\overline{\omega}^*}{\partial r} + \frac{\partial\overline{\omega}}{\partial z}\frac{\partial\overline{\omega}^*}{\partial z}\Big) \\ & + \frac{(\lambda_1-\lambda_2)}{(1+2in\lambda_1)(1+in\lambda_1)}\Big[\Big(\frac{\partial\overline{\omega}}{\partial r}\Big)^2 + \Big(\frac{\partial\overline{\omega}}{\partial z}\Big)^2\Big]e^{2int_0}\Big\}. \end{aligned}$$

This suggests that $\psi^{(1)}(r,z,t_0)$ has the form

$$\psi^{(1)}(r,z,t_0) = \mathrm{Re}(\psi_0(r,z) + \psi_2(r,z)e^{2int_0}), \tag{3.2.23}$$

i.e. a steady component as well as a t_0-periodic component with twice the frequency of the forcing agent. It has been pointed out (P. W. James, private communication) that the secondary streaming, as represented by the function $\psi^{(1)}$, can be expressed in a form that may have more direct physical appeal. Equation (3.2.23) may be rewritten in the form

$$\begin{aligned}\psi^{(1)} &= \mathrm{Re}(\psi_0(r,z) + \psi_2(r,z)e^{-2in(t-t_0)} \cdot e^{2int}) \\ &= \mathrm{Re}(\psi_0(r,z) + \psi_2(r,z)[1 + O(t-t_0)] \cdot e^{2int}).\end{aligned}$$

Thus, consistent with the approximations hitherto made,

$$\psi^{(1)} = \mathrm{Re}(\psi_0(r,z) + \psi_2(r,z)e^{2int}),$$

a form which can be identified with that given by Frater (1964), (1964) for the eventual, fully developed, secondary streaming motion in axially symmetric oscillatory flows when the amplitude of oscillation is small[25]. It is seen as a form which lends more credence to the description of $\psi_0(r,z)$ as the component which characterizes the *steady* secondary streaming.

Substituting (3.2.23) into (3.2.22) the following two equations result:

$$\frac{\partial^2\psi_0}{\partial r^2} - \frac{1}{r}\frac{\partial\psi_0}{\partial r} + \frac{\partial^2\psi_0}{\partial z^2} = \frac{r^2}{2}\frac{\partial}{\partial z}\{\bar{\omega}\bar{\omega}^* - 2K_1(\frac{\partial\overline{\omega}}{\partial r}\frac{\partial\overline{\omega}^*}{\partial r} + \frac{\partial\overline{\omega}}{\partial z}\frac{\partial\overline{\omega}^*}{\partial z})\}, \tag{3.2.24}$$

[25] It is well known that associated with an oscillatory flow in general there is a *steady* streaming motion, referred to as 'acoustic streaming' (see, for example, Riley (1967)).

$$\frac{\partial^2\psi_2}{\partial r^2} - \frac{1}{r}\frac{\partial\psi_2}{\partial r} + \frac{\partial^2\psi_2}{\partial z^2} = \frac{r^2}{2}\frac{\partial}{\partial z}\{\bar{\omega}^2 - 2K_2[(\frac{\partial\overline{\omega}}{\partial r})^2 + (\frac{\partial\overline{\omega}}{\partial z})^2]\}, \qquad (3.2.25)$$

where

$$K_1 = \frac{\eta_0(\lambda_1 - \lambda_2)}{\rho(1 + n^2\lambda_1^2)}, \qquad (3.2.26)$$

$$K_2 = \frac{\eta_0(\lambda_1 - \lambda_2)}{\rho(1 + 2in\lambda_1)(1 + in\lambda_1)}, \qquad (3.2.27)$$

and where the real part is understood. These equations are to be associated with boundary conditions

$$\psi_0(r,z) = 0, \quad \psi_2(r,z) = 0 \text{ on the wall } f(r,z) = 0, \qquad (3.2.28a)$$

$$\psi_0(r,z) = 0, \quad \psi_2(r,z) = 0 \text{ on the free surface } z = b, \qquad (3.2.28b)$$

together with the understood condition that $\psi_0(r,z)$ and $\psi_2(r,z)$ are finite throughout the region of flow.

The secondary streaming, as characterized by the function $\psi(r,z,t_0)$, is seen to be made up of a steady component and an oscillatory component with frequency twice that of the forcing agent. The steady component $\psi_0(r,z)$ - the average of the (secondary) flow over a single time cycle $2\pi/n$ - *even if weak,* leads (within an apparent oscillatory system) to extensive migration of fluid elements within the well. This unique type of convection or 'stirring' of the mixture associated with such steady streamings has especial significance within the present study in that it accelerates the translational rate process of the reagents within the well[26]. It is appropriate, therefore, that the next phase should include an investigation of the nature of the time-invariant streaming described by the function $\psi_0(r,z)$.

[26] As well, the steady streamings give rise to (steady) stresses at the boundary wall and these may be significant in the continual removal of loosely adhering reagents on the wall surface.

3.3 References

Frater, K. R.,"Flow of an elastico-viscous fluid between torsionally oscillating disks", 1964, *J. Fluid Mech.*, **19**, 175.

Frater, K. R.,"Secondary flow in an elastico-viscous fluid caused by rotational oscillations of sphere. Part 1", 1964, *J. Fluid Mech.*, **20**, 369.

Griffiths, D. F., Jones, D. T. and Walters, K.,"A flow reversal due to edge effects", 1969, *J. Fluid Mech.*, **36**, part 1, 161.

James, P. W., "Unsteady elastico-viscous flow in a curved pipe", 1975, *Rheol. Acta,* **14**, 679.

James, P. W., "A study of time-variant flows of elastico-viscous liquids", PhD Thesis, University of Wales, 1975.

Jones, J. R., "Non-Newtonian effects in axially symmetric oscillatory flows of some elastico-viscous liquids",1970, *Proc. Cambridge Philos. Soc.*, **68**, 731.

Jones, J. R., "A further note on axially symmetric flows of elastico-viscous liquids",1973, *Proc. Cambridge Philos. Soc.*, **73**, 239.

Lyne, W. H., "Unsteady flow in a curved pipe", 1970, *J. Fluid Mech.*, **45,** 13.

Riley, N., "Oscillatory viscous flows. Review and extension", 1967, *J. Inst. Maths Applies,* **3**, 419.

Zalosh, R. G. and Nelson, W. G., "Pulsating flow in a curved tube", 1973, *J. Fluid Mech.*, **59**, part 4, 693.

CHAPTER 4

ANALYSIS FOR A HEMISPHERICAL-SHAPED WELL

The equations governing the large scale motion of the fluid mixture within an axially symmetric well associated with the 'jiggle' mode are now formulated (Eqs. (3.2.16), (3.2.24)). It is the aim and purpose of the present chapter to seek their solutions when the well is supposed to be hemispherical in shape. Although the choice of geometry is intended, in the main, to facilitate the mathematical analysis, it is proper to stress that it is not all that wayward a description of the actual well configuration. The advantages that follow in the wake of this geometrical representation are considerable: *exact* analytical solutions, in simple closed forms, can be constructed for both primary and secondary flows, solutions which allow for a description of the motion within the well over the whole spectrum of values of the Reynolds number, from small to large.

4.1 Primary Flow

Within the cylindrical polar coordinate description r, ϕ, z ($r = 0$ representing the well axis), the primary flow is characterized by equation (3.2.16), viz.

$$\frac{\partial^2 \overline{\omega}}{\partial r^2} + \frac{3}{r}\frac{\partial \overline{\omega}}{\partial r} + \frac{\partial^2 \overline{\omega}}{\partial z^2} + k^2 \overline{\omega} = 0, \tag{4.1.1}$$

with associated boundary conditions

$$\overline{\omega}(r,z) = \Omega_0 \text{ on the wall } f(r,z) = 0, \tag{4.1.2a}$$

$$\frac{\partial \overline{\omega}(r,z)}{\partial z} = 0 \text{ on the free surface } z = b, \tag{4.1.2b}$$

together with the understood condition that $\overline{\omega}(r,z)$ is finite throughout the region of flow. Here

$$k^2 = -\frac{in\rho(1+in\lambda_1)}{\eta_0(1+in\lambda_2)}.$$

For a hemispherical well of radius a, it is more convenient to refer the motion to spherical polar coordinates R, θ, ϕ defined by

$$r = R\sin\theta, \quad \phi = \phi, \quad z = R\cos\theta. \tag{4.1.3}$$

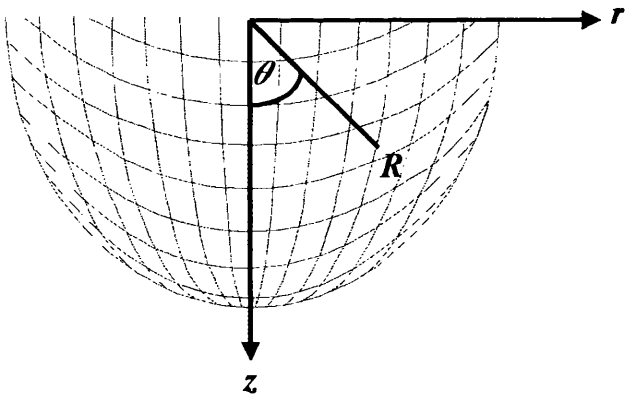

Fig. 4.1.1 Hemispherical-shaped well in (R, θ, ϕ) coordinates.

To proceed, it is first required to express the above equation for $\overline{\omega}$ in terms of the variables R, θ. It is a simple matter to do this by observing the operator relationships

$$\frac{\partial}{\partial r} \equiv \sin\theta\frac{\partial}{\partial R} + \frac{\cos\theta}{R}\frac{\partial}{\partial \theta}, \tag{4.1.4a}$$

$$\frac{\partial}{\partial z} \equiv \cos\theta\frac{\partial}{\partial R} - \frac{\sin\theta}{R}\frac{\partial}{\partial \theta}. \tag{4.1.4b}$$

However, there is some advantage in placing the transformation process within a wider context. Equation (4.1.1) can be rewritten in the form

$$\frac{\partial}{\partial r}(r^3\frac{\partial\overline{\omega}}{\partial r})+\frac{\partial}{\partial z}(r^3\frac{\partial\overline{\omega}}{\partial z})+k^2r^3\overline{\omega}=0. \tag{4.1.5}$$

Hence, on regarding the variables r, z as plane Cartesian coordinates, the equation for $\overline{\omega}$ may be represented in a wider sense by

$$\nabla\cdot(r^3\nabla\overline{\omega})+k^2r^3\overline{\omega}=0. \tag{4.1.6}$$

Thus, in a general transformation from supposedly Cartesians r, z to (plane) orthogonal curvilinear coordinates ξ_1, ξ_2 with vector line element $(h_1d\xi_1, h_2d\xi_2)$, the equation for $\overline{\omega}$ transforms into

$$\frac{1}{h_1h_2}[\frac{\partial}{\partial\xi_1}(r^3\frac{h_2}{h_1}\frac{\partial\overline{\omega}}{\partial\xi_1})+\frac{\partial}{\partial\xi_2}(r^3\frac{h_1}{h_2}\frac{\partial\overline{\omega}}{\partial\xi_2})]+k^2r^3\overline{\omega}=0, \tag{4.1.7}$$

where $r = r(\xi_1, \xi_2)$ is a prescribed function of ξ_1, ξ_2. The transformation $(r, z) \rightarrow (R, \theta)$, as defined by equation (4.1.3), is of the above class of transformations, i.e. one from supposedly Cartesians r, z to (plane) polar coordinates R, θ ($h_1 = 1$, $h_2 = R$, and $r = r(R, \theta) = R\sin\theta$). Thus, the equation for $\overline{\omega}(R, \theta)$ reduces to

$$\frac{\partial^2\bar{\omega}}{\partial R^2}+\frac{4}{R}\frac{\partial\bar{\omega}}{\partial R}+\frac{1}{R^2}\frac{\partial^2\bar{\omega}}{\partial\theta^2}+\frac{3\cot\theta}{R^2}\frac{\partial\bar{\omega}}{\partial\theta}+k^2\bar{\omega}=0, \tag{4.1.8}$$

and is to be associated with boundary conditions

$$\bar{\omega}=\Omega_0 \text{ on the wall } R=a, \tag{4.1.9a}$$

$$\frac{\partial\bar{\omega}}{\partial\theta}=0 \text{ on the free surface } \theta=\frac{\pi}{2}^{27}. \tag{4.1.9b}$$

[27] Here b is supposed zero, i.e. the origin is taken in the free surface.

Symmetry, and the nature of the boundary conditions, suggest one looks for a solution of the form $\bar{\omega} = \bar{\omega}(R)$, a function of the radial coordinate R only. In this event, equation (4.1.7) takes on the simple form

$$\frac{d^2\bar{\omega}}{dR^2} + \frac{4}{R}\frac{d\bar{\omega}}{dR} + k^2\bar{\omega} = 0, \tag{4.1.10}$$

and is to be associated with the *single* boundary condition

$$\bar{\omega} = \Omega_0 \text{ on the wall } R = a. \tag{4.1.11}$$

(As well, it is understood that $\bar{\omega}$ is required to be finite throughout the region of flow.)

Equation (4.1.10) is of the class

$$x^2y'' + \alpha xy' + \beta^2x^2y = 0,$$

which, on using the transformation $y = x^{(1-\alpha)/2}g(x)$, reduces to the equation

$$x^2g'' + xg' + (\beta^2x^2 - \frac{(\alpha-1)^2}{4})g = 0,$$

and is recognized as a Bessel equation. Hence, on writing

$$\bar{\omega}(R) = R^{-3/2}G(R), \tag{4.1.12}$$

the following equation for $G(R)$ results:

$$R^2G'' + RG' + (k^2R^2 - \frac{9}{4})G = 0. \tag{4.1.13}$$

Its general solution is expressible in the form

$$G(R) = AJ_{3/2}(kR) + BJ_{-3/2}(kR), \tag{4.1.14}$$

where $J_{3/2}(kR)$ and $J_{-3/2}(kR)$ are Bessel functions of the first kind of orders $3/2$ and $-3/2$ respectively, and A and B are arbitrary constants. Thus the general solution of (4.1.10) is

$$\bar{\omega}(R) = R^{-3/2}(AJ_{3/2}(kR) + BJ_{-3/2}(kR)).$$

Bessel functions of order half an odd integer are expressible as finite combinations of elementary functions; in particular

$$J_{3/2}(kR) = \sqrt{\frac{2}{\pi kR}}\left(\frac{\sin kR}{kR} - \cos kR\right), \tag{4.1.15}$$

$$J_{-3/2}(kR) = \sqrt{\frac{2}{\pi kR}}\left(\frac{\cos kR}{kR} + \sin kR\right). \tag{4.1.16}$$

It is seen that $R^{-\frac{3}{2}}J_{-3/2}(kR)$ is unbounded at $R = 0$, and hence, to ensure finiteness of the primary flow everywhere within the well, it is required that $B = 0$. The condition at the wall surface, viz. $\bar{\omega} = \Omega_0$ on $R = a$, requires $A = \Omega_0\sqrt{a^3}/J_{3/2}(ka)$. Thus, finally, the appropriate solution for the primary flow is

$$\bar{\omega}(R) = \Omega_0\left(\frac{a}{R}\right)^{3/2}\frac{J_{3/2}(kR)}{J_{3/2}(ka)}, \tag{4.1.17}$$

which, in turn, gives for the velocity field

$$v_{(\phi)} = \Omega_0 R\sin\theta\,\mathrm{Re}([(\frac{a}{R})^{3/2}\frac{J_{3/2}(kR)}{J_{3/2}(ka)} - 1]e^{int}). \tag{4.1.18}$$

4.1.1 Numerical Results

An exact analytical solution (in simple closed form) has been constructed for the primary flow and it is a simple matter to illustrate how this flow varies with the Reynolds-type number $R_a = \sqrt{(n\rho a^2/\eta_0)}$. However, it is interesting first to look

analytically at this behaviour in two extreme cases: (i) when R_a is small (i.e. when the angular frequency n (or $|k|$) of the forcing agent is small), and (ii) when R_a is large (i.e. when the angular frequency n (or $|k|$) of the forcing agent is large).

I. Small Values of n

In this case $|kR|$ is small throughout the region of flow $0 \leq R \leq a$, i.e. $|kR| << 1$. In such a slowly oscillating scheme it is convenient to express the Bessel function $J_{3/2}(kR)$ as an ascending power series in its (small) argument kR. On using the finite expression (4.1.15) for $J_{3/2}(kR)$, it is straightforward to obtain the series representation

$$J_{3/2}(kR) = \sqrt{\frac{2}{\pi}}\left(\frac{1}{3}(kR)^{3/2} - \frac{1}{30}(kR)^{7/2} + O((kR)^{11/2})\right), \tag{4.1.19}$$

which, in turn, gives

$$\overline{\omega}(R) = \Omega_0[1 + \frac{1}{10}k^2(a^2 - R^2) + O(k^4)]. \tag{4.1.20}$$

On neglecting terms $O(k^4)$, it is seen that the profile $|\overline{\omega}(R) - \Omega_0|$ is parabolic, varying from zero on the boundary wall to a maximum $\Omega_0 |k|^2 a^2/10$ at the centre ($R = 0$) of the well. It is found that the profiles flatten out, i.e. $|\overline{\omega}(R) - \Omega_0|$ becomes smaller, as the Reynolds-type number R_a becomes smaller, whilst the effect of elasticity is to delay, *somewhat strikingly*, this feature. Further, it is found that $\overline{\omega}(R) - \Omega_0 \to 0$ as $k \to 0$ (i.e. as $n \to 0$), i.e. for very small values of the angular frequency n the fluid moves as if rigid with angular velocity which, at any instant, matches that of the well boundary, a motion exhibiting no secondary flow effects. These general comments, valid for sufficiently slowly varying regimes, are reflected in the *exact* flow diagrams illustrated in Figs. 4.2.1a,b.

II. Large Values of n

For this regime, it is necessary to look separately at two regions, that remote from the centre ($R = 0$), and that near the centre.

Region remote from the centre:

In this region both $|ka|$ and $|kR|$ are large, i.e. $|ka|\,,\ |kR| \gg 1$. Now

$$\begin{aligned}\frac{\sin kR}{kR} - \cos kR &= \frac{e^{ikR} - e^{-ikR}}{2ikR} - \frac{e^{ikR} + e^{-ikR}}{2} \\ &= \frac{1}{2}[(\frac{1}{ikR} - 1)e^{ikR} + (\frac{-1}{ikR} - 1)e^{-ikR}] \\ &= \frac{1}{2}[(\frac{1}{i\,|kR|\,e^{-i\chi}} - 1)e^{i|kR|e^{-i\chi}} - (\frac{1}{i\,|kR|\,e^{-i\chi}} + 1)e^{-i|kR|e^{-i\chi}}].\end{aligned}$$

Here $k = |k|\,e^{-i\chi}$, where

$$|k| = \sqrt{\frac{n\rho}{\eta_0}}\left(\frac{1 + n^2\lambda_1^2}{1 + n^2\lambda_2^2}\right)^{1/4}, \quad \chi = \frac{\pi}{4} - \frac{1}{2}(\tan^{-1} n\lambda_1 - \tan^{-1} n\lambda_2).$$

Again as $e^{i|kR|e^{-i\chi}} = e^{|kR|(\sin\chi + i\cos\chi)}$, $e^{-i|kR|e^{-i\chi}} = e^{-|kR|(\sin\chi + i\cos\chi)}$ and, on observing that $|kR| \gg 1$, the second term is seen to be negligibly small compared with the first. Thus

$$\frac{\sin kR}{kR} - \cos kR \simeq -\frac{1}{2}e^{i|kR|(\cos\chi - i\sin\chi)}.$$

Similarly

$$\frac{\sin ka}{ka} - \cos ka \simeq -\frac{1}{2}e^{i|ka|(\cos\chi - i\sin\chi)}.$$

Hence, $\bar{\omega}(R)$ may written

$$\bar{\omega}(R) \simeq \Omega_0(\frac{a}{R})^2 e^{-i(a-R)|k|(\cos\chi - i\sin\chi)}, \tag{4.1.21}$$

and, in turn, gives for the velocity field

$$v_{(\phi)} \simeq \Omega_0 R\sin\theta\,\mathrm{Re}\{[(\frac{a}{R})^2 e^{-i(a-R)|k|(\cos\chi - i\sin\chi)} - 1]e^{int}\}. \tag{4.1.22}$$

Now when n (or $|k|$) is large the exponential term $e^{-i(a-R)|k|(\cos\chi - i\sin\chi)}$ in the above expression is appreciable only when $a - R$ is small, i.e. in a region immediately adjacent to the wall, i.e. in a layer near the wall whose thickness is $O[(n\rho/\eta_0)^{-1/2}]$, i.e. $O(aR_a^{-1})$. Outside this layer the above exponential factor is negligible and, effectively, $\varpi \simeq 0$ or, equally, $v_{(\phi)} \simeq \Omega_0 R\sin\phi\,\mathrm{Re}[e^{i(nt-\pi)}]$, independent of the rheological properties of the mixture. This represents a rigid body (oscillatory) rotation with angular amplitude Ω_0 and frequency $n/2\pi$, but of phase π behind that of the boundary wall.

Region near the centre:

In this region $|ka| \gg 1$ but $|kR| \ll 1$. Now

$$\frac{\sin kR}{kR} - \cos kR \simeq \frac{1}{3}(kR)^2,$$

and

$$\frac{\sin ka}{ka} - \cos ka \simeq -\frac{1}{2}e^{ika}.$$

Thus

$$\begin{aligned}\bar{\omega}(R) &\simeq -\frac{2}{3}\Omega_0 a^2 k^2 e^{-ika} \\ &\simeq -\frac{2}{3}\Omega_0 a^2 k^2 e^{-i|ka|(\cos\chi - i\sin\chi)},\end{aligned}$$

i.e. $\varpi(R) = 0$ on neglect of exponentially small terms, and so,

$$v_{(\phi)} \simeq \Omega_0 R\sin\theta\,\mathrm{Re}(-e^{int}) = \Omega_0 R\sin\phi\,\mathrm{Re}[e^{i(nt-\pi)}]. \qquad (4.1.23)$$

It is seen that in a region sufficiently near the centre ($R = 0$), the fluid moves as if rigid with angular amplitude Ω_0 and frequency $n/2\pi$ but with phase π behind that of

the boundary wall, exactly as that predicted above for the flow outside the boundary layer.

One concludes that for large values of n(or of R_a) the primary flow varies rapidly in the region immediately adjacent to the well wall, attaining there a high peak, but elsewhere moves as if rigid with angular amplitude and frequency that of the forcing agent but of phase π behind it. The effects of elasticity are to increase, *substantially*, the high peak value of the flow close to the boundary wall, while having no great effect elsewhere, and to decrease somewhat the thickness of the boundary region in which flow changes rapidly.

For illustration purposes, the *exact* profiles of the square magnitude of the 'angular' velocity $|\overline{\omega}(R)/\Omega_0 - 1|^2$, i.e. of $\left|v_{(\phi)}/\Omega_0 R\sin\theta\right|^2$, for various values of Reynolds-type number ($R_a = \sqrt{(n\rho a^2/\eta_0)}$)[28], and for various values of the elastic parameters $n\lambda_1$, $n\lambda_2$, are exhibited in Figs. 4.2.1c-f. Here 'distance from the wall' is to be interpreted as the dimensionless measure $(a - R)/a$.

[28] Rosenblat (1960) has shown, in case of viscous liquids, that, within a different context, the above approximations to the primary flow are valid provided that $(n\rho a^2/\eta_0) < 10$ (for small values of n) and $(n\rho a^2/\eta_0) > 20$ (for large values of n).

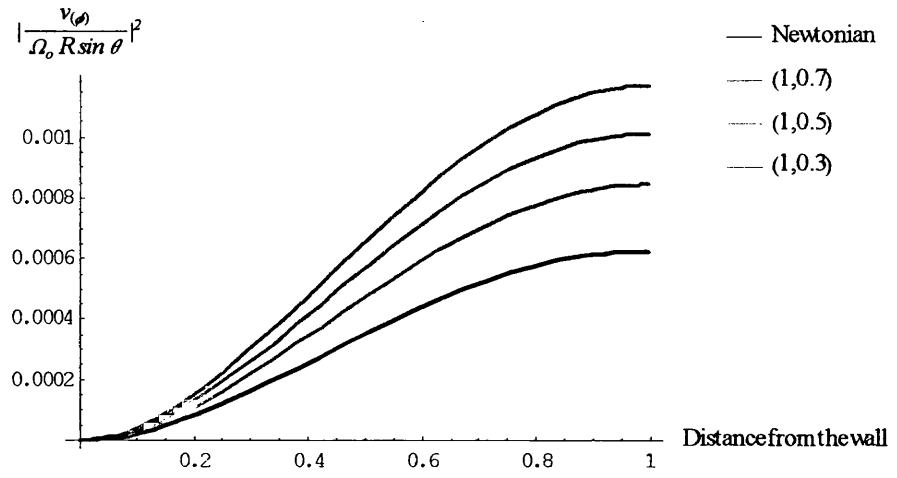

Fig. 4.2.1a Primary flow profiles for various values of the elastic parameters $(n\lambda_1, n\lambda_2)$ when $R_a = 0.5$.

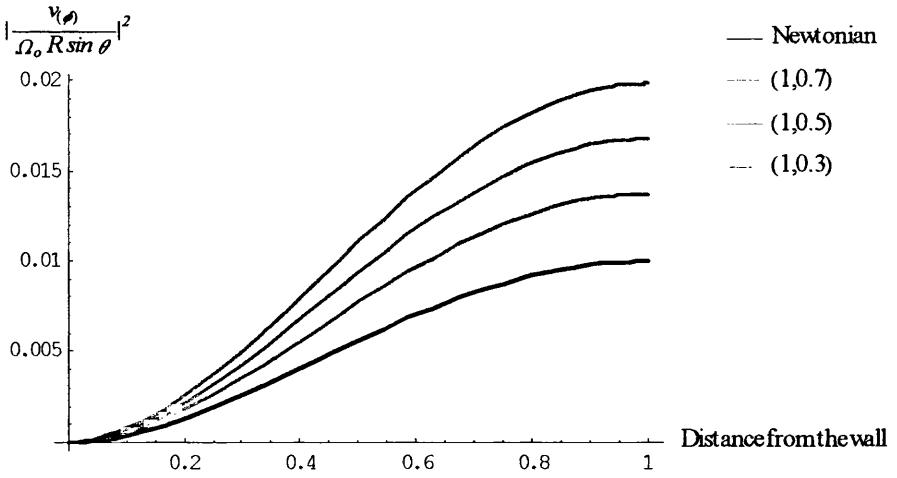

Fig. 4.2.1b Primary flow profiles for various values of the elastic parameters $(n\lambda_1, n\lambda_2)$ when $R_a = 1$.

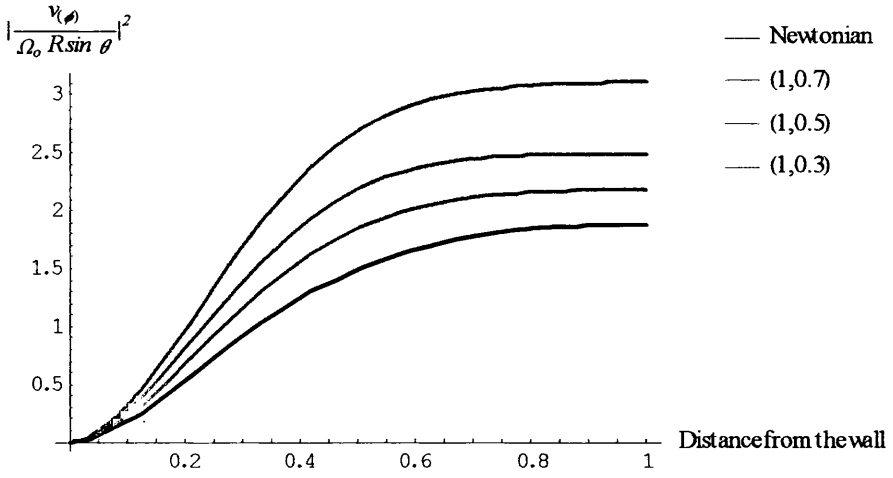

Fig. 4.2.1c Primary flow profiles for various values of the elastic parameters $(n\lambda_1, n\lambda_2)$ when $R_a = 6$.

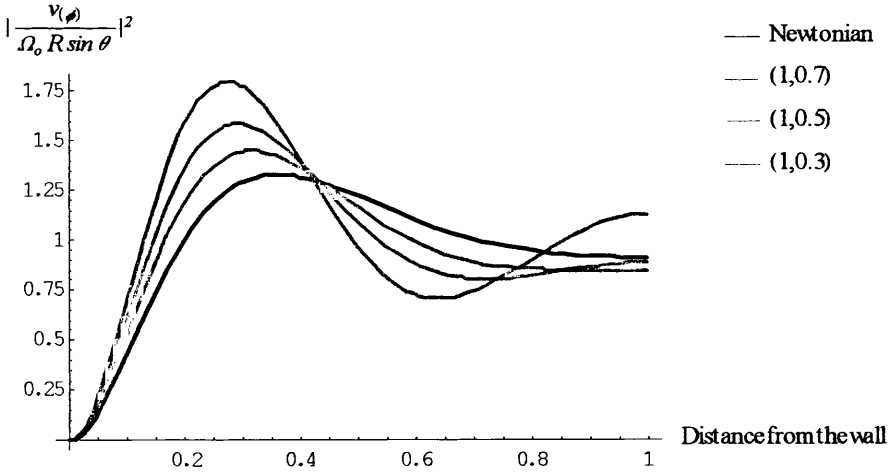

Fig. 4.2.1d Primary flow profiles for various values of the elastic parameters $(n\lambda_1, n\lambda_2)$ when $R_a = 8$.

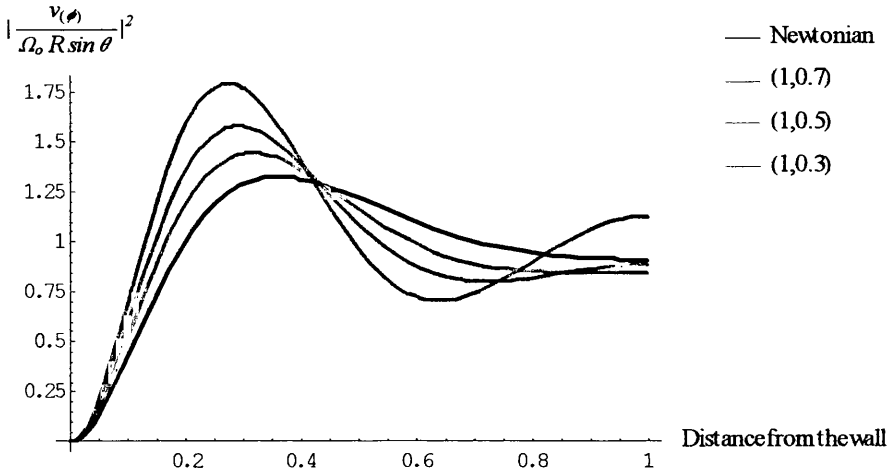

Fig. 4.2.1e Primary flow profiles for various values of the elastic parameters $(n\lambda_1, n\lambda_2)$ when $R_a = 10$.

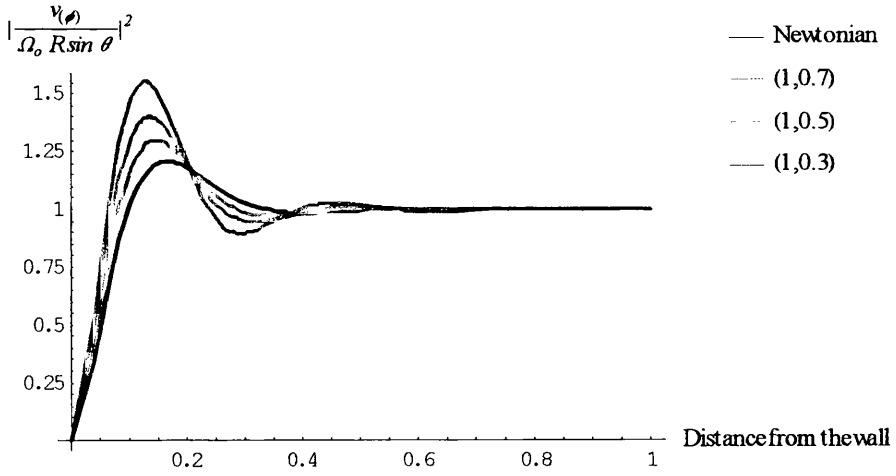

Fig. 4.2.1f Primary flow profiles for various values of the elastic parameters $(n\lambda_1, n\lambda_2)$ when $R_a = 20$.

4.2 Secondary Flow

Within the cylindrical polar description r, ϕ, z, the steady streaming flow as characterized by the stream function $\psi_0(r,z)$ is defined by equation (3.2.24), viz.

$$\frac{\partial^2\psi_0}{\partial r^2} - \frac{1}{r}\frac{\partial\psi_0}{\partial r} + \frac{\partial^2\psi_0}{\partial z^2} = \frac{r^2}{2}\frac{\partial}{\partial z}\{\bar{\omega}\bar{\omega}^* - 2K_1(\frac{\partial\bar{\omega}}{\partial r}\frac{\partial\bar{\omega}^*}{\partial r} + \frac{\partial\bar{\omega}}{\partial z}\frac{\partial\bar{\omega}^*}{\partial z})\}, \qquad (4.2.1)$$

and is associated with the boundary conditions

$$\psi_0(r,z) = 0 \text{ on the wall } f(r,z) = 0, \qquad (4.2.2a)$$

$$\psi_0(r,z) = 0 \text{ on the free surface } z = 0, \qquad (4.2.2b)$$

together with the understood condition that $\psi_0(r,z)$ is finite throughout the region of flow. Here K_1 is the purely elastic parameter $\eta_0(\lambda_1 - \lambda_2)/\rho(1 + n^2\lambda_1^2)$.

The differential equation for $\psi_0(r,z)$ can, in much the same way as that for the primary flow $\bar{\omega}(r,z)$, be represented within a somewhat wider domain. Equation (4.2.1) may be rewritten in the form

$$\frac{\partial}{\partial r}(\frac{1}{r}\frac{\partial\psi_0}{\partial r}) + \frac{\partial}{\partial z}(\frac{1}{r}\frac{\partial\psi_0}{\partial z}) = \frac{1}{2}r\frac{\partial}{\partial z}\{\bar{\omega}\bar{\omega}^* - 2K_1(\frac{\partial\bar{\omega}}{\partial r}\frac{\partial\bar{\omega}^*}{\partial r} + \frac{\partial\bar{\omega}}{\partial z}\frac{\partial\bar{\omega}^*}{\partial z})\}, \qquad (4.2.3)$$

which, on regarding r, z as plane Cartesian coordinates, may be identified as the equation

$$\nabla\cdot(\frac{1}{r}\nabla\psi_0) = \frac{1}{2}r\frac{\partial}{\partial z}\{|\bar{\omega}|^2 - 2K_1|\nabla\bar{\omega}|^2\}. \qquad (4.2.4)$$

Thus, in a transformation $(r,z) \to (\xi_1, \xi_2)$, a transformation from supposedly Cartesians r, z to (plane) orthogonal curvilinear coordinates ξ_1, ξ_2, equation (4.2.4) transforms into

$$\begin{aligned} &\frac{1}{h_1h_2}[\frac{\partial}{\partial\xi_1}(\frac{h_2}{rh_1}\frac{\partial\psi_0}{\partial\xi_1}) + \frac{\partial}{\partial\xi_2}(\frac{h_1}{rh_2}\frac{\partial\psi_0}{\partial\xi_2})] \\ = &\frac{1}{2}r(\frac{\partial\xi_1}{\partial z}\frac{\partial}{\partial\xi_1} + \frac{\partial\xi_2}{\partial z}\frac{\partial}{\partial\xi_2})\{\bar{\omega}\bar{\omega}^* - 2K_1[\frac{1}{h_1^2}\frac{\partial\bar{\omega}}{\partial\xi_1}\frac{\partial\bar{\omega}^*}{\partial\xi_1} + \frac{1}{h_2^2}\frac{\partial\bar{\omega}}{\partial\xi_2}\frac{\partial\bar{\omega}^*}{\partial\xi_2}]\}, \end{aligned} \qquad (4.2.5)$$

where $r = r(\xi_1, \xi_2)$. Thus under the transformation $(r, z) \rightarrow (R, \theta)$, as defined by equation (4.1.3), and on noting that $\bar{\omega} = \bar{\omega}(R)$, the equation for the steady streaming flow reduces to

$$\frac{\partial^2 \psi_0}{\partial R^2} - \frac{\cot\theta}{R^2}\frac{\partial \psi_0}{\partial \theta} + \frac{1}{R^2}\frac{\partial^2 \psi_0}{\partial \theta^2} = \frac{R^2}{2}\frac{d}{dR}(\bar{\omega}\bar{\omega}^* - 2K_1 \frac{d\bar{\omega}}{dR}\frac{d\bar{\omega}^*}{dR}) \sin^2\theta \cos\theta, \quad (4.2.6)$$

and is to be associated with boundary conditions

$$\psi_0(R, \theta) = 0 \text{ on the wall } R = a, \quad (4.2.7a)$$

$$\psi_0(R, \theta) = 0 \text{ on the free surface } \theta = \frac{\pi}{2}. \quad (4.2.7b)$$

Now, from (4.1.17),

$$\bar{\omega}(R) = \Omega_0 \left(\frac{a}{R}\right)^{3/2} \frac{J_{3/2}(kR)}{J_{3/2}(ka)}, \quad (4.2.8)$$

and so it follows that

$$\bar{\omega}(R)\bar{\omega}^*(R) = \Omega_0^2 \left(\frac{a}{R}\right)^3 \frac{J_{3/2}(kR)}{J_{3/2}(ka)} \frac{J_{3/2}(k^*R)}{J_{3/2}(k^*a)}, \quad (4.2.9)$$

and

$$\frac{d\bar{\omega}}{dR}\frac{d\bar{\omega}^*}{dR} = \Omega_0^2 |k|^2 \left(\frac{a}{R}\right)^3 \frac{J_{5/2}(kR)}{J_{3/2}(ka)} \frac{J_{5/2}(k^*R)}{J_{3/2}(k^*a)}. \quad (4.2.10)$$

Here, one has made use of the identity

$$\frac{d}{dx}(x^{-3/2} J_{3/2}(x)) = -x^{-3/2} J_{5/2}(x),$$

it being useful to note the expansion

$$J_{5/2}(kR) = \sqrt{\frac{2}{\pi kR}} \left((\frac{3}{k^2R^2} - 1) \sin kR - \frac{3}{kR} \cos kR \right). \quad (4.2.11)$$

On writing

$$G(R) = \bar{\omega}\bar{\omega}^* - 2K_1 \frac{d\bar{\omega}}{dR}\frac{d\bar{\omega}^*}{dR}, \quad (4.2.12)$$

equation (4.2.6) reduces to

$$\frac{\partial^2\psi_0}{\partial R^2} - \frac{\cot\theta}{R^2}\frac{\partial\psi_0}{\partial\theta} + \frac{1}{R^2}\frac{\partial^2\psi_0}{\partial\theta^2} = \frac{R^2}{2}G'(R)\sin^2\theta\cos\theta. \tag{4.2.13}$$

The form of this equation suggests that ψ_0 may be written in the form

$$\psi_0(R,\theta) = F(R)\sin^2\theta\cos\theta, \tag{4.2.14}$$

which on substitution into equation (4.2.13) results in the following equation for $F(R)$:

$$(F'' - \frac{6}{R^2}F) = \frac{R^2}{2}G'(R). \tag{4.2.15}$$

This equation is to be integrated subject to the boundary condition

$$F(R) = 0 \text{ on } R = a, \tag{4.2.16}$$

together with the constraint that $F(R)$ be finite in the region of flow $0 < R < a$, $0 < \theta < \pi/2$. One observes that the associated homogeneous differential equation of (4.2.15) has the two linearly independent solutions R^3, R^{-2}, and so it is a simple matter to use the method of variation of parameters to construct the general solution of the non-homogeneous equation. The result is

$$F(R) = v_1(R)R^3 + v_2(R)R^{-2},$$

where

$$v_1(R) = A + \frac{1}{10}\int^R G'(\xi)d\xi, \quad v_2(R) = B - \frac{1}{10}\int^R \xi^5 G'(\xi)d\xi.$$

A and B being arbitrary constants. By rearrangement

$$F(R) = AR^3 + BR^{-2} + \frac{1}{2}R^{-2}\int^R \xi^4 G(\xi)d\xi. \tag{4.2.17}$$

Now

$$\int R^4 G(R)dR = \frac{\Omega_0^2 a^4}{\left|\frac{\sin ka}{ka} - \cos ka\right|^2}\left(\int M(R)dR - 2\left|k\right|^2 K_1 \int N(R)dR\right), \quad (4.2.18)$$

where

$$M(R) = \left(\frac{\sin kR}{kR} - \cos kR\right)\left(\frac{\sin k^* R}{k^* R} - \cos k^* R\right),$$

and

$$\begin{aligned} N(R) &= ([1 - \frac{3}{k^2R^2}]\sin kR + \frac{3}{kR}\cos kR)([1 - \frac{3}{(k^*R)^2}]\sin k^*R \\ &\quad + \frac{3}{k^*R}\cos k^*R). \end{aligned}$$

By repeated integration by parts, it is found that

$$\int^R M(R)dR = \frac{-\sin kR \sin k^*R}{kk^*R} + \frac{\sin(k+k^*)R}{2(k+k^*)} + \frac{\sin(k-k^*)R}{2(k-k^*)}, \quad (4.2.19)$$

$$\begin{aligned} \int^R N(R)dR &= \frac{1}{2}\frac{\sin(k-k^*)R}{(k-k^*)} - \frac{1}{2}\frac{\sin(k+k^*)R}{(k+k^*)} - \frac{3\cos kR\cos k^*R}{kk^*R} \\ &\quad + \frac{3\sin kR\cos k^*R}{k^2k^*R^2} + \frac{3\cos kR\sin k^*R}{k(k^*)^2R^2} - \frac{3\sin kR\sin k^*R}{(kk^*)^2R^3}. \end{aligned} \quad (4.2.20)$$

Inspection shows that finiteness of $F(R)$ within the region of flow requires $B = 0$, and the boundary condition (4.2.16) gives the appropriate value of A. Finally, one obtains the solution

$$
\begin{aligned}
F(R) \;=\; & \frac{\Omega_0^2}{2\left|\frac{\sin ka}{ka}-\cos ka\right|^2}\{\frac{a^4}{R^2}(\frac{-\sin kR\sin k^*R}{|k|^2R}+\frac{1}{2}\frac{\sin(k+k^*)R}{(k+k^*)} \\
& +\frac{1}{2}\frac{\sin(k-k^*)R}{(k-k^*)})-\frac{R^3}{a}(\frac{-\sin ka\sin k^*a}{|k|^2a}+\frac{1}{2}\frac{\sin(k+k^*)a}{(k+k^*)} \\
& +\frac{1}{2}\frac{\sin(k-k^*)a}{(k-k^*)})-2|k|^2K_1[\frac{a^4}{R^2}(\frac{1}{2}\frac{\sin(k-k^*)R}{(k-k^*)}-\frac{1}{2}\frac{\sin(k+k^*)R}{(k+k^*)} \\
& -\frac{3\cos kR\cos k^*R}{kk^*R}+\frac{3\sin kR\cos k^*R}{k^2k^*R^2}+\frac{3\cos kR\sin k^*R}{k(k^*)^2R^2} \\
& -\frac{3\sin kR\sin k^*R}{(kk^*)^2R^3})-\frac{R^3}{a}(\frac{1}{2}\frac{\sin(k-k^*)a}{(k-k^*)}-\frac{1}{2}\frac{\sin(k+k^*)a}{(k+k^*)} \\
& -\frac{3\cos ka\cos k^*a}{kk^*a}+\frac{3\sin ka\cos k^*a}{k^2k^*a^2}+\frac{3\cos ka\sin k^*a}{k(k^*)^2a^2} \\
& -\frac{3\sin ka\sin k^*a}{(kk^*)^2a^3})]\}. \qquad (4.2.21)
\end{aligned}
$$

The associated *steady* velocity field is defined by

$$v_{(R)}^{(1)}=-\frac{1}{R^2\sin\theta}\frac{\partial\psi_0}{\partial\theta}=\frac{1}{R^2}F(R)(3\sin^2\theta-2), \qquad (4.2.22a)$$

$$v_{(\theta)}^{(1)}=\frac{1}{R\sin\theta}\frac{\partial\psi_0}{\partial R}=\frac{1}{R}F'(R)\sin\theta\cos\theta, \qquad (4.2.22b)$$

It is thus seen that the initial acceleration vector has a non-zero component tangential to the boundary wall $R=a$.

4.2.1 Numerical Results

Secondary *steady* streaming flows, as characterized by $\psi_0(R,\theta)$ above, are associated with oscillatory flow but not with steady flow. It is relevant within our study to look closely at the behaviour of $\psi_0(R,\theta)$ with the Reynolds-type number R_a and with the parameters λ_1,λ_2 characterizing the elasticity of the fluid. Although the expression for $\psi_0(R,\theta)$ is in the form of a finite combination of elementary functions, it is still somewhat complicated in mathematical form. Nevertheless, it is possible to

make some general deductions about the nature of the secondary flow in two special cases: (i) when the frequency n of oscillation is small, and (ii) when the frequency n of oscillation is large.

Before one turns to look at these two special regimes, it may be appropriate to ascertain the nature of the secondary flow when the mixture is supposed Newtonian, in which case the expression for $\psi_0(R,\theta)$ reduces to

$$\begin{aligned}\psi_0(R,\theta) &= \frac{\Omega_0^2}{2\left|\frac{\sin ka}{ka}-\cos ka\right|^2}\{\frac{a^4}{R^2}(\frac{-\sin kR\sin k^*R}{|k|^2R}+\frac{1}{2}\frac{\sin(k+k^*)R}{(k+k^*)}\\ &+\frac{1}{2}\frac{\sin(k-k^*)R}{(k-k^*)})-\frac{R^3}{a}(\frac{-\sin ka\sin k^*a}{|k|^2a}+\frac{1}{2}\frac{\sin(k+k^*)a}{(k+k^*)}\\ &+\frac{1}{2}\frac{\sin(k-k^*)a}{(k-k^*)})\}\sin^2\theta\cos\theta. \qquad (4.2.23)\end{aligned}$$

Although this expression for $\psi_0(R,\theta)$ is much simpler in mathematical form than that represented by (4.2.14) and (4.2.21), it is not sufficiently simple to allow one to make a broad analytical comment on the flow structure. However, its numerical evaluation over a wide range of values of the Reynolds-type number R_a shows that the flow is little changed by variation of frequency, fluid being *always* thrown outwards near the boundary wall and drawn inwards near the well axis, i.e. a flow much as expected by centrifugal effects. The numerical findings are exhibited in Figs 4.2.1a-d.

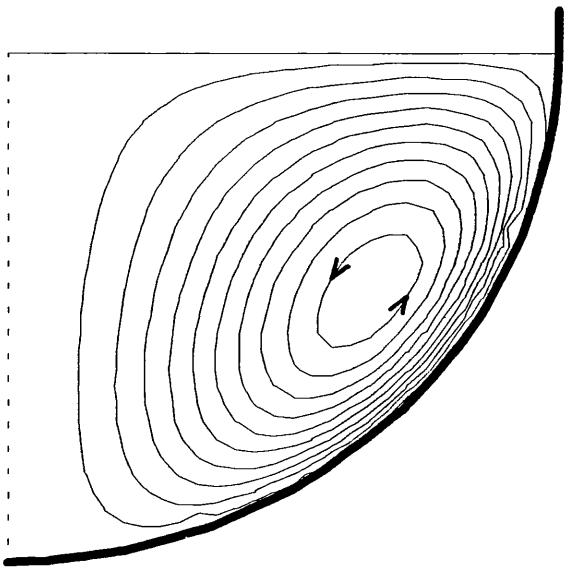

Fig. 4.2.1a Secondary (steady) streaming $\psi_0(R,\theta) = \textit{constant}$ for a Newtonian fluid when $R_a = 1$.

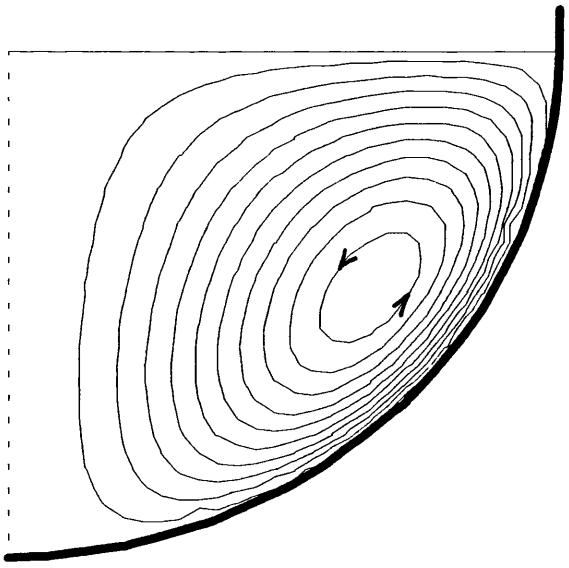

Fig. 4.2.1b Secondary (steady) streaming $\psi_0(R,\theta) = \textit{constant}$ for a Newtonian fluid when $R_a = 4$.

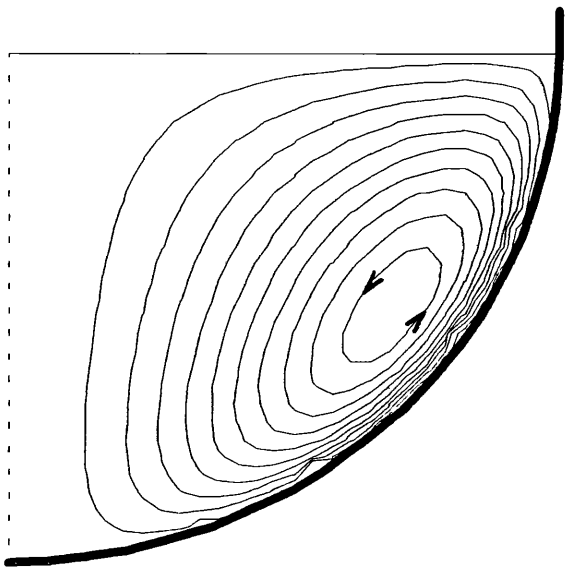

Fig. 4.2.1c Secondary (steady) streaming $\psi_0(R,\theta) = \textit{constant}$ for a Newtonian fluid when $R_a = 10$.

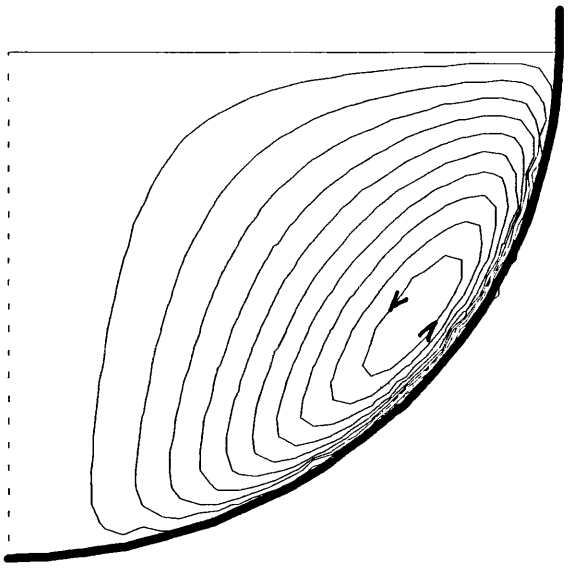

Fig. 4.2.1d Secondary (steady) streaming $\psi_0(R,\theta) = \textit{constant}$ for a Newtonian fluid when $R_a = 20$.

One now turns to look at the two special cases remarked on above.

I. Small Values of n

For small values of n, i.e. when $|kR|$ and $|ka|$ are both small, it is convenient to express the trigonometric functions in the *exact* expression for $\psi_0(R,\theta)$ in ascending powers of their (small) arguments. After long and tedious algebraic manoeuvers, it is found that

$$\psi_0(R,\theta) \simeq \Omega_0^2 |k|^4 R^3(a^2-R^2)[-\frac{1}{6300}(a^2+R^2)+\frac{1}{50}\Lambda(1-\frac{\lambda_2}{\lambda_1})a^2]\sin^2\theta\cos\theta, \tag{4.2.24}$$

where Λ is the dimensionless parameter $\eta_0\lambda_1/(\rho a^2)$. This result shows that $\psi_0(R,\theta) = O(n^2)$. Thus for small values of the frequency $n/2\pi$ the secondary (steady) streaming flow is a very weak affair. However, it varies strikingly with elasticity. When $\lambda_1 = \lambda_2$, corresponding to a Newtonian mixture, the flow is seen to be dominated by centrifugal actions, fluid being thrown outwards near the boundary wall ($R = a$) and drawn inwards along the axis of rotation ($\theta = 0$) consistent with the numerical illustration in Figs. 4.2.1a-d. However, when $\lambda_1 > \lambda_2 \geq 0$, it is seen that non-Newtonian actions counteract, and may even dominate, centrifugal actions. The indication is that *low* (critical) values of the frequency $n/2\pi$ exist for which non-Newtonian actions can overwhelm centrifugal actions, and in the region of flow within the well in which this is the case the direction of the flow would be spectacularly reversed[29]. Such effects are somewhat surprising, but are indeed reflected in

[29] It is seen from formula (4.2.24) that the ratio of Newtonian actions to non-Newtonian actions decreases as R decreases, i.e. as one approaches the centre of the well. This shows that as elasticity increases flow reversal is manifest first in the interior as is indeed shown in the exact streamline patterns exhibited in Fig. 4.2.3b.

the *exact* streamline projections $\psi_0(R,\theta) = constant$ exhibited in Figs. 4.2.2a,b.

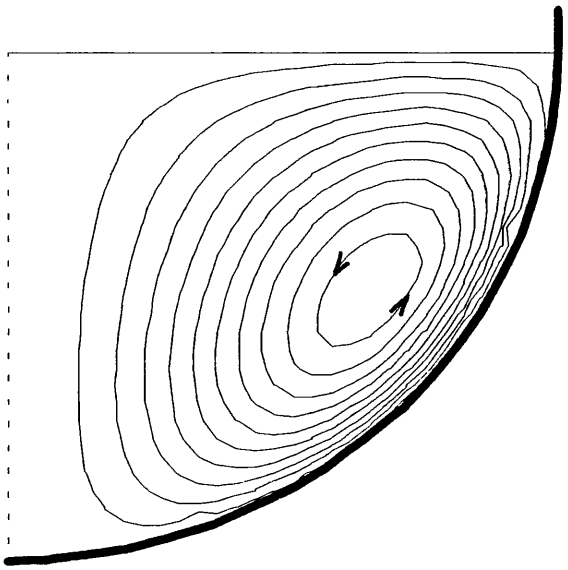

Fig. 4.2.2a Secondary (steady) streaming $\psi_0(R,\theta) = constant$ for an elastico-viscous fluid ($n\lambda_1 = 0$, $n\lambda_2 = 0$) when $R_a = 1$.

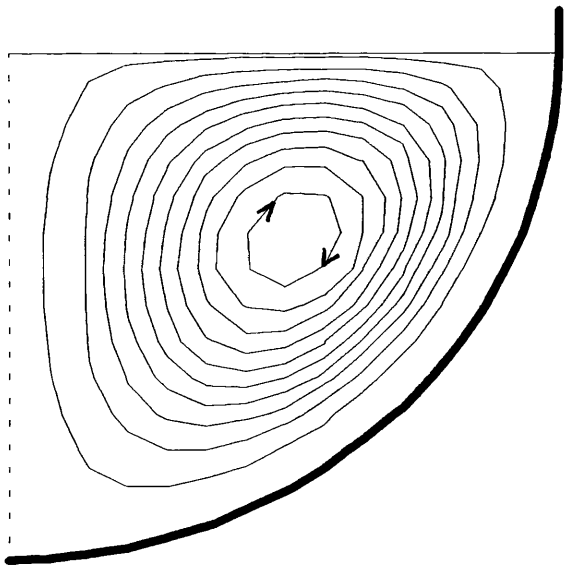

Fig. 4.2.2b Secondary (steady) streaming $\psi_0(R,\theta) = constant$ for an elastico-viscous fluid ($n\lambda_1 = 0.02$, $n\lambda_2 = 0.005$) when $R_a = 1$.

II. Large Values of n

As previously made clear in the analysis of the primary flow, it is necessary to look separately at two regions, that remote from the centre ($R = 0$), and that near the centre.

Region remote from the centre:

In this region both $|kR|$ and $|ka|$ are large, for which regime, on neglecting exponentially small terms, it is found that[30]

$$\psi_0(R,\theta) \simeq \frac{\Omega_0^2}{4\,|k|\sin\chi}[1-2K_1\,|k|^2](\frac{a^4}{R^2}e^{-2|k|(a-R)\sin\chi} - \frac{R^3}{a})\sin^2\theta\cos\theta. \quad (4.2.25)$$

This representation reveals much about the nature of the secondary flow when the frequency of oscillation is large. In particular:

(i) The exponential term $e^{-2|k|(a-R)\sin\chi}$ is negligibly small other than in a thin layer immediately adjacent to the boundary wall $R = a$. Within this layer, whose thickness is $O(aR_a^{-1})$, the streamline projection gradients are large, whilst (relatively) small elsewhere, i.e. in the main body of the well. The steady streaming that is generated is thus seen to be more significant (or intense) in a region near the wall and less so elsewhere within the well.

(ii) Accompanying this rapid change in the steady streaming, in the region close to the wall, one finds that the direction of the flow is controlled by the parameter $1-2K_1\,|k|^2$, flow reversal being associated with a change of sign of $1-2K_1\,|k|^2$, a function of the frequency of the forcing agent and of the parameters characterizing

[30] Here it is supposed that $1-2K_1\,|k|^2$ is not zero.

the rheological properties of the mixture[31]. In the illustrations undertaken here, corresponding to the values $\lambda_2/\lambda_1 = 1/4$, $\rho a^2/\eta_0\lambda_1 = 50$, it is found that $1-2K_1\,|k|^2$ vanishes for two distinct values of n, namely n_1, n_2 $(n_1 < n_2)$, where

$$n_1, n_2 = (46.99, 212.82)\,\frac{\eta_0}{\rho a^2}.$$

When $n < n_1$, the flow is similar to a Newtonian fluid, i.e. a flow controlled by centrifugal actions; when $n_1 < n < n_2$, the flow is spectacularly reversed, i.e. a flow in which non-Newtonian actions overwhelm centrifugal actions; and when $n > n_2$ the flow is again similar to that of a Newtonian fluid. This pattern of flow is well reflected in the *exact* streamline projections $\psi_0(R,\theta) =$ *constant* illustrated in Figs. 4.2.4a-e.

Region near the centre:

In this region $|ka| \gg 1$ but $|kR| \ll 1$. For such a regime, it is found that

$$\psi_0(R,\theta) \simeq \frac{2}{45}\Omega_0^2 a^4\,|k|^4\,e^{-2a|k|\sin\chi}R^3\sin^2\theta\cos\theta, \qquad (4.2.26)$$

which result shows that $\nabla\psi_0(R,\theta)$ is exponentially small, indicating that the secondary streaming flow is 'weak'.

Two groups of streamline projection curves $\psi_0(R,\theta) =$ *constant* are exhibited:

(i) Figs. 4.2.3a-e show the way the secondary flow varies with elasticity for a fixed Reynolds-type number R_a. Fig. 4.2.3a shows the flow, for sufficiently small elasticity, to be dominated everywhere by centrifugal actions, fluid being thrown outwards near the boundary wall and drawn inwards near the axis of rotation. As

[31] The zeros of this parameter can be matched with those of the function Φ_1 of Frater (1964) and of the function N_1 of Jones (1970), functions associated with flows between rotating parallel plates.

elasticity increases, Figs. 4.2.3b-e show that a region of flow reversal begins to develop in the inner region and that this region expands with increasing elasticity until it envelopes the whole region within the well. These results are more in keeping with the findings of Frater (1964) which indicate that non-Newtonian effects emanate from within the main body of fluid and not from the boundary wall as indicated by Jones (1970). As elasticity proceeds to increase centrifugal actions again begin to dominate in the near-wall region, eventually overwhelming non-Newtonian actions throughout the well.

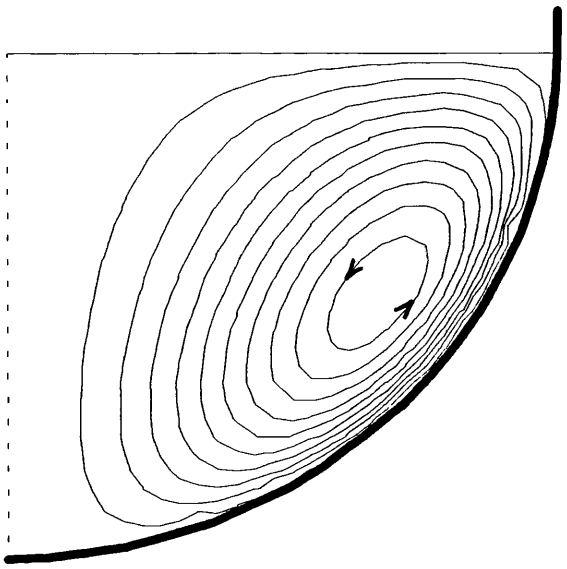

Fig. 4.2.3a Secondary (steady) streaming $\psi_0(R,\theta) = \textit{constant}$ for an elastico-viscous fluid ($n\lambda_1 = 0.2$, $n\lambda_2 = 0.05$) when $R_a = 5$.

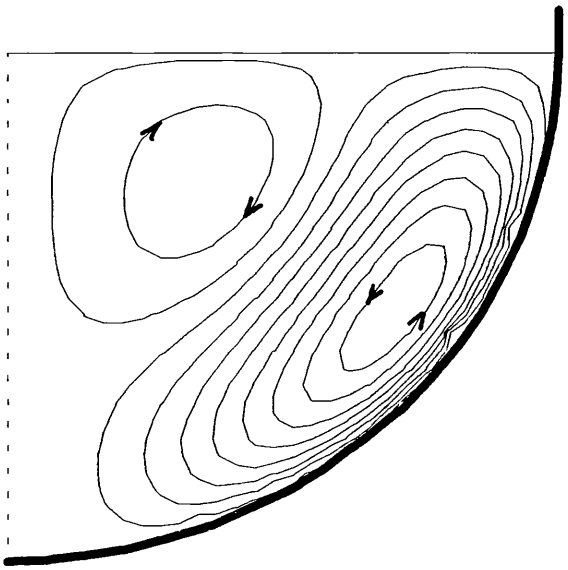

Fig. 4.2.3b Secondary (steady) streaming $\psi_0(R,\theta) = \textit{constant}$ for an elastico-viscous fluid ($n\lambda_1 = 0.4$, $n\lambda_2 = 0.1$) when $R_a = 5$.

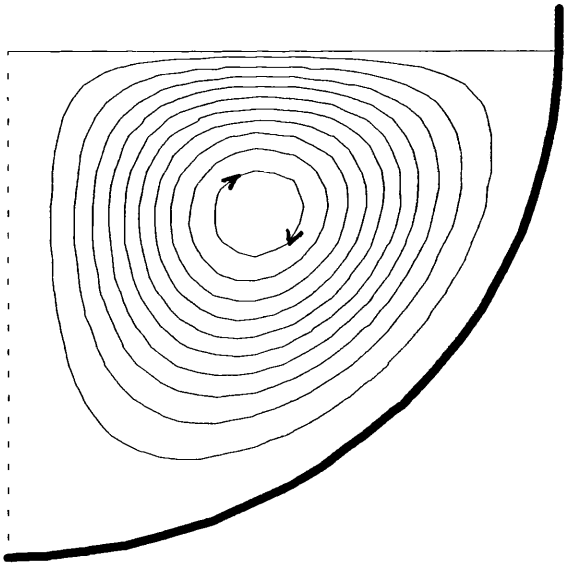

Fig. 4.2.3c Secondary (steady) streaming $\psi_0(R,\theta) = \textit{constant}$ for an elastico-viscous fluid ($n\lambda_1 = 1$, $n\lambda_2 = 0.25$) when $R_a = 5$.

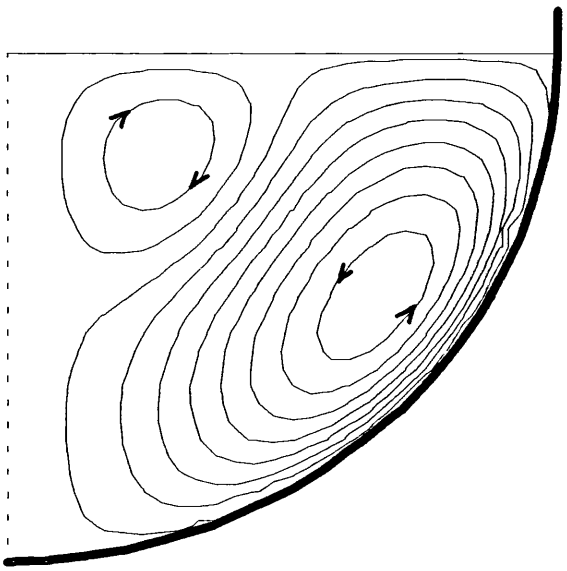

Fig. 4.2.3d Secondary (steady) streaming $\psi_0(R,\theta) = \textit{constant}$ for an elastico-viscous fluid ($n\lambda_1 = 4$, $n\lambda_2 = 1$) when $R_a = 5$.

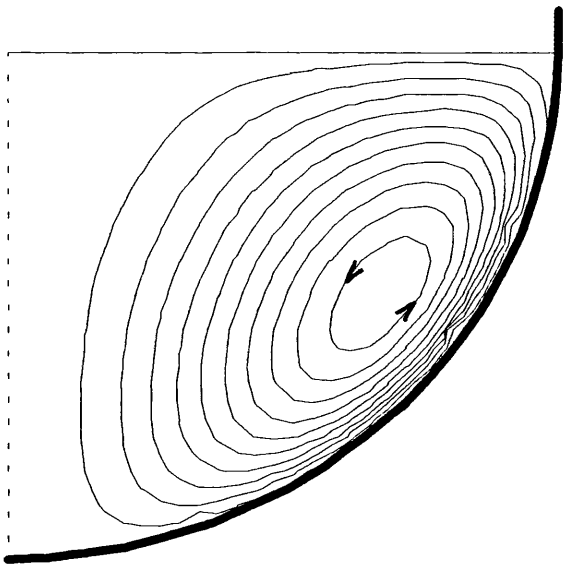

Fig. 4.2.3e Secondary (steady) streaming $\psi_0(R,\theta) = \textit{constant}$ for an elastico-viscous fluid ($n\lambda_1 = 6$, $n\lambda_2 = 1.5$) when $R_a = 5$.

(ii) Figs. 4.2.4a-c show the way the secondary flow varies with the Reynolds-type number R_a for fixed elasticity. For sufficiently small values of R_a (i.e. of n), for the measure of elasticity chosen, the flow is dominated throughout the well by non-Newtonian actions, fluid being drawn inwards along the boundary wall and thrown outwards along the axis of rotation[32]. As the Reynolds-type number increases, a region develops near the boundary wall in which centrifugal actions dominate, a region which expands to occupy the whole well. The exact reverse pattern of events occurs as R_a increases further, until the whole well is dominated by centrifugal actions. This type of regime remains unchanged as R_a proceeds to higher values.

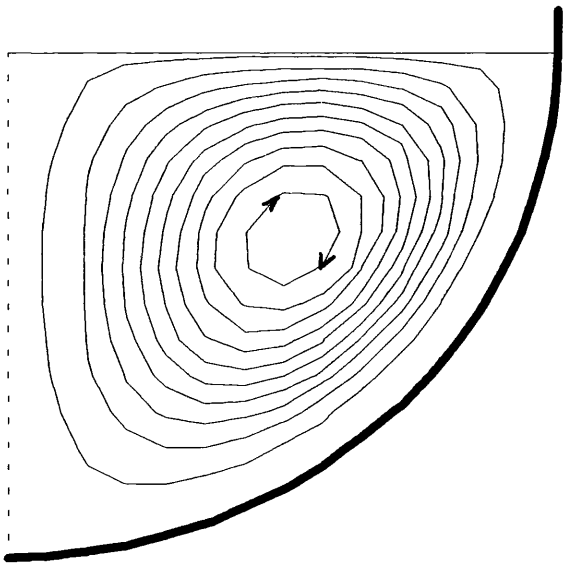

Fig. 4.2.4a Secondary (steady) streaming $\psi_0(R,\theta) = \textit{constant}$ for an elastico-viscous fluid ($n\lambda_1 = 0.02$, $n\lambda_2 = 0.005$) when $R_a = 1$.

[32] For a Newtonian fluid ($\lambda_1 = \lambda_2$), the effect is the opposite, centrifugal actions being everywhere in control.

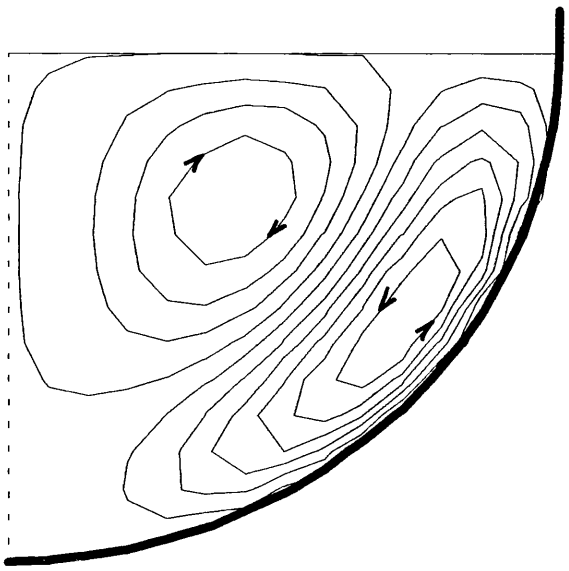

Fig. 4.2.4b Secondary (steady) streaming $\psi_0(R,\theta) = \textit{constant}$ for an elastico-viscous fluid ($n\lambda_1 = 0.245$, $n\lambda_2 = 0.06$) when $R_a = 3.5$.

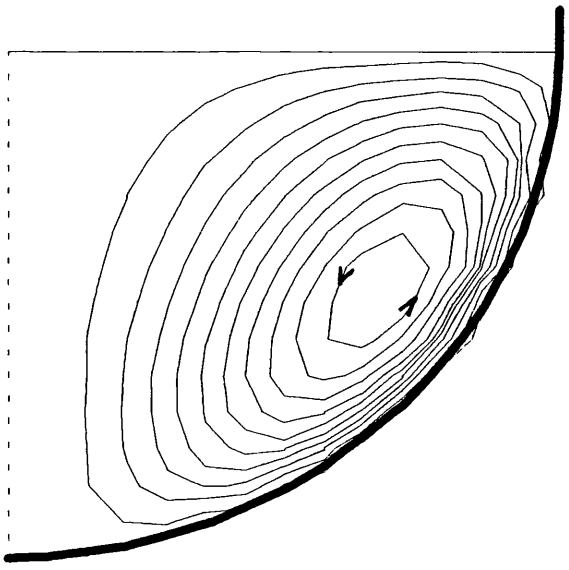

Fig. 4.2.4c Secondary (steady) streaming $\psi_0(R,\theta) = \textit{constant}$ for an elastico-viscous fluid ($n\lambda_1 = 0.5$, $n\lambda_2 = 0.125$) when $R_a = 5$.

The above (*exact*) pattern of the secondary steady streaming flow is much in keeping with the approximate analysis for small and large values of the frequency $n/2\pi$.

4.3 Concluding Remark

A qualitative picture of the flow of the mixture within the well whilst in motion on the outer carousel ring has now been obtained. Within the main 'inner' body of the well the mixture moves nearly as if rigid, a motion virtually free of any migratory motion of fluid elements. Whereas, within a thin layer adjacent to the well wall, the flow varies rapidly, and is associated with vigorous (steady) stirrings of the mixture.

4.4 References

Frater, K. R.,"Flow of an elastico-viscous fluid between torsionally oscillating disks", 1964, *J. Fluid Mech.*, **19**, 175.

Frater, K. R.,"Secondary flow in an elastico-viscous fluid caused by rotational oscillations of sphere. Part 1", 1964, *J. Fluid Mech.*, **20**, 369.

Jones, J. R., "Non-Newtonian effects in axially symmetric oscillatory flows of some elastico-viscous liquids", 1970, *Proc. Cambridge Philos. Soc.*, **68**, 731.

Rosenblat, S., "Flow between torsionally oscillating disks", 1960, *J. Fluid Mech.*, **8**, 388.

CHAPTER 5

ANALYSIS FOR A CYLINDRICAL-SHAPED WELL

The study of the large scale flow of the mixture within the well, whilst in motion on the outer carousel ring, is continued in the present chapter, the well geometry being now supposed cylindrical in shape. An exact solution for the primary flow is developed in the form of an infinite series, a series which converges rapidly when the frequency of oscillation is large as in the 'jiggle' regime. However, it has not been found possible to construct an exact solution for the steady streaming as characterized by the function $\psi_0(r,z)$, but reasonably accurate representations can be found when the ratio of radius to depth of the well is either large or small.

5.1 Primary Flow

Within a cylindrical polar description r, ϕ, z, in which $r = 0$ represents the well axis, the governing equation for the primary flow is defined by equation (3.2.16), viz.

$$\frac{\partial^2 \overline{\omega}}{\partial r^2} + \frac{3}{r}\frac{\partial \overline{\omega}}{\partial r} + \frac{\partial^2 \overline{\omega}}{\partial z^2} + k^2 \bar{\omega} = 0, \tag{5.1.1}$$

and is associated with the boundary conditions

$$\overline{\omega}(r,z) = \Omega_0 \text{ on the wall } r = a, \tag{5.1.2a}$$

$$\overline{\omega}(r,z) = \Omega_0 \text{ on the wall } z = 0, \tag{5.1.2b}$$

$$\frac{\partial \overline{\omega}(r,z)}{\partial z} = 0 \text{ on the free surface } z = b, \tag{5.1.2c}$$

together with the understood condition that $\overline{\omega}(r,z)$ is finite throughout the region of flow. Here

$$k = |k|\, e^{-i\chi},\ |k| = \sqrt{\frac{n\rho}{\eta_0}}\left(\frac{1+n^2\lambda_1^2}{1+n^2\lambda_2^2}\right)^{\frac{1}{4}} \text{ and } \chi = \frac{\pi}{4} - \frac{1}{2}(\tan^{-1} n\lambda_1 - \tan^{-1} n\lambda_2).$$

The solution of the differential system (5.1.1)-(5.1.2a-c) is easily constructed in the case of a 'shallow' well and in the case of a 'deep' well. It is appropriate, in the first instance, to look at these two special cases separately.

I. Shallow Well

In this case it is supposed that $a \gg b$. Hence, approximately, $\bar{\omega} = \bar{\omega}(z)$, in which event the equation for $\bar{\omega}$ reduces to

$$\frac{d^2\bar{\omega}}{dz^2} + k^2\bar{\omega} = 0, \tag{5.1.3}$$

and is associated with the boundary conditions

$$\bar{\omega}(z) = \Omega_0 \text{ on } z = 0, \tag{5.1.4a}$$

$$\frac{\partial \bar{\omega}(z)}{\partial z} = 0 \text{ on } z = b, \tag{5.1.4b}$$

together with the understood condition that $\bar{\omega}(z)$ is finite throughout the region of flow $0 \le z \le b$. Equations (5.1.3)-(5.1.4a,b) are seen to admit the solution

$$\bar{\omega}(z) = \Omega_0 \frac{\cos k(b-z)}{\cos kb}, \tag{5.1.5}$$

and, in turn, gives for the velocity field

$$v_{(\phi)} = \Omega_0 r\, \mathrm{Re}[(\frac{\cos k(b-z)}{\cos kb} - 1)e^{int}]. \tag{5.1.6}$$

II. Deep Well

In this case it is supposed that $a \ll b$. Hence, approximately $\bar{\omega} = \bar{\omega}(r)$, in which event equation (5.1.1) reduces to

$$\frac{d^2\bar{\omega}}{dr^2} + \frac{3}{r}\frac{d\bar{\omega}}{dr} + k^2\bar{\omega} = 0, \tag{5.1.7}$$

and is associated with the boundary condition

$$\bar{\omega}(r) = \Omega_0 \text{ on } r = a, \tag{5.1.8}$$

together with the understood condition that $\bar{\omega}(r)$ is finite throughout the region of flow $0 \leq r \leq a$. Equations (5.1.7) and (5.1.8) are seen to admit the solution

$$\bar{\omega}(r) = \Omega_0 \frac{aJ_1(kr)}{rJ_1(ka)}, \tag{5.1.9}$$

with associated velocity field

$$v_{(\phi)} = \Omega_0 r \,\mathrm{Re}[(\frac{aJ_1(kr)}{rJ_1(ka)} - 1)e^{int}], \tag{5.1.10}$$

J_1 being the Bessel function of the first kind of order unity.

One next looks at equations (5.1.1)-(5.1.2a-c) with a view of constructing a **general** solution for a cylindrical well of radius a and depth b, the above two solutions being derivable as special cases (corresponding to two extreme configurations). Two different, but *exact*, representations are derived for $\overline{\omega}(r, z)$, one suitable for application in the case of a shallow well when $a \gg b$, and one suitable for application in the case of a deep well when $b \gg a$. (See Jones & Walters (1966)).

First, with a view of constructing a solution suitable for application in the case of a *shallow* well, it is convenient to consider the (more) symmetrical flow regime

defined by the differential equation (5.1.1) in the region $0 \leq r \leq a$, $0 \leq z \leq 2b$ subject to the boundary conditions

$$\bar{\omega}(r,z) = \Omega_0 \text{ on } r = a, \tag{5.1.11a}$$

$$\bar{\omega}(r,z) = \Omega_0 \text{ on } z = 0, \tag{5.1.11b}$$

$$\bar{\omega}(r,z) = \Omega_0 \text{ on } z = 2b. \tag{5.1.11c}$$

Symmetry will demand that the solution be such that $\partial\bar{\omega}(r,z)/\partial z$ is identically zero on $z = b$. Hence, the solution of the above parallel problem, when restricted to the region $0 \leq z \leq b$, will correspond to that in a well of radius a and depth b.

In the analysis of the above scheme, it is convenient to introduce the finite Fourier sine transform $\bar{\omega}_F(r,m)$ of $\bar{\omega}(r,z)$ defined by

$$\bar{\omega}_F(r,m) = \frac{1}{b}\int_0^{2b} \bar{\omega}(r,z)\sin(\frac{m\pi z}{2b})dz. \tag{5.1.12}$$

Multiplying equation (5.1.1) by $\frac{1}{b}\sin(\frac{m\pi}{2b})z$ and integrating with respect to z between the limits 0 and $2b$ results in the equation

$$\frac{d^2\bar{\omega}_F}{dr^2} + \frac{3}{r}\frac{d\bar{\omega}_F}{dr} + h_m^2\bar{\omega}_F = \Omega_0\frac{m\pi}{2b^2}[(-1)^m - 1], \tag{5.1.13}$$

and is to be associated with the Fourier sine transform of the boundary conditions (5.1.11a-c), viz.

$$\bar{\omega}_F(r,m) = -\frac{2\Omega_0}{m\pi}[(-1)^m - 1] \text{ on } r = a, \tag{5.1.14}$$

together with the understood condition that $\bar{\omega}_F(r,m)$ is finite throughout the region of flow. Here $h_m^2 = k^2 - (\frac{m\pi}{2b})^2$. The general solution of the differential equation (5.1.13) is

$$\bar{\omega}_F(r,m) = \frac{A}{r}J_1(h_m r) + \frac{B}{r}Y_1(h_m r) + \Omega_0\frac{m\pi}{2b^2h_m^2}[(-1)^m - 1], \tag{5.1.15}$$

where $J_1(h_m r)$, $Y_1(h_m r)$ are Bessel functions of the first and second kind of order unity, A and B being arbitrary constants. On imposing the boundary condition (5.1.14), the appropriate solution finite throughout the region of flow is

$$\bar{\omega}_F(r,m) = \frac{\Omega_0[(-1)^m - 1]}{h_m^2}\left(\frac{m\pi}{2b^2} - \frac{2k^2}{m\pi}\frac{aJ_1(h_m r)}{rJ_1(h_m a)}\right). \tag{5.1.16}$$

Thus, on using the inversion formula

$$\bar{\omega}(r,z) = \sum_{m=1}^{\infty} \bar{\omega}_F(r,m)\sin(\frac{m\pi z}{2b}), \tag{5.1.17}$$

it is found that

$$\bar{\omega}(r,z) = \sum_{m=1}^{\infty} \frac{\Omega_0[(-1)^m - 1]}{h_m^2}\left(\frac{m\pi}{2b^2} - \frac{2k^2}{m\pi}\frac{aJ_1(h_m r)}{rJ_1(h_m a)}\right)\sin(\frac{m\pi z}{2b}). \tag{5.1.18}$$

This expression for $\bar{\omega}(r,z)$, applicable in the region $0 \le z \le b$, can be rearranged in a more convenient form. Now

$$\begin{aligned}
&\frac{1}{b}\int_0^{2b} \frac{\Omega_0 \cos k(b-z)}{\cos kb}\sin(\frac{m\pi z}{2b})dz \\
&= \frac{\Omega_0}{2b\cos kb}\int_0^{2b}\{\sin[(\frac{m\pi}{2b}+k)z - kb] + \sin[(\frac{m\pi}{2b}-k)z + kb]\}dz \\
&= \frac{-\Omega_0}{2b\cos kb}\left[\frac{\cos[(\frac{m\pi}{2b}+k)z - kb]}{\frac{m\pi}{2b}+k} + \frac{\cos[(\frac{m\pi}{2b}-k)z + kb]}{\frac{m\pi}{2b}-k}\right]_0^{2b} \\
&= \frac{\Omega_0 m\pi}{2b^2 h_m^2}[(-1)^m - 1],
\end{aligned}$$

and so $\Omega_0 m\pi[(-1)^m - 1]/2b^2h_m^2$ is recognized as the finite Fourier sine transform of $\Omega_0 \cos k(b-z)/\cos kb$, i.e.,

$$\sum_{m=1}^{\infty} \frac{\Omega_0 m\pi}{2b^2 h_m^2}[(-1)^m - 1]\sin(\frac{m\pi z}{2b}) = \frac{\Omega_0 \cos k(b-z)}{\cos kb}. \tag{5.1.19}$$

Hence the expression for $\bar{\omega}(r,z)$ can be rearranged to give

$$\bar{\omega}(r,z) = \frac{\Omega_0 \cos k(b-z)}{\cos kb} + \frac{4\Omega_0 ak^2}{\pi r}\sum_{m=0}^{\infty} \frac{J_1(h_{2m+1}r)}{(2m+1)h_{2m+1}^2 J_1(h_{2m+1}a)}\sin[\frac{(2m+1)\pi z}{2b}], \tag{5.1.20}$$

where $h_{2m+1}^2 = k^2 - ((2m+1)\pi/2b)^2$. It is now seen that the first term in (5.1.20) is the solution represented by equation (5.1.5), appropriate to the case of the shallow well, and so (5.1.20) is a representation of $\bar{\omega}(r,z)$ that is particularly well suited for application in the case $a \gg b$. The corresponding (oscillatory) primary flow within a cylindrical well of radius a and depth b is

$$\begin{aligned} v_{(\phi)} &= \Omega_0 r \,\mathrm{Re}\{(-1 + \frac{\cos k(b-z)}{\cos kb} \\ &\quad + \frac{4ak^2}{\pi r} \sum_{m=0}^{\infty} \frac{J_1(h_{2m+1}r)}{(2m+1)h_{2m+1}^2 J_1(h_{2m+1}a)} \sin[\frac{(2m+1)\pi z}{2b}])e^{int}\}. \end{aligned} \tag{5.1.21}$$

Second, with a view of constructing a solution suitable for application in the case of a *deep* well, it is convenient to reverse the role of the variables r, z and to consider a transformation on the variable r. The Hankel transform $\bar{\omega}_H(q_i, z)$ of $\bar{\omega}(r,z)$ is introduced, defined by

$$\bar{\omega}_H(q_i, z) = \int_0^a r^2 J_1(q_i r)\bar{\omega}(r,z)dr, \tag{5.1.22}$$

where q_i is a positive root of $J_1(q_i a) = 0$. On multiplying equation (5.1.1) by $r^2 J_1(q_i r)$ and integrating with respect to r between the limits 0 and a, the following equation results

$$\frac{d^2\bar{\omega}_H}{dz^2} + (k^2 - q_i^2)\bar{\omega}_H = \Omega_0 a^2 q_i J_1'(q_i a), \tag{5.1.23}$$

and is to be associated with the boundary condition

$$\bar{\omega}_H(q_i, z) = -\frac{a^2\Omega_0}{q_i} J_0(q_i a) \text{ on } z = 0, \tag{5.1.24a}$$

$$\frac{\partial\bar{\omega}_H(q_i, z)}{\partial z} = 0 \text{ on } z = b, \tag{5.1.24b}$$

together with the understood condition that $\bar{\omega}_H(q_i, z)$ is finite throughout the region of flow. Here one has made use of the identities

$$\int x^n J_{n-1}(x)dx = x^n J_n(x) \text{ and } J_{n+1}(x) = \frac{2n}{x}J_n(x) - J_{n-1}(x).$$

It is a simple matter to construct the general solution of (5.1.23): it is

$$\bar{\omega}_H(q_i, z) = A\cos l_i z + B\sin l_i z + \frac{\Omega_0 a^2 q_i}{l_i^2}J_0(q_i a), \tag{5.1.25}$$

where $l_i^2 = k^2 - q_i^2$. Here one has made use of the further identity

$$\frac{d}{dx}(xJ_1(x)) = xJ_0(x).$$

On applying boundary condition (5.1.24a,b), one finds

$$\bar{\omega}_H(q_i, z) = -\frac{\Omega_0 a^2}{l_i^2}\left(\frac{k^2}{q_i}\frac{\cos l_i(b-z)}{\cos l_i b} - q_i\right)J_0(q_i a). \tag{5.1.26}$$

Therefore, on using the inversion formula

$$\bar{\omega}(r, z) = \sum_{i=1}^{\infty}\frac{2}{a^2 r}\frac{J_1(q_i r)}{[J_2(q_i a)]^2}\bar{\omega}_H(q_i, z), \tag{5.1.27}$$

one obtains the solution

$$\bar{\omega}(r, z) = \sum_{i=1}^{\infty}\frac{-2\Omega_0}{l_i^2 r}\left(\frac{k^2}{q_i}\frac{\cos l_i(b-z)}{\cos l_i b} - q_i\right)\frac{J_1(q_i r)}{J_0(q_i a)}. \tag{5.1.28}$$

Expression (5.1.28) for $\bar{\omega}(r, z)$ may be rearranged in a more convenient form as follows. Now

$$\begin{aligned}\int_0^a r^2 J_1(q_i r)[\Omega_0\frac{aJ_1(kr)}{rJ_1(ka)}]dr &= \frac{\Omega_0 a}{J_1(ka)}\left(\frac{kaJ_1(q_i a)J_0(ka) - q_i a J_1(ka)J_0(q_i a)}{q_i^2 - k^2}\right)\\ &= \frac{\Omega_0 a^2 q_i}{l_i^2}J_0(q_i a),\end{aligned}$$

and is recognized as the Hankel transform of $\Omega_0 a J_1(kr)/rJ_1(ka)$. Hence

$$\Omega_0 \frac{aJ_1(kr)}{rJ_1(ka)} = \sum_{i=1}^{\infty} \frac{2\Omega_0 q_i}{l_i^2 r} \frac{J_1(q_i r)}{J_0(q_i a)}. \tag{5.1.29}$$

Thus $\bar{\omega}(r,z)$ may be expressed in the form

$$\bar{\omega}(r,z) = \Omega_0 \frac{aJ_1(kr)}{rJ_1(ka)} - \frac{2\Omega_0 k^2}{r} \sum_{i=1}^{\infty} \frac{1}{q_i l_i^2} \frac{\cos l_i(b-z)}{\cos l_i b} \frac{J_1(q_i r)}{J_0(q_i a)}. \tag{5.1.30}$$

The first term in (5.1.30) is recognized as the solution appropriate to the case of a deep well, and so (5.1.30) is a representation of $\bar{\omega}(r,z)$ particularly well suited for application in the case when $b \gg a$. Finally, the associated (oscillatory) primary velocity field may be written

$$v_{(\phi)} = \Omega_0 r \,\mathrm{Re}\{(-1 + \frac{aJ_1(kr)}{rJ_1(ka)} - \frac{2\Omega_0 k^2}{r} \sum_{i=1}^{\infty} \frac{1}{q_i l_i^2} \frac{\cos l_i(b-z)}{\cos l_i b} \frac{J_1(q_i r)}{J_0(q_i a)}) e^{int}\}. \tag{5.1.31}$$

5.1.1 Numerical Results

Although the primary (oscillatory) motion, as represented by equation (5.1.21), or equally by equation (5.1.31), is complicated in mathematical form, it is nevertheless possible to make some general deductions about the nature of the flow in certain regions when the frequency of oscillation $n/2\pi$ is sufficiently small or large. Two special configurations are assessed: the shallow well and the deep well.

I. Small Values of n

i. Shallow well ($a \gg b$)

Sufficiently far away from the wall ($r = a$) of the well, the primary flow may be approximated by

$$\bar{\omega} = \bar{\omega}(z) = \Omega_0 \frac{\cos k(b-z)}{\cos kb}, \tag{5.1.32}$$

and so for small values of the frequency $n/2\pi$, i.e., of $|kz|$ $(0 \leq z \leq b)$, one may write

$$\bar{\omega}(z) = \Omega_0[1 + \frac{1}{2}k^2 z(2b - z) + O(k^4)], \tag{5.1.33}$$

and, in turn, gives for the primary velocity

$$v_{(\phi)} = \mathrm{Re}[\{\frac{1}{2}\Omega_0 k^2 r z(2b - z) + O(k^4)\}e^{int}]. \tag{5.1.34}$$

It is thus seen that the angular velocity profiles $v_{(\phi)}(z)/r$, i.e. $|\overline{\omega}(z) - \Omega_0|$, are approximately parabolic, varying from zero on the wall $z = 0$ to a maximum at the free surface $z = b$. The effect of elasticity is to heighten these profiles across the whole depth of the well, i.e. to increase the velocity at all points in the well. As the frequency decreases the variation of $v_{(\phi)}/r$ with z becomes less marked, and eventually the primary flow $v_{(\phi)}$ approaches zero at all points in the well as n approaches zero, i.e. as the forcing agent approaches a steady value. These features of the flow are seen to be reflected in the *exact* profiles exhibited in Figs. 5.1.1a-d.

The notation is that $R_a = \sqrt{(\rho a^2 n/\eta_0)}$ and $R_b = \sqrt{(\rho b^2 n/\eta_0)}$, i.e. Reynolds-type numbers with characteristic lengths based respectively on the radius and depth of the well, the ratio $R_a : R_b$ being identified with the ratio $a : b$; and , again, as in the previous chapter, the 'distance from the wall' is to be interpreted as the appropriate dimensionless measure.

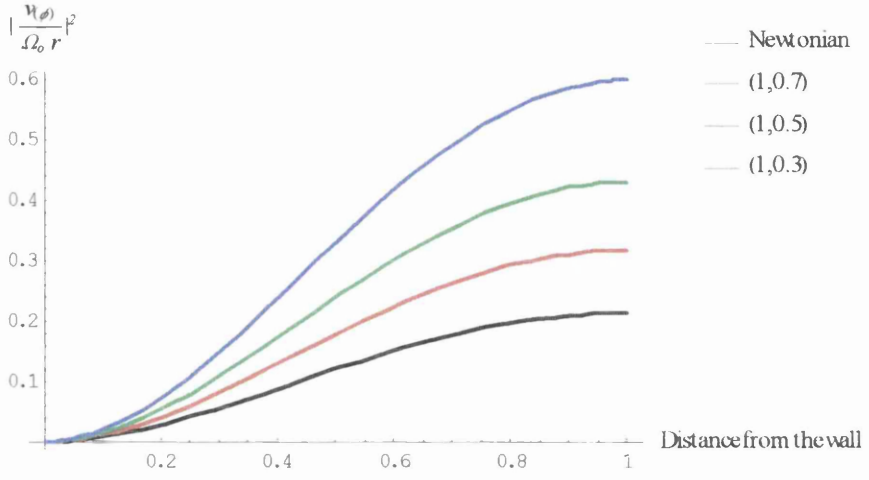

Fig. 5.1.1a Primary flow profiles for various values of the elastic parameters $(n\lambda_1, n\lambda_2)$ when $R_b = 1, R_b/R_a = 0.2$ and $r = 0.01$.

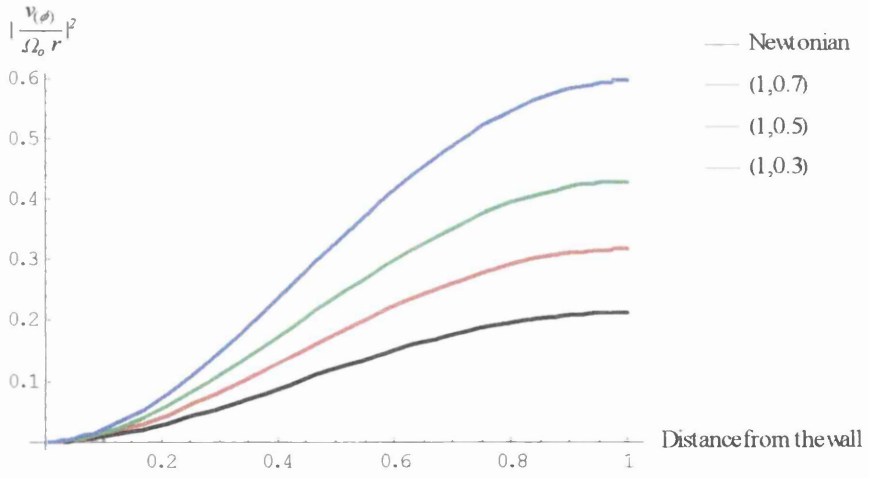

Fig. 5.1.1b Primary flow profiles for various values of the elastic parameters $(n\lambda_1, n\lambda_2)$ when $R_b = 1, R_b/R_a = 0.2$ and $r = 0.2$.

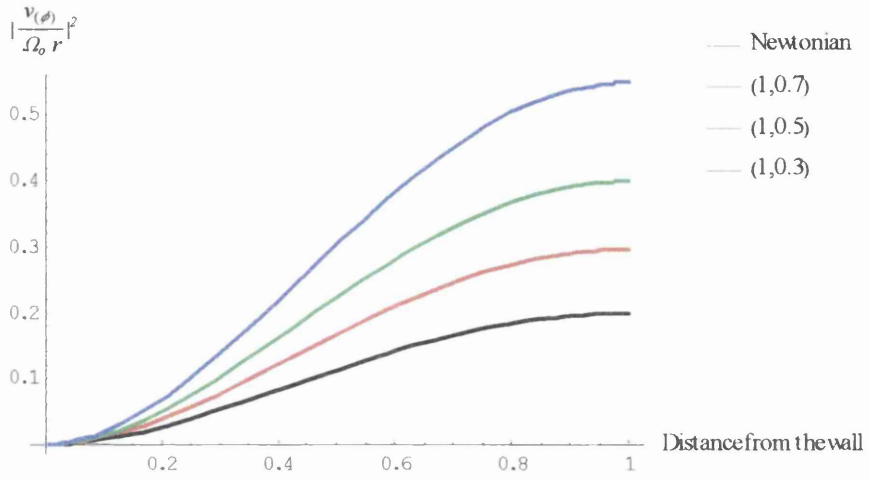

Fig. 5.1.1c Primary flow profiles for various values of the elastic parameters $(n\lambda_1, n\lambda_2)$ when $R_b = 1, R_b/R_a = 0.2$ and $r = 0.5$.

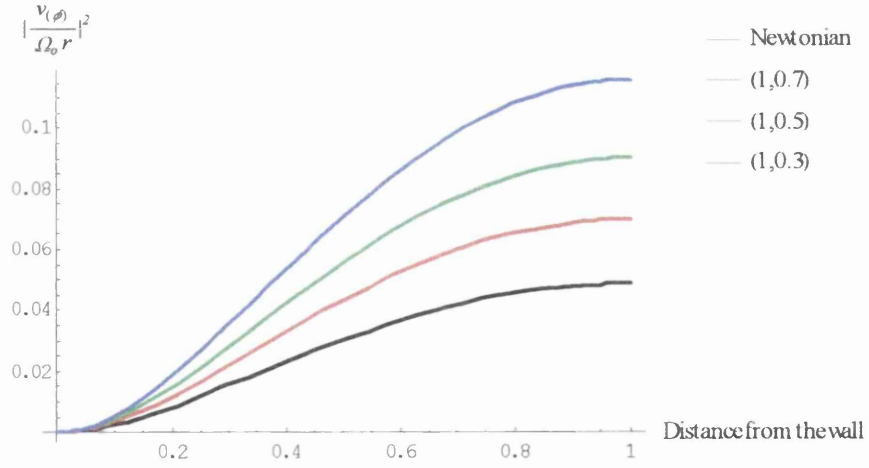

Fig. 5.1.1d Primary flow profiles for various values of the elastic parameters $(n\lambda_1, n\lambda_2)$ when $R_b = 1, R_b/R_a = 0.2$ and $r = 0.9$.

ii. Deep well ($b \gg a$)

Here, sufficiently far away from the floor wall ($z = 0$) of the well, the primary flow may be approximated by

$$\bar{\omega} = \bar{\omega}(r) = \Omega_0 \frac{aJ_1(kr)}{rJ_1(ka)}. \tag{5.1.35}$$

On using the infinite series representation for the Bessel function $J_1(kr)$, one obtains, for sufficiently small values of n, i.e. of $|kr|$ $(0 \leq r \leq a)$,

$$\bar{\omega}(r) = \Omega_0[1 + \frac{1}{8}k^2(a^2 - r^2) + O(k^4)], \tag{5.1.36}$$

and, in turn, gives the velocity field

$$v_{(\phi)} = \mathrm{Re}[\{\Omega_0 \frac{1}{8}k^2 r(a^2 - r^2) + O(k^4)\}e^{int}]. \tag{5.1.37}$$

The results are seen to be similar in all ways with those in the previous case, the $v_{(\phi)}(r)/r$ velocity profiles are again parabolic, varying from zero on the wall $r = a$ to a maximum on the axis of symmetry $r = 0$. Likewise, the effect of elasticity is to increase somewhat the velocity throughout the well. Again, $v_{(\phi)}$ approaches zero as the forcing agent approaches a steady value (i.e. as n approaches zero). These general features of the flow as seen to be reflected in the *exact* profiles exhibited in Figs. 5.1.2a-d.

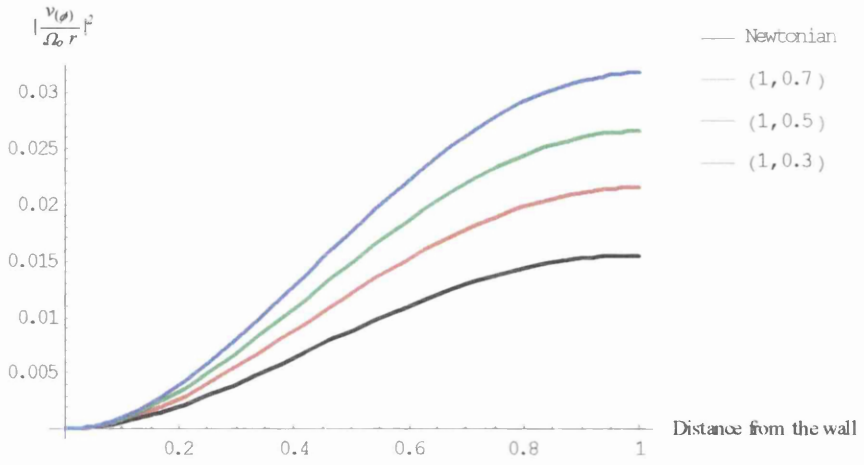

Fig. 5.1.2a Primary flow profiles for various values of the elastic parameters $(n\lambda_1, n\lambda_2)$ when $R_a = 1, R_a/R_b = 0.2$ and $z = 1$.

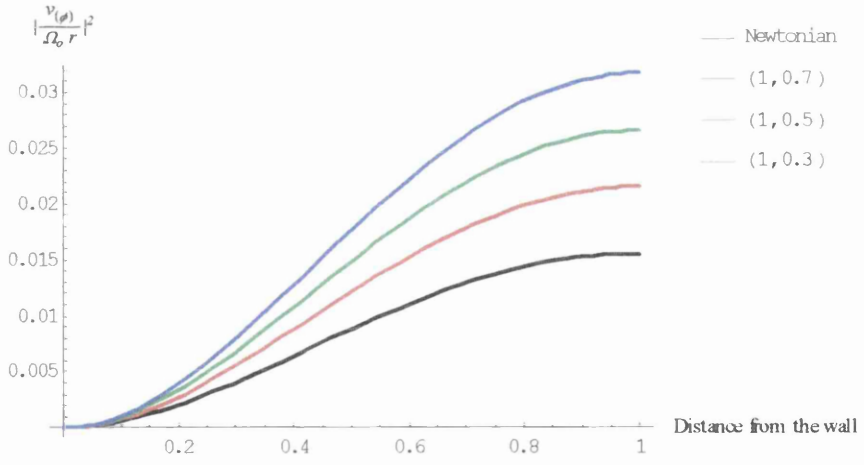

Fig. 5.1.2b Primary flow profiles for various values of the elastic parameters $(n\lambda_1, n\lambda_2)$ when $R_a = 1, R_a/R_b = 0.2$ and $z = 0.8$.

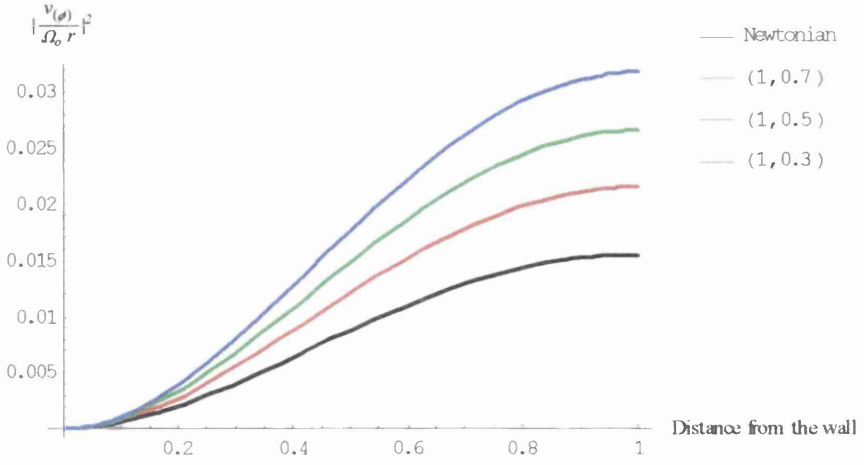

Fig. 5.1.2c Primary flow profiles for various values of the elastic parameters $(n\lambda_1, n\lambda_2)$ when $R_a = 1, R_a/R_b = 0.2$ and $z = 0.5$.

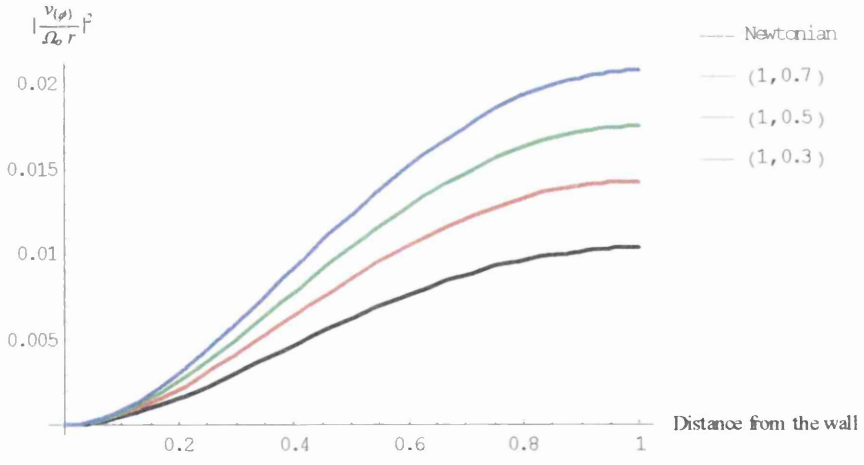

Fig. 5.1.2d Primary flow profiles for various values of the elastic parameters $(n\lambda_1, n\lambda_2)$ when $R_a = 1, R_a/R_b = 0.2$ and $z = 0.1$.

Although the above analyses apply to extreme well configurations, they are deemed sufficient to indicate the general nature of the flow of the mixture within the well when n is very small: the mixture rotates as if rigid with angular velocity which at any instant equals that of the wall at the same instant. These results are in exact parallel with those in the previous chapter, i.e. those results relating to flow within a hemispherical-shaped well. The general deduction that can be made, based on the primary flow, is that no appreciable mixing takes place within the well when the frequency of oscillation is small.

II. Large Values of n

i. Shallow well ($a \gg b$)

One now seeks to analyse the behaviour of $\bar{\omega}$, as defined approximately by (5.1.32), for large values of n, i.e. of $|k|$. In such a regime, one needs to look separately at two regions: a region near the floor wall ($z = 0$) of the well in which region $|k|\, b$ and $|k|\,(b - z)$ are both large, and a region remote from the wall in which region $|k|\, b$ is large whilst $|k|\,(b - z)$ is small.

Region near the wall $z = 0$:

It is convenient to write

$$\begin{aligned} \cos k(b - z) &= \frac{1}{2}(e^{ikb}e^{-ikz} + e^{-ikb}e^{ikz}), \\ \cos kb &= \frac{1}{2}(e^{ikb} + e^{-ikb}). \end{aligned}$$

Now, since within this region $|k|\, b$ and $|k|\,(b - z)$ are both large (i.e. $|k|\, b \gg 1$ and $|k|\, z \ll 1$), one obtains, on neglecting exponentially small terms,

$$\bar{\omega} = \bar{\omega}(z) \simeq \Omega_0 e^{-|k|z\,(\sin\chi + i\cos\chi)},$$

and, in turn, gives for the velocity field

$$v_{(\phi)} \simeq \Omega_0 r \,\mathrm{Re}[(e^{-|k|z\,(\sin\chi + i\cos\chi)} - 1)e^{int}]. \tag{5.1.38}$$

The exponential factor here is negligibly small everywhere except in a thin layer adjacent to the wall $z = 0$. The velocity field varies rapidly within this layer, attaining a high peak value near the wall. Outside this layer, one obtains, on neglecting exponentially small terms,

$$v_{(\phi)} \simeq \Omega_0 r \,\mathrm{Re}[-e^{int}],$$

i.e. a flow which is, approximately, a rigid body rotation with the same angular amplitude (Ω_0) and frequency ($n/2\pi$) of the boundary wall, but of phase π behind it. The effects of elasticity are to increase *substantially* the value of $\left|v_{(\phi)}/r\right|^2$ close to the wall, while having no great effect on its magnitude over the rest of the region of flow, and to decrease somewhat the thickness of the boundary layer region in which the velocity changes rapidly. These general features are seen to be reflected in the *exact* profiles exhibited in Figs. (5.1.3a-d) and (5.1.4a-d).

Region remote from the wall $z = 0$:

Within this region both $|k|\,b$ and $|k|\,z$ are large. Thus, on neglecting exponentially small terms,

$$\frac{\cos k(b - z)}{\cos kb} \simeq 2e^{-ikb} \simeq 0.$$

Hence

$$\bar{\omega}(z) \simeq 0,$$

and

$$v_{(\phi)} \simeq \Omega_0 r \,\mathrm{Re}[-e^{int}], \tag{5.1.39}$$

i.e. the flow is, effectively, a rigid body rotation of angular amplitude and frequency that of the wall, but of phase π behind it.

The nature of the primary flow is now ascertained: the velocity varies rapidly in a thin layer adjacent to the wall, there attaining a high peak, whereas elsewhere the flow approaches a rigid body rotation.

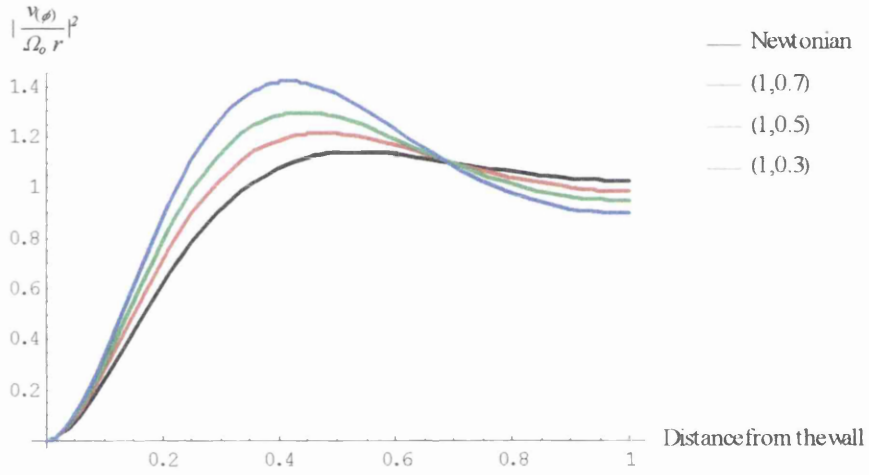

Fig. 5.1.3a Primary flow profiles for various values of the elastic parameters $(n\lambda_1, n\lambda_2)$ when $R_b = 6, R_b/R_a = 0.2$ and $r = 0.01$.

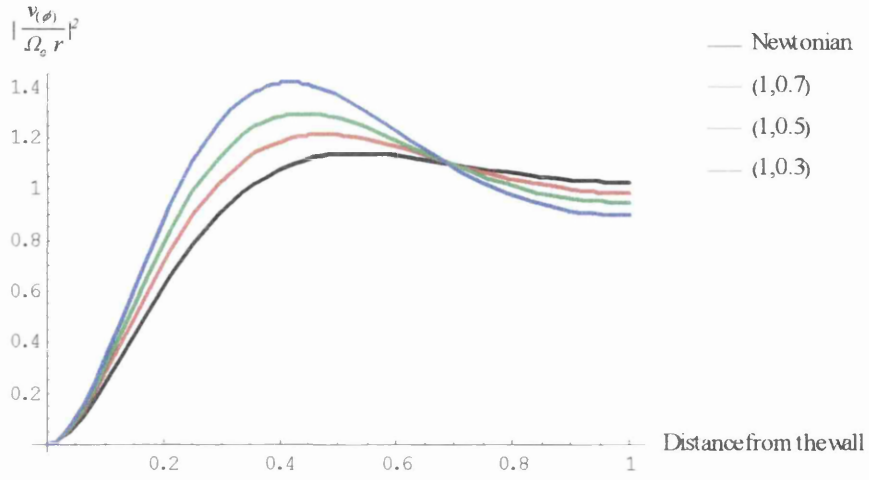

Fig. 5.1.3b Primary flow profiles for various values of the elastic parameters $(n\lambda_1, n\lambda_2)$ when $R_b = 6, R_b/R_a = 0.2$ and $r = 0.2$.

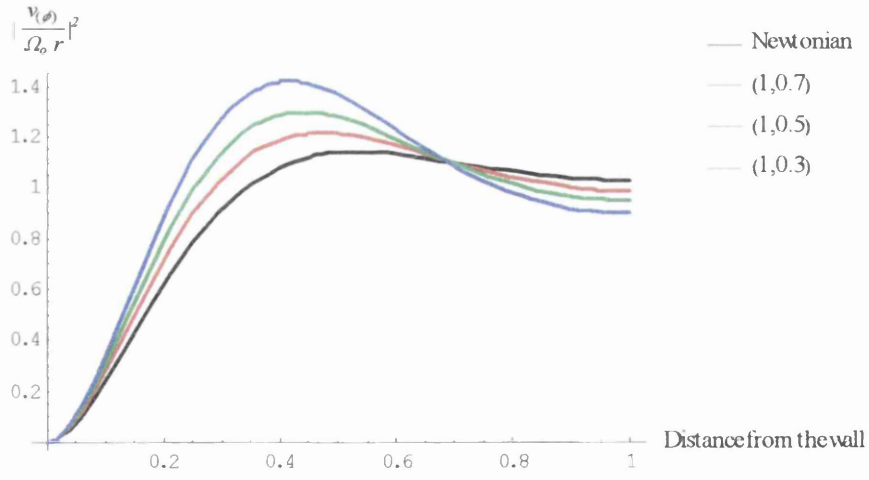

Fig. 5.1.3c Primary flow profiles for various values of the elastic parameters $(n\lambda_1, n\lambda_2)$ when $R_b = 6, R_b/R_a = 0.2$ and $r = 0.5$.

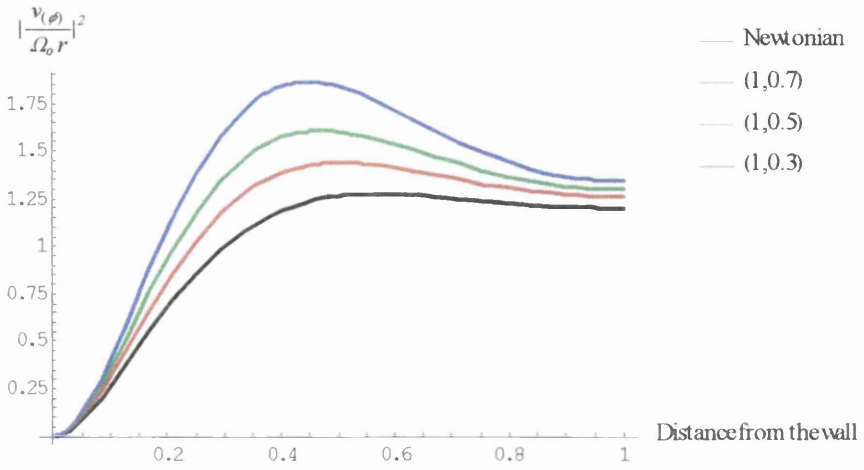

Fig. 5.1.3d Primary flow profiles for various values of the elastic parameters $(n\lambda_1, n\lambda_2)$ when $R_b = 6, R_b/R_a = 0.2$ and $r = 0.9$.

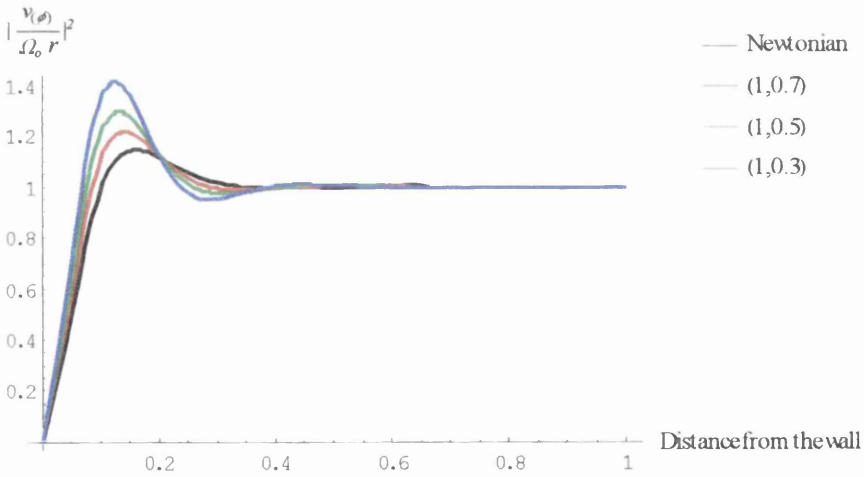

Fig. 5.1.4a Primary flow profiles for various values of the elastic parameters $(n\lambda_1, n\lambda_2)$ when $R_b = 20, R_b/R_a = 0.2$ and $r = 0.01$.

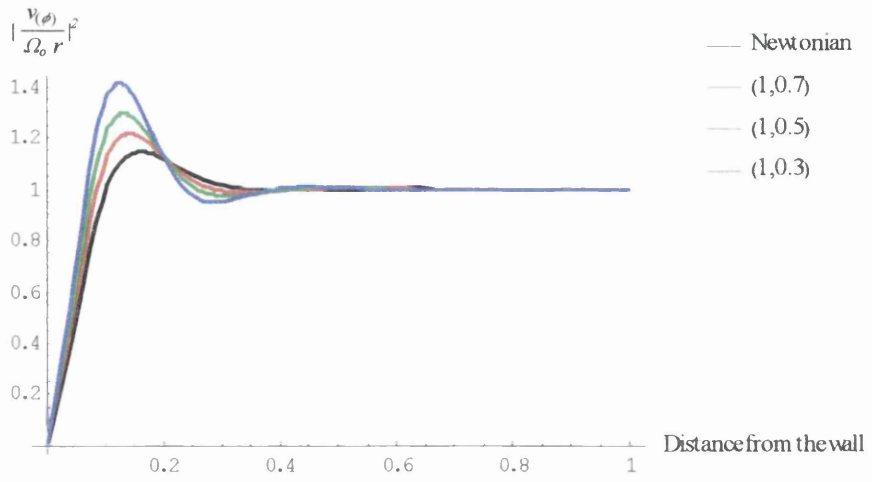

Fig. 5.1.4b Primary flow profiles for various values of the elastic parameters $(n\lambda_1, n\lambda_2)$ when $R_b = 20, R_b/R_a = 0.2$ and $r = 0.2$.

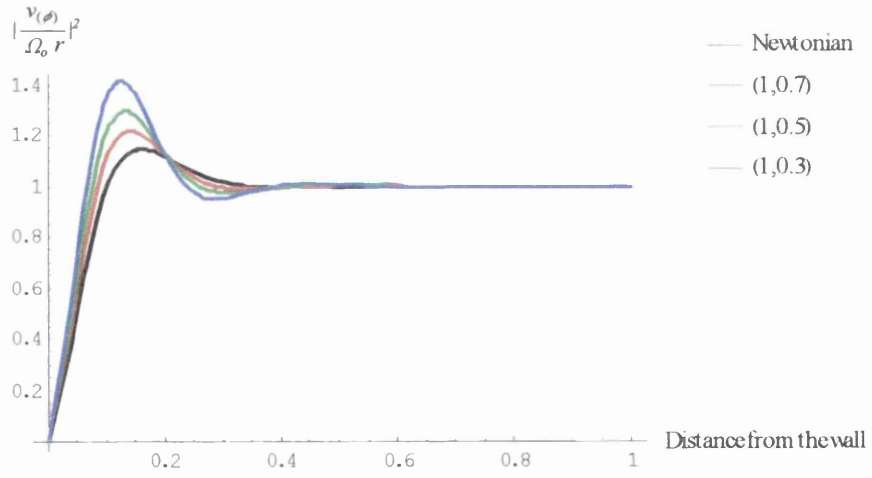

Fig. 5.1.4c Primary flow profiles for various values of the elastic parameters $(n\lambda_1, n\lambda_2)$ when $R_b = 20, R_b/R_a = 0.2$ and $r = 0.5$.

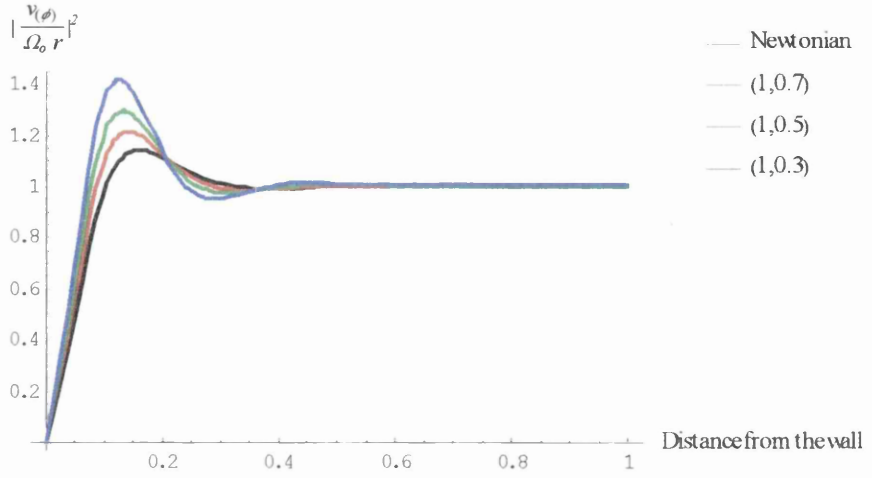

Fig. 5.1.4d Primary flow profiles for various values of the elastic parameters $(n\lambda_1, n\lambda_2)$ when $R_b = 20$, $R_b/R_a = 0.2$ and $r = 0.9$.

ii. Deep well $(b \gg a)$

Region remote from the axis $r = 0$:

In this region of flow both $|k|\,a$ and $|k|\,r$ are large, and so on using the asymptotic expansions for the Bessel functions in equation (5.1.35), it is found that, on neglecting exponentially small terms,

$$\bar{\omega}(r) \simeq \Omega_0 \left(\frac{a}{r}\right)^{\frac{3}{2}} e^{-(a-r)|k|(\sin\chi + i\cos\chi)},$$

and

$$v_{(\phi)} \simeq \Omega_0 r\, \mathrm{Re}[(\left(\frac{a}{r}\right)^{\frac{3}{2}} e^{-(a-r)|k|(\sin\chi + i\cos\chi)} - 1)e^{int}]. \qquad (5.1.40)$$

The exponential term here has only appreciable effect in a thin layer adjacent to the wall $r = a$. Within this *boundary-layer* the velocity varies rapidly, there attaining a high peak; but elsewhere, outside this layer, the flow approaches that of a rigid body rotation of the same angular amplitude (Ω_0) and frequency $(n/2\pi)$ as that of the

boundary wall, but of phase π behind it. The effect of elasticity is again to decrease somewhat the thickness of this boundary layer where the velocity varies rapidly and to increase the peak value of the velocity.

Region near the central axis:

In this region $|k|\,a \gg 1$ and $|k|\,r \ll 1$, and it is not difficult to show that, on neglecting exponentially small terms,

$$\bar{\omega}(z) \simeq 0,$$

and

$$v_{(\phi)} \simeq \Omega_0 r\, \mathrm{Re}[-e^{int}], \tag{5.1.41}$$

corresponding to a flow as described above in the region outside the wall boundary layer. The above general features of the flow are fairly accurately reflected in the *exact* profiles exhibited in Figs. (5.1.5a-d) and (5.1.6a-d).

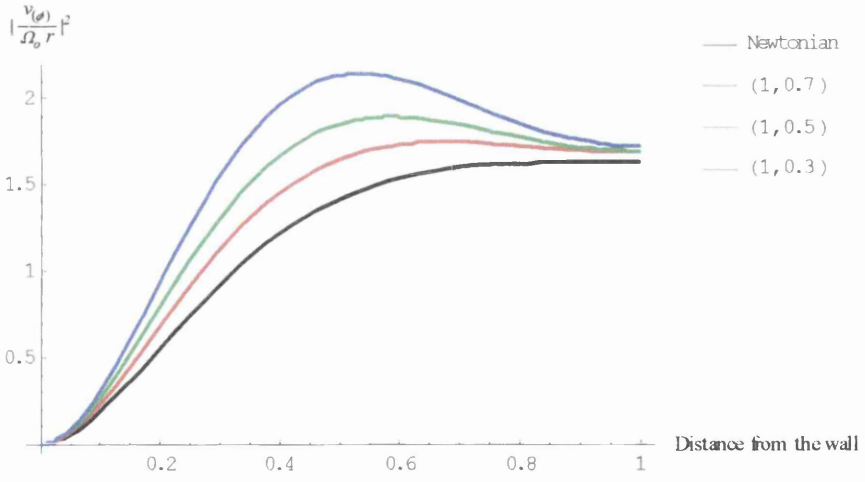

Fig. 5.1.5a Primary flow profiles for various values of the elastic parameters $(n\lambda_1, n\lambda_2)$ when $R_a = 6, R_a/R_b = 0.2$ and $z = 1$.

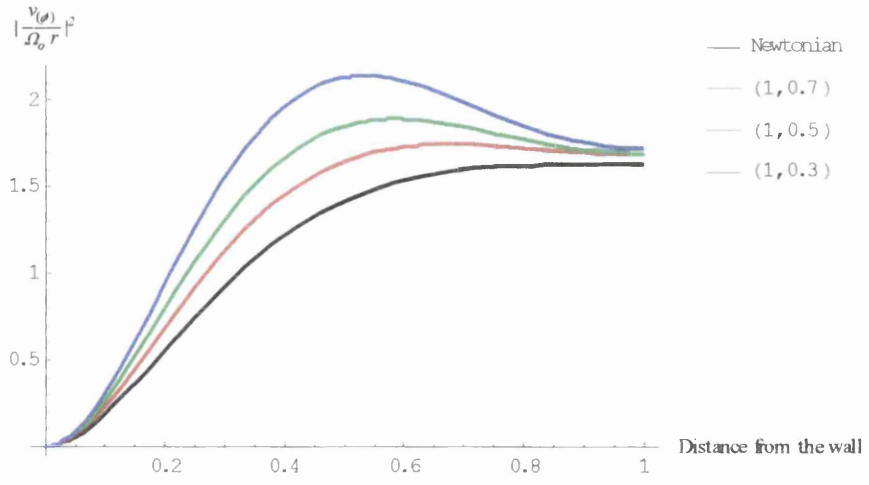

Fig. 5.1.5b Primary flow profiles for various values of the elastic parameters $(n\lambda_1, n\lambda_2)$ when $R_a = 6, R_a/R_b = 0.2$ and $z = 0.8$.

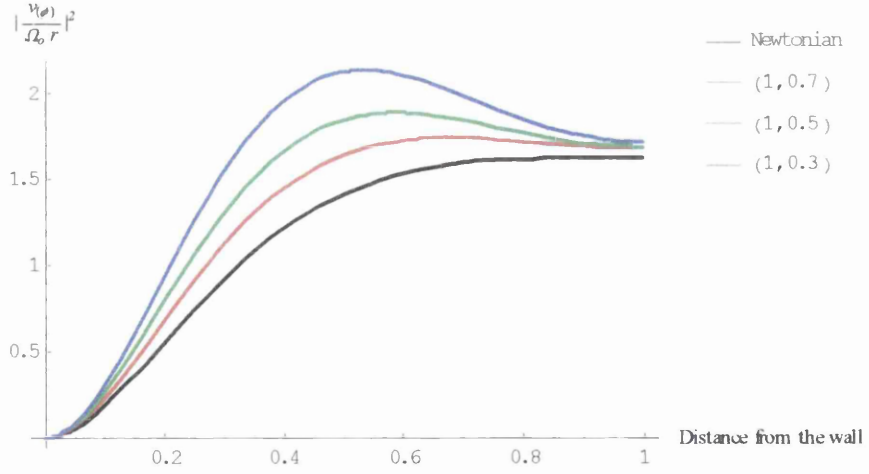

Fig. 5.1.5c Primary flow profiles for various values of the elastic parameters $(n\lambda_1, n\lambda_2)$ when $R_a = 6, R_a/R_b = 0.2$ and $z = 0.5$.

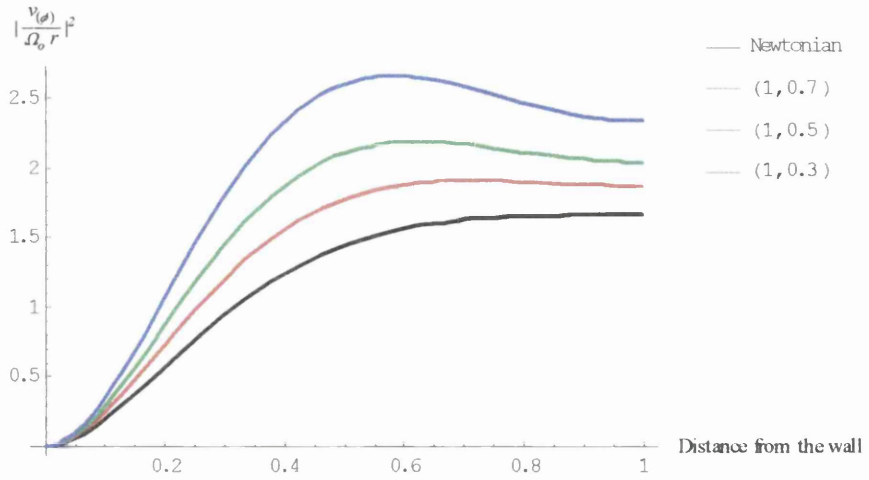

Fig. 5.1.5d Primary flow profiles for various values of the elastic parameters $(n\lambda_1, n\lambda_2)$ when $R_a = 6, R_a/R_b = 0.2$ and $z = 0.1$.

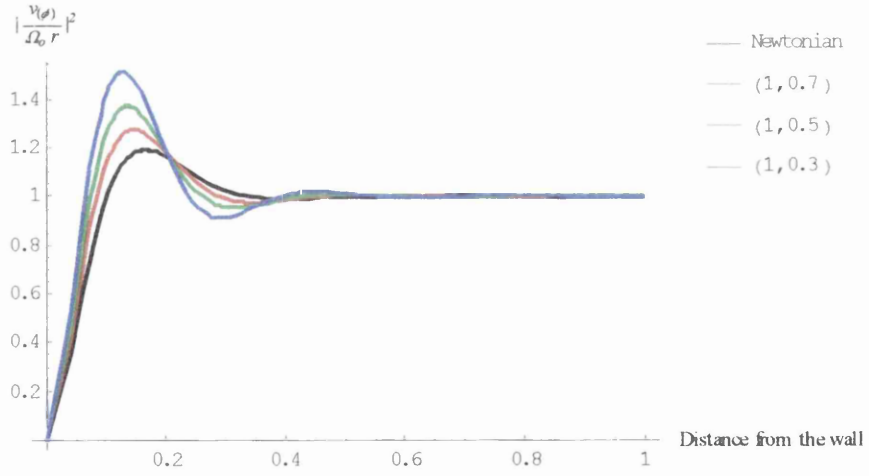

Fig. 5.1.6a Primary flow profiles for various values of the elastic parameters $(n\lambda_1, n\lambda_2)$ when $R_a = 20, R_a/R_b = 0.2$ and $z = 1$.

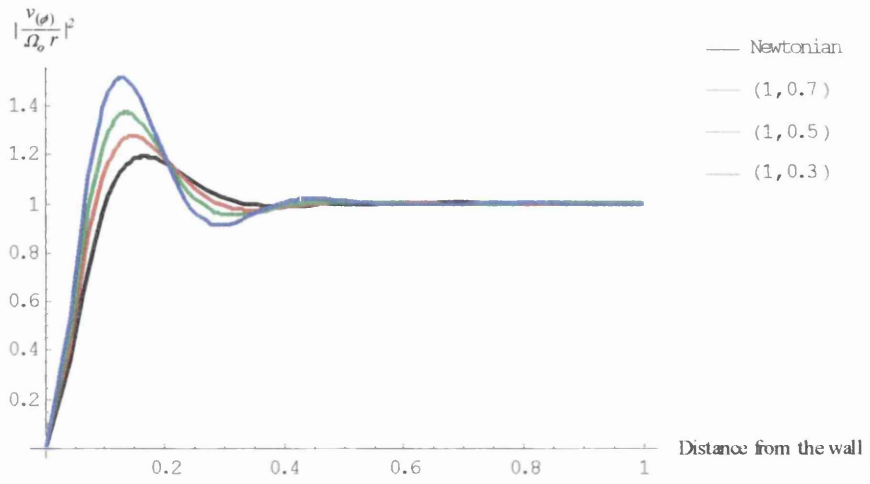

Fig. 5.1.6b Primary flow profiles for various values of the elastic parameters $(n\lambda_1, n\lambda_2)$ when $R_a = 20, R_a/R_b = 0.2$ and $z = 0.8$.

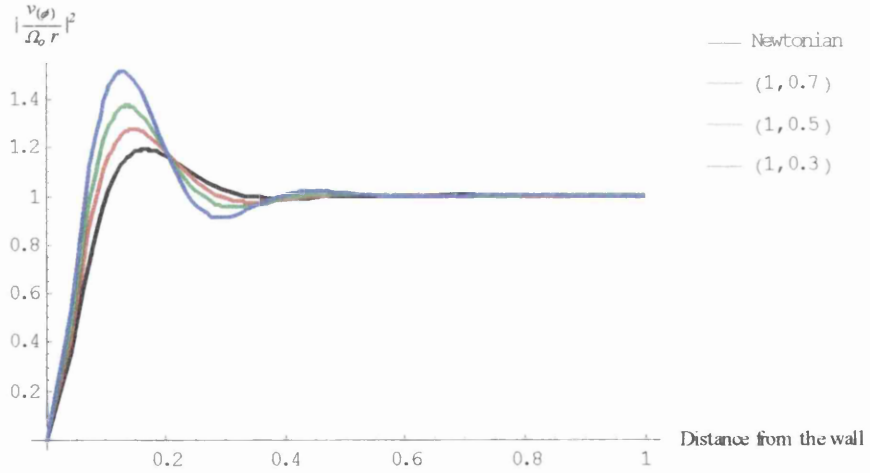

Fig. 5.1.6c Primary flow profiles for various values of the elastic parameters $(n\lambda_1, n\lambda_2)$ when $R_a = 20, R_a/R_b = 0.2$ and $z = 0.5$.

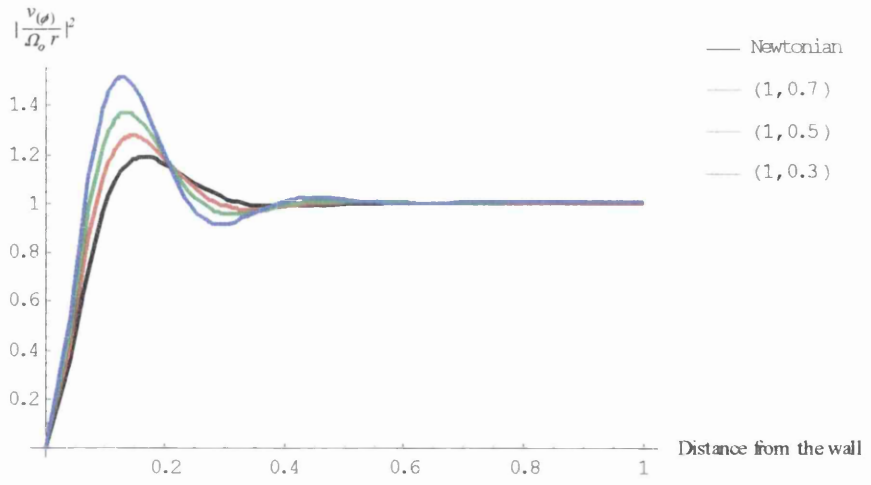

Fig. 5.1.6d Primary flow profiles for various values of the elastic parameters $(n\lambda_1, n\lambda_2)$ when $R_a = 20, R_a/R_b = 0.2$ and $z = 0.1$.

The general nature of the (primary) flow within the well *when n is large* is now ascertained in general terms:

(i) the main body of the mixture rotates as if rigid with the same angular amplitude (Ω_0) and frequency $(n/2\pi)$ as that of the boundary wall, but of phase π behind it, and hence *in space* its motion is one of pure translation (without rotation);

(ii) the motion of the mixture immediately adjacent to the boundary wall varies intensely with distance from the wall, there attaining a high peak value, these variations in the flow being significantly changed by the presence of elasticity.

5.2 Secondary Flow

The equation governing the (secondary) steady streaming flow, as characterized by the stream function $\psi_0(r,z)$, is given by equation (3.2.24), viz.

$$\frac{\partial^2\psi_0}{\partial r^2}-\frac{1}{r}\frac{\partial\psi_0}{\partial r}+\frac{\partial^2\psi_0}{\partial z^2}=\frac{r^2}{2}\frac{\partial}{\partial z}\{\bar{\omega}\bar{\omega}^*-2K_1(\frac{\partial\bar{\omega}}{\partial r}\frac{\partial\bar{\omega}^*}{\partial r}+\frac{\partial\bar{\omega}}{\partial z}\frac{\partial\bar{\omega}^*}{\partial z})\}, \qquad (5.2.1)$$

and is to be associated with the boundary conditions

$$\psi_0(r,z) = 0 \text{ on } r=a, \qquad (5.2.2a)$$

$$\psi_0(r,z) = 0 \text{ on } z=0, \qquad (5.2.2b)$$

$$\psi_0(r,z) = 0 \text{ on } z=b, \qquad (5.2.2c)$$

together with the understood condition that $\psi_0(r,z)$ is finite throughout the region of flow. Here $K_1=\eta_0(\lambda_1-\lambda_2)/\rho(1+n^2\lambda_1^2)$. No progress can be reported in the finding of an exact analytical solution of this equation for $\psi_0(r,z)$, the difficulty arising from the unwieldy representation of the primary flow, a rather complicated infinite series, whichever of the two representations (5.1.21), (5.1.31) is chosen. The steady streaming flow, as characterized by $\psi_0(r,z)$, is the mechanism within the oscillatory 'jiggle' mode whereby fluid elements are transported from one region of the well to another, and it is thus important to be able to comment, even if only in a vague way, on its overall structure. Some progress can be made in this direction within two schemes: that in which $a \gg b$ (or, equally, $R_a(=\sqrt{(n\rho a^2/\eta_0)}) \gg R_b(=\sqrt{(n\rho b^2/\eta_0)})$); and that in which $b \gg a$ ($R_b \gg R_a$).

I. The case in which $a \gg b$, i.e. $R_a \gg R_b$

When $a \gg b$ it is suitable to express $\bar{\omega}(r,z)$ in the form (5.1.20), viz.

$$\bar{\omega}(r,z) = \frac{\Omega_0 \cos k(b-z)}{\cos kb} + \frac{4\Omega_0 ak^2}{\pi r} \sum_{m=0}^{\infty} \frac{J_1(h_{2m+1}r)}{(2m+1)h_{2m+1}^2 J_1(h_{2m+1}a)} \sin[\frac{(2m+1)\pi z}{2b}]. \tag{5.2.3}$$

In the illustrations undertaken here, corresponding to the values $R_b/R_a = 0.2$, $\lambda_2/\lambda_1 = 0.25$, $b^2\rho/\eta_0\lambda_1 = 50$, it is interesting to look at the errors involved in truncating the infinite series in (5.2.3) at $m = 1$. Figs 5.2.1a,b give a numerical plot of the size of the error involved.

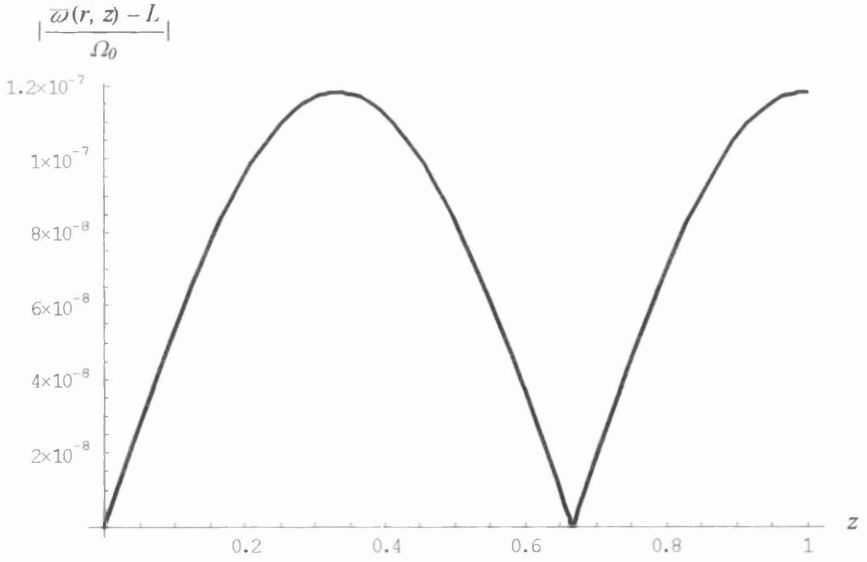

Fig 5.2.1a The plot of $|(\bar{\omega}(r,z) - L)/\Omega_0|$ vs. z, where $L = \Omega_0\{\frac{\cos k(b-z)}{\cos kb} + \frac{4ak^2}{\pi r}\frac{J_1(h_1 r)}{h_1^2 J_1(h_1 a)} \sin[\frac{\pi z}{2b}]\}$, $R_b = 1$ and $r = 0.5$.

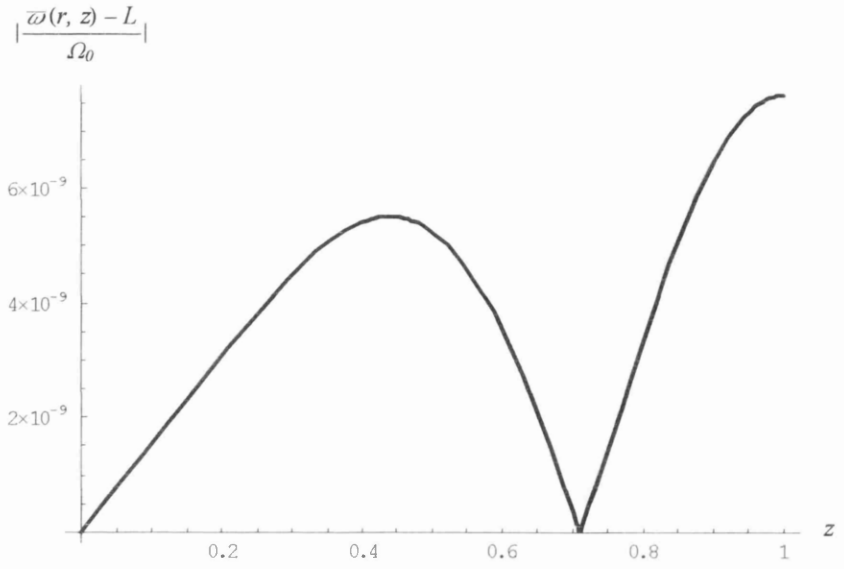

Fig 5.2.1b The plot of $|(\bar{\omega}(r,z)-L)/\Omega_0|$ vs. z, where $L=\Omega_0\{\frac{\cos k(b-z)}{\cos kb}+\frac{4ak^2}{\pi r}\frac{J_1(h_1 r)}{h_1^2 J_1(h_1 a)}\sin[\frac{\pi z}{2b}]\}$, $R_b=10$ and $r=0.5$.

It may be concluded that the first term in the infinite series on the right hand side of (5.2.3), i.e. the term defined by

$$\frac{4ak^2}{\pi r}\frac{J_1(h_1 r)}{h_1^2 J_1(h_1 a)}\sin[\frac{\pi z}{2b}],$$

is by far the dominant term. Thus within such a scheme one may write

$$\bar{\omega}(r,z)\simeq\Omega_0\left(\frac{\cos k(b-z)}{\cos kb}+\frac{4ak^2}{\pi r}\frac{J_1(h_1 r)}{h_1^2 J_1(h_1 a)}\sin[\frac{\pi z}{2b}]\right). \qquad (5.2.4)$$

It is important to stress that this expression for $\bar{\omega}(r,z)$, although approximate, satisfies not only the governing differential equation (5.1.1) but also the exact boundary conditions on the wall $z=0$ and on the free surface $z=b$. It fails only to satisfy the *single* condition $\bar{\omega}(r,z)=\Omega_0$ on the boundary wall $r=a$, which wall is deemed too distant to have any appreciable effect on the flow.

Consistent with the above approximation, one finds that

$$\begin{aligned}\bar{\omega}\bar{\omega}^* &= \Omega_0^2[(\cosh\alpha_1+\cos\alpha_2)^{-1}\{\cosh[\alpha_1(1-\frac{z}{b})]+\cos[\alpha_2(1-\frac{z}{b})]\} \\ &+(\frac{2k^2aJ_1(h_1r)}{\pi h_1^2 r J_1(h_1a)\cos k^*b}\{\sin[k^*(b-z)+\frac{\pi z}{2b}]-\sin[k^*(b-z)-\frac{\pi z}{2b}]\} \\ &+\textit{the complex conjugate expression)}], \qquad (5.2.5)\end{aligned}$$

$$\begin{aligned}\frac{\partial\bar{\omega}}{\partial z}\frac{\partial\bar{\omega}^*}{\partial z} &= \Omega_0^2[\,|k|^2\,(\cosh\alpha_1+\cos\alpha_2)^{-1}\{\cosh[\alpha_1(1-\frac{z}{b})]+\cos[\alpha_2(1-\frac{z}{b})]\} \\ &+(\frac{k^*k^2aJ_1(h_1r)}{bh_1^2rJ_1(h_1a)\cos k^*b}\{\sin[k^*(b-z)+\frac{\pi z}{2b}]+\sin[k^*(b-z)-\frac{\pi z}{2b}]\} \\ &+\textit{the complex conjugate expression)}], \qquad (5.2.6)\end{aligned}$$

where $\alpha_1 = 2\,|k|\,b\sin\chi$ and $\alpha_2 = 2\,|k|\,b\cos\chi$. Thus, the equation for $\psi_0(r,z)$ reduces to[33]

$$\begin{aligned}\frac{\partial^2\psi_0}{\partial r^2}-\frac{1}{r}\frac{\partial\psi_0}{\partial r}+\frac{\partial^2\psi_0}{\partial z^2} &= \frac{\Omega_0^2r^2}{2}[(\cosh\alpha_1+\cos\alpha_2)^{-1}\{-\frac{\alpha_1}{b}[1-2\,|k|^2\,K_1] \\ &\sinh[\alpha_1(1-\frac{z}{b})]+\frac{\alpha_2}{b}[1+2\,|k|^2\,K_1] \\ &\sin[\alpha_2(1-\frac{z}{b})]\}+(\frac{2k^2aJ_1(h_1r)}{h_1^2rJ_1(h_1a)\cos k^*b} \\ &\{(\frac{1}{\pi}-\frac{k^*K_1}{b})(\frac{\pi}{2b}-k^*)\cos[k^*(b-z)+\frac{\pi z}{2b}] \\ &+(\frac{1}{\pi}+\frac{k^*K_1}{b})(\frac{\pi}{2b}+k^*)\cos[k^*(b-z)-\frac{\pi z}{2b}]\} \\ &+\textit{the complex conjugate expression)}]. \qquad (5.2.7)\end{aligned}$$

On writing $\psi_0(r,z)$ in the form

$$\psi_0(r,z) = r^2F_1(z)+[rJ_1(h_1r)F_2(z)+\textit{the complex conjugate expression}], \qquad (5.2.8)$$

[33] Here $(\partial\bar{\omega}/\partial r)(\partial\bar{\omega}^*/\partial r)$ is of lower order of magnitude compared with $(\partial\bar{\omega}/\partial z)(\partial\bar{\omega}^*/\partial z)$.

the following equations for $F_1(z)$ and $F_2(z)$ result:

$$F_1''(z) = \frac{\Omega_0^2}{2}\frac{d}{dz}[(\cosh\alpha_1+\cos\alpha_2)^{-1}\{[1-2|k|^2K_1]\cosh[\alpha_1(1-\frac{z}{b})] + [1+2|k|^2K_1]\cos[\alpha_2(1-\frac{z}{b})]\}], \tag{5.2.9}$$

$$F_2''(z)-h_1^2F_2(z) = \frac{\Omega_0^2k^2a}{\pi h_1^2J_1(h_1a)\cos k^*b}\{-M_1(k^*-\frac{\pi}{2b})\cos[k^*(b-z)+\frac{\pi z}{2b}] + M_2(k^*+\frac{\pi}{2b})\cos[k^*(b-z)-\frac{\pi z}{2b}]\}, \tag{5.2.10}$$

where $M_1 = 1-\pi k^*K_1/b$ and $M_2 = 1+\pi k^*K_1/b$. These equations are to be associated with the boundary conditions

$$F_i(0) = F_i(b) = 0, \quad (i=1,2), \tag{5.2.11}$$

together with the understood condition that $F_1(z)$ and $F_2(z)$ are finite throughout the region of flow.

By integration of equation (5.2.9)

$$F_1(z) = -b\Omega_0^2(\cosh\alpha_1+\cos\alpha_2)^{-1}\{N_1\sinh[\alpha_1(1-\frac{z}{b})]+N_2\sin[\alpha_2(1-\frac{z}{b})]\}+Az+B, \tag{5.2.12}$$

where $N_1 = (1-2|k|^2K_1)/2\alpha_1$ and $N_2 = (1+2|k|^2K_1)/2\alpha_2$, A and B being arbitrary constants. On imposing the boundary conditions (5.2.11), one obtains

$$F_1(z) = b\Omega_0^2(\cosh\alpha_1+\cos\alpha_2)^{-1}\{N_1[(1-\frac{z}{b})\sinh\alpha_1-\sinh[\alpha_1(1-\frac{z}{b})]] + N_2[(1-\frac{z}{b})\sin\alpha_2-\sin[\alpha_2(1-\frac{z}{b})]]\}. \tag{5.2.13}$$

Next, to construct the solution of the differential equation (5.2.10). Two linearly independent solutions of the associated homogeneous equation are seen to be $\cosh h_1z$,

$\sinh h_1 z$. To proceed, one writes by the usual method of variation of parameters

$$F_2(z) = v_1(z)\cosh h_1 z + v_2(z)\sinh h_1 z. \tag{5.2.14}$$

It is then straightforward to show that

$$\begin{aligned} v_1(z) &= A + \frac{\Omega_0^2 k^2 a}{\pi h_1^3 J_1(h_1 a)\cos k^* b}\{\frac{M_1(k^* - \frac{\pi}{2b})}{h_1^2 + (k^* - \frac{\pi}{2b})^2}(h_1 \cosh h_1 z \\ &\quad \cos[k^*(b-z) + \frac{\pi z}{2b}] - (k^* - \frac{\pi}{2b})\sinh h_1 z \sin[k^*(b-z) + \frac{\pi z}{2b}]) \\ &\quad - \frac{M_2(k^* + \frac{\pi}{2b})}{h_1^2 + (k^* + \frac{\pi}{2b})^2}(h_1 \cosh h_1 z \cos[k^*(b-z) - \frac{\pi z}{2b}] \\ &\quad - (k^* + \frac{\pi}{2b})\sinh h_1 z \sin[k^*(b-z) - \frac{\pi z}{2b}])\}, \end{aligned}$$

and

$$\begin{aligned} v_2(z) &= B + \frac{\Omega_0^2 k^2 a}{\pi h_1^3 J_1(h_1 a)\cos k^* b}\{\frac{-M_1(k^* - \frac{\pi}{2b})}{h_1^2 + (k^* - \frac{\pi}{2b})^2}(h_1 \sinh h_1 z \\ &\quad \cos[k^*(b-z) + \frac{\pi z}{2b}] - (k^* - \frac{\pi}{2b})\cosh h_1 z \sin[k^*(b-z) + \frac{\pi z}{2b}]) \\ &\quad + \frac{M_2(k^* + \frac{\pi}{2b})}{h_1^2 + (k^* + \frac{\pi}{2b})^2}(h_1 \sinh h_1 z \cos[k^*(b-z) - \frac{\pi z}{2b}] \\ &\quad - (k^* + \frac{\pi}{2b})\cosh h_1 z \sin[k^*(b-z) - \frac{\pi z}{2b}])\}, \end{aligned}$$

A and B being arbitrary constants. Finally, on imposing the boundary conditions (5.2.11), one obtains

$$\begin{aligned} F_2(z) &= \frac{\Omega_0^2 k^2 a}{\pi h_1^2 J_1(h_1 a)}\{(-\frac{M_1(k^* - \frac{\pi}{2b})}{h_1^2 + (k^* - \frac{\pi}{2b})^2} + \frac{M_2(k^* + \frac{\pi}{2b})}{h_1^2 + (k^* + \frac{\pi}{2b})^2})\frac{\sinh h_1(b-z)}{\sinh h_1 b} \\ &\quad + \frac{M_1(k^* - \frac{\pi}{2b})}{h_1^2 + (k^* - \frac{\pi}{2b})^2}\frac{\cos[k^*(b-z) + \frac{\pi z}{2b}]}{\cos k^* b} \\ &\quad - \frac{M_2(k^* + \frac{\pi}{2b})}{h_1^2 + (k^* + \frac{\pi}{2b})^2}\frac{\cos[k^*(b-z) - \frac{\pi z}{2b}]}{\cos k^* b}\}. \end{aligned} \tag{5.2.15}$$

Thus, the solution of (5.2.1), (5.2.2a-c) in the case when $a \gg b$, or when $R_a \gg R_b$, is

$$\psi_0(r,z) = r^2 F_1(z) + r J_1(h_1 r) F_2(z) + r J_1(h_1^* r) F_2^*(z), \tag{5.2.16}$$

where $F_1(z)$ and $F_2(z)$ are as given by equations (5.2.13) and (5.2.15).

The expression for $\psi_0(r,z)$ is too complicated in mathematical form to allow any broad analytical comment to be made on the structure of the flow. Any comment has to be guided by numerical evaluation. The streamline projection exhibited in Figs. 5.2.2a-d correspond to the values $R_b/R_a = 0.2$, $\lambda_2/\lambda_1 = 0.25$, $b^2\rho/\eta_0\lambda_1 = 50$, and for a range of values of R_b. For small values of R_b (i.e. of n) the flow is seen to be similar to that of a Newtonian fluid, i.e. a flow controlled by centrifugal actions. As the Reynolds-type number R_b increases a region develops in the interior within which non-Newtonian actions dominate resulting in a region of flow reversal. This region of flow reversal expands with increasing R_b to occupy the whole region within the well. With ever increasing values of R_b the process is put in reverse until, eventually, the whole region again becomes dominated by centrifugal actions.

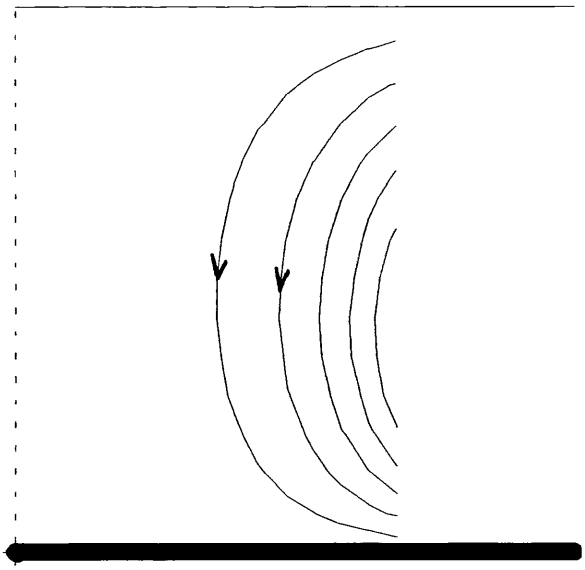

Fig. 5.2.2a Secondary (steady) streaming $\psi_0(r,z) = \textit{constant}$ when $R_b = 1$.

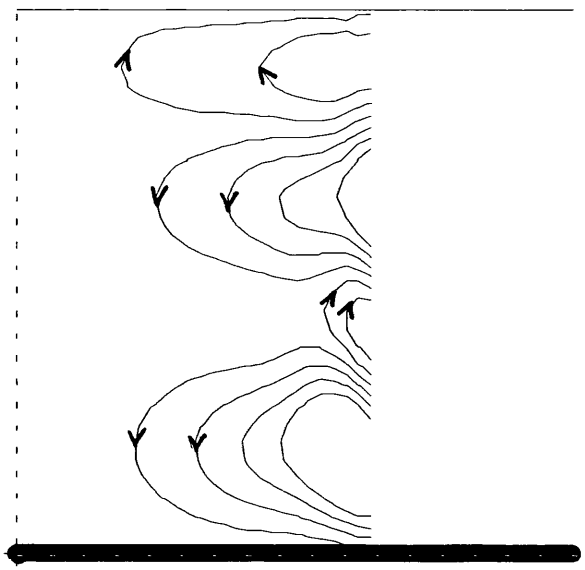

Fig. 5.2.2b Secondary (steady) streaming $\psi_0(r, z) = \textit{constant}$ when $R_b = 6.85$.

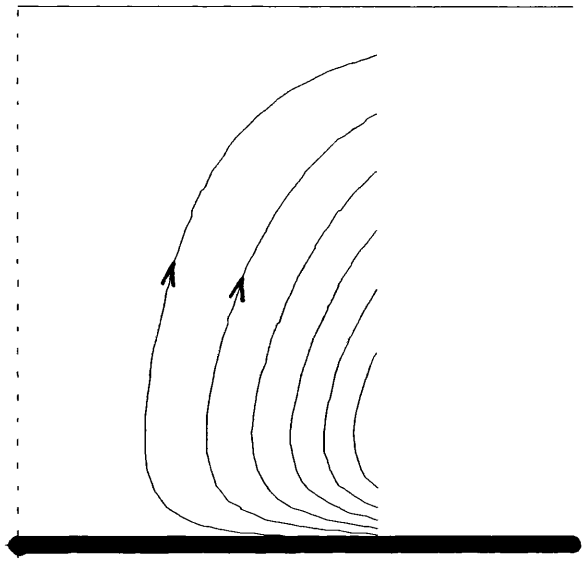

Fig. 5.2.2c Secondary (steady) streaming $\psi_0(r, z) = \textit{constant}$ when $R_b = 10$.

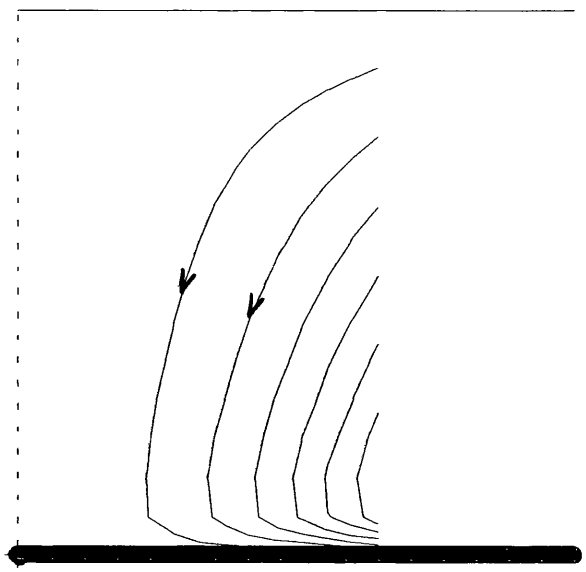

Fig. 5.2.2d Secondary (steady) streaming $\psi_0(r,z) = \textit{constant}$ when $R_b = 16$.

II. The case in which $b \gg a$, i.e. $R_b \gg R_a$

When $b \gg a$, it is appropriate to express $\bar{\omega}(r,z)$ in the form (5.1.30),viz.

$$\bar{\omega}(r,z) = \Omega_0 \frac{aJ_1(kr)}{rJ_1(ka)} - \frac{2\Omega_0 k^2}{r} \sum_{i=1}^{\infty} \frac{1}{q_i l_i^2} \frac{\cos l_i(b-z)}{\cos l_i b} \frac{J_1(q_i r)}{J_0(q_i a)}. \tag{5.2.17}$$

As previously remarked, the infinite series representation of the primary flow $\bar{\omega}(r,z)$ makes the construction of an analytic solution of equation (5.2.1) prohibitive. However, in the case under consideration, i.e. that in which $b \gg a$, and for the values $R_a/R_b = 0.2$, $\lambda_2/\lambda_1 = 0.25$, $a^2\rho/\eta_0\lambda_1 = 50$, viz. the numerical parameters chosen for illustration purposes, inspection shows that, even for reasonably large values of the Reynolds-type number R_a, the infinite series (5.2.17) for $\bar{\omega}(r,z)$ converges rapidly. The numerical findings, exhibited graphically in Figs 5.2.2a,b, show that the error involved in replacing the infinite series by a finite series ($i = 1$) is negligibly small.

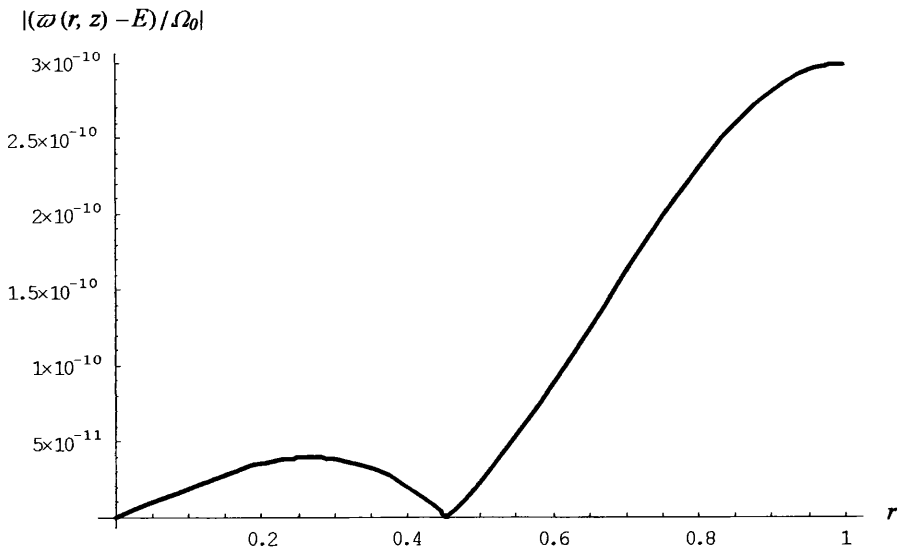

Fig 5.2.2a The plot of $|(\bar{\omega}(r,z) - E)/\Omega_0|$ vs. r where $E = \Omega_0\{\frac{aJ_1(kr)}{rJ_1(ka)} - \frac{2k^2}{q_1 l_1^2 r}\frac{\cos l_1(b-z)}{\cos l_1 b}\frac{J_1(q_1 r)}{J_0(q_1 a)}\}$, $R_a = 1$ and $z = 0.5$.

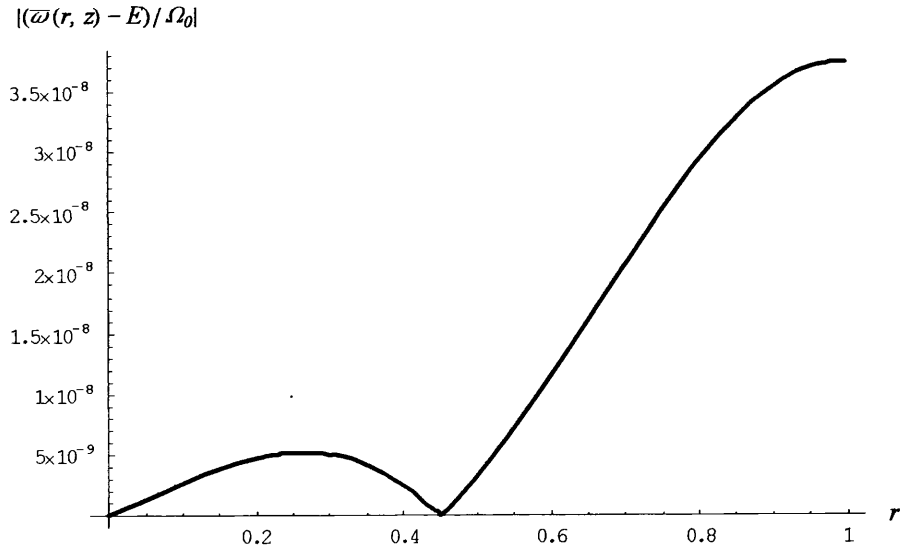

Fig 5.2.2b The plot of $|(\bar{\omega}(r,z) - E)/\Omega_0|$ vs. r where $E = \Omega_0\{\frac{aJ_1(kr)}{rJ_1(ka)} - \frac{2k^2}{q_1 l_1^2 r}\frac{\cos l_1(b-z)}{\cos l_1 b}\frac{J_1(q_1 r)}{J_0(q_1 a)}\}$, $R_a = 10$ and $z = 0.5$.

There is ample justification, therefore, in proceeding with the analysis by writing

$$\bar{\omega}(r,z) \simeq \Omega_0 \left(\frac{aJ_1(kr)}{rJ_1(ka)} - \frac{2k^2}{q_1 l_1^2 r} \frac{\cos l_1(b-z)}{\cos l_1 b} \frac{J_1(q_1 r)}{J_0(q_1 a)} \right). \tag{5.2.18}$$

Again, it is significant to observe that the expression for $\bar{\omega}(r,z)$ here, although approximate, satisfies all the required conditions other than the *single* condition $\bar{\omega}(r,z) = \Omega_0$ on the boundary wall $z = 0$, which wall is deemed too distant from the region of flow under investigation to have any significant effect.

It follows that, to the same order of approximation,

$$\begin{aligned} \bar{\omega}\bar{\omega}^* \;=\; & \Omega_0^2 [\frac{a^2}{r^2} \frac{J_1(kr)}{J_1(ka)} \frac{J_1(k^*r)}{J_1(k^*a)} - (\frac{2ak^2}{q_1 l_1^2 r^2} \frac{\cos l_1(b-z)}{\cos l_1 b} \frac{J_1(k^*r)}{J_1(k^*a)} \frac{J_1(q_1 r)}{J_0(q_1 a)} \\ & + \textit{the complex conjugate expression})], \end{aligned} \tag{5.2.19}$$

$$\begin{aligned} \frac{\partial \bar{\omega}}{\partial r} \frac{\partial \bar{\omega}^*}{\partial r} \;=\; & \Omega_0^2 [\frac{a^2 |k|^2}{r^2} \frac{J_2(kr)}{J_1(ka)} \frac{J_2(k^*r)}{J_1(k^*a)} - (\frac{2ak |k|^2}{l_1^2 r^2} \frac{\cos l_1(b-z)}{\cos l_1 b} \frac{J_2(k^*r)}{J_1(k^*a)} \frac{J_2(q_1 r)}{J_0(q_1 a)} \\ & + \textit{the complex conjugate expression})]. \end{aligned} \tag{5.2.20}$$

The resulting equation for $\psi_0(r,z)$ then reduces to[34]

$$\begin{aligned} \frac{\partial^2 \psi_0}{\partial r^2} - \frac{1}{r} \frac{\partial \psi_0}{\partial r} + \frac{\partial^2 \psi_0}{\partial z^2} \;=\; & -\frac{\Omega_0^2 a k^2}{q_1 l_1} (\frac{J_1(k^*r) J_1(q_1 r) - 2k^* q_1 K_1 J_2(k^*r) J_2(q_1 r)}{J_1(k^*a) J_0(q_1 a)}) \\ & \frac{\sin l_1(b-z)}{\cos l_1 b} + \textit{the complex conjugate expression.} \end{aligned} \tag{5.2.21}$$

By writing $\psi_0(r,z)$ in the form

$$\psi_0(r,z) = F(r) \sin l_1(b-z) + \textit{the complex conjugate expression,} \tag{5.2.22}$$

[34] Here $(\partial\bar{\omega}/\partial z)(\partial\bar{\omega}^*/\partial z)$ is of lower order of magnitude compared with $(\partial\bar{\omega}/\partial r)(\partial\bar{\omega}^*/\partial r)$.

equation (5.2.21) reduces to give the following ordinary differential equation for $F(r)$

$$F''(r) - \frac{1}{r}F'(r) - l_1^2 F(r) = \frac{-\Omega_0^2 a k^2}{q_1 l_1 \cos l_1 b}\left(\frac{J_1(k^* r)J_1(q_1 r) - 2k^* q_1 K_1 J_2(k^* r)J_2(q_1 r)}{J_1(k^* a)J_0(q_1 a)}\right), \tag{5.2.23}$$

and is subject to the conditions

$$F(r) \text{ is finite in } 0 \leq r \leq a, \tag{5.2.24a}$$

$$F(a) = 0, \tag{5.2.24b}$$

The associated homogeneous differential equation of (5.2.23) may be written in the more recognizable form

$$r^2 \frac{d^2}{dr^2}\left(\frac{F(r)}{r}\right) + r\frac{d}{dr}\left(\frac{F(r)}{r}\right) + [(il_1 r)^2 - 1]\left(\frac{F(r)}{r}\right) = 0, \tag{5.2.25}$$

two linearly independent solutions of which are seen to be $rJ_1(il_1 r)$ and $rY_1(il_1 r)$. Thus, the general solution of (5.2.23) can be constructed by the usual method of variation of parameters. By writing

$$F(r) = v_1(r) r J_1(il_1 r) + v_2(r) r Y_1(il_1 r), \tag{5.2.26}$$

it is not difficult to show that

$$\begin{aligned} v_1(r) &= A + \frac{\Omega_0^2 \pi a k^2 \sec l_1 b}{2q_1 l_1 J_1(k^* a)J_0(q_1 a)} \int_a^r Y_1(il_1 \xi)[J_1(k^* \xi)J_1(q_1 \xi) \\ &\quad -2k^* q_1 K_1 J_2(k^* \xi)J_2(q_1 \xi)]d\xi, \end{aligned}$$

and

$$\begin{aligned} v_2(r) &= B + \frac{-\Omega_0^2 \pi a k^2 \sec l_1 b}{2q_1 l_1 J_1(k^* a)J_0(q_1 a)} \int_a^r J_1(il_1 \xi)[J_1(k^* \xi)J_1(q_1 \xi) \\ &\quad -2k^* q_1 K_1 J_2(k^* \xi)J_2(q_1 \xi)]d\xi, \end{aligned}$$

A and B being arbitrary constants. In the process of solving one has made use of the result $J_n(x)Y_n'(x) - J_n'(x)Y_n(x) = \frac{2}{\pi x}$. Hence, the general solution of (5.2.23) may be written as

$$\begin{aligned} F(r) &= ArJ_1(il_1r) + BrY_1(il_1r) + \frac{\Omega_0^2\pi ak^2 \sec l_1 b}{2q_1l_1J_1(k^*a)J_0(q_1a)} \\ &\quad [rJ_1(il_1r)\int_a^r Y_1(il_1\xi)[J_1(k^*\xi)J_1(q_1\xi) - 2k^*q_1K_1J_2(k^*\xi)J_2(q_1\xi)]d\xi \\ &\quad -rY_1(il_1r)\int_a^r J_1(il_1\xi)[J_1(k^*\xi)J_1(q_1\xi) - 2k^*q_1K_1J_2(k^*\xi)J_2(q_1\xi)]d\xi]. \end{aligned} \tag{5.2.27}$$

By imposing conditions (5.2.24a,b), one obtains the result

$$\begin{aligned} F(r) &= \frac{\Omega_0^2\pi ak^2 \sec l_1 b}{2q_1l_1J_1(k^*a)J_0(q_1a)}\{rJ_1(il_1r)\frac{Y_1(il_1a)}{J_1(il_1a)}\int_0^a J_1(il_1\xi)[J_1(k^*\xi)J_1(q_1\xi) \\ &\quad -2k^*q_1K_1J_2(k^*\xi)J_2(q_1\xi)]d\xi - rY_1(il_1r)\int_0^r J_1(il_1\xi)[J_1(k^*\xi)J_1(q_1\xi) \\ &\quad -2k^*q_1K_1J_2(k^*\xi)J_2(q_1\xi)]d\xi + rJ_1(il_1r)\int_a^r Y_1(il_1\xi)[J_1(k^*\xi)J_1(q_1\xi) \\ &\quad -2k^*q_1K_1J_2(k^*\xi)J_2(q_1\xi)]d\xi. \end{aligned} \tag{5.2.28}$$

Finally

$$\psi_0(r,z) = F(r)\sin l_1(b-z) + F^*(r)\sin l_1^*(b-z), \tag{5.2.29}$$

$F(r)$ being as defined by (5.2.28).

The expression for $\psi_0(r,z)$ is far too complicated in mathematical form to allow one to make any general analytical deduction on the nature of flow. However, one may obtain a fair idea of the structure of flow by numerical evaluation. The streamline projections exhibited in Figs. 5.2.3a-f correspond to the values $R_a/R_b = 0.2$, $\lambda_2/\lambda_1 = 0.25$, $a^2\rho/\eta_0\lambda_1 = 50$, and for various values of R_a.

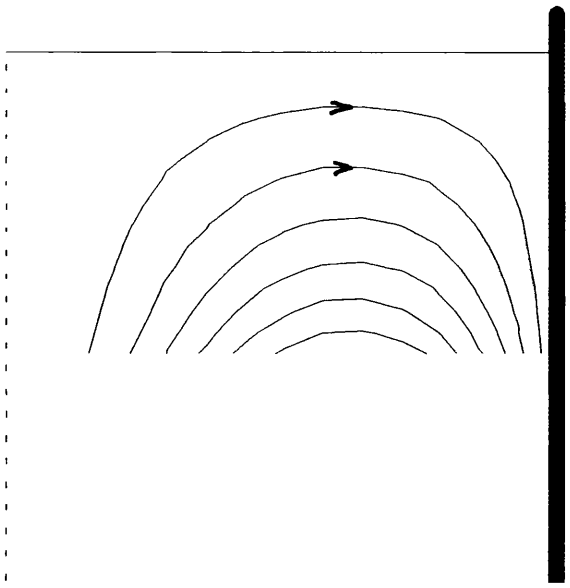

Fig. 5.2.3a Secondary (steady) streaming $\psi_0(r, z) = \textit{constant}$ when $R_a = 1$.

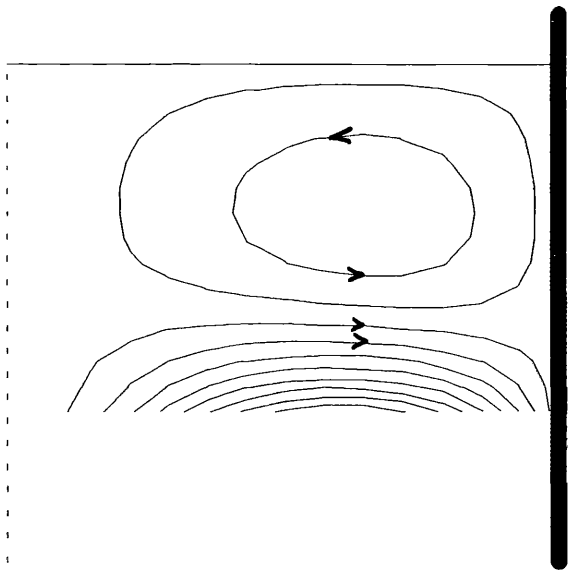

Fig. 5.2.3b Secondary (steady) streaming $\psi_0(r, z) = \textit{constant}$ when $R_a = 1.6535$.

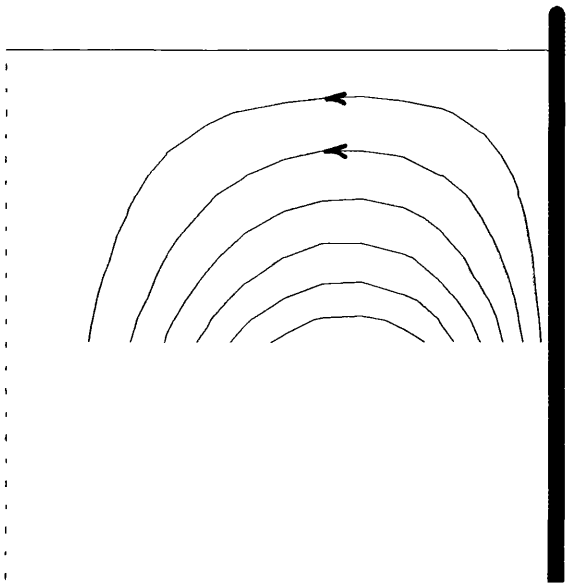

Fig. 5.2.3c Secondary (steady) streaming $\psi_0(r, z) = \textit{constant}$ when $R_a = 2$.

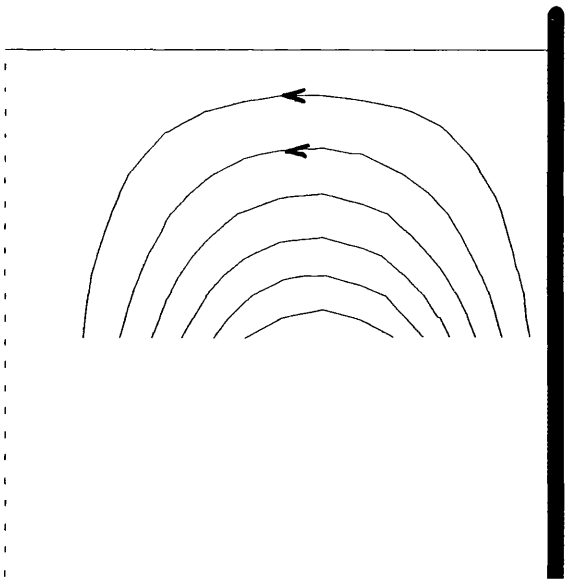

Fig. 5.2.3d Secondary (steady) streaming $\psi_0(r, z) = \textit{constant}$ when $R_a = 4$.

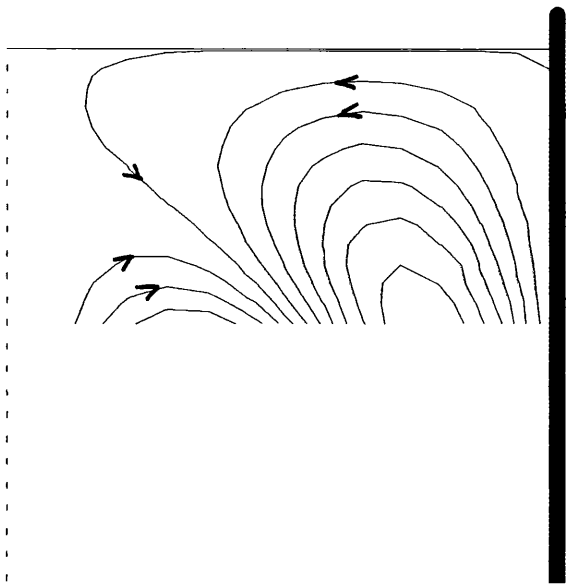

Fig. 5.2.3e Secondary (steady) streaming $\psi_0(r,z) = \textit{constant}$ when $R_a = 5$.

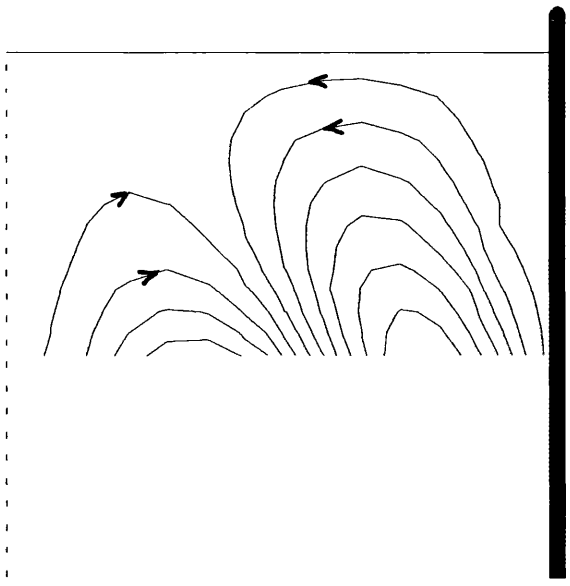

Fig. 5.2.3f Secondary (steady) streaming $\psi_0(r,z) = \textit{constant}$ when $R_a = 6$.

The pattern of events run very much in parallel to those described above for the case $a \gg b$, except that the roles of r, z are reversed. However, for values of R_a much in excess of 10 the accuracy of the development is brought into question.

5.3 References

Jones, J. R., and Walters, T. S., "Oscillatory motion of an elastico-viscous liquid contained in a cylindrical cup I. Theoretical", 1966, *Brit. J. Appl. Phys.*, **17,** 937.

CHAPTER 6
DRIFT PATTERN OF THE REAGENTS

The nature of the flow within the well whilst in motion on the outer carousel ring is now known in broad outline. The next (and final) stage is to determine the way in which the (particulate) reagents *drift* through the patient sample, supposing their concentration not sufficiently large to affect the structural nature of the flow; and , moreover, to determine the pattern which the reagents make when they eventually accumulate on the boundary wall. It is the purpose of the present chapter to address this problem, which investigation would complete the study of the hydro-mechanics associated with the Vitros Immunodiagnostic System.

6.1 Introduction

It is now necessary to give identity to the suspended (particulate) reagents. Again, as in previous discussions, all kinematic variables are measured relative to the (moving) Cartesian frame $Oxyz$ fixed relative to the well (cf. Chapter 3): Oz is vertically upwards and coincides with the well axis and Ox is along the radial direction CO. Relative to this frame, $\mathbf{x} = \mathbf{x}(\mathbf{x}_0, t)$ denotes the position of a suspended element at time t, the parameter $\mathbf{x}_0$, the position of the element at time t_0, being that which identifies the element and distinguishes it from all other elements. (No two elements can occupy the same position $\mathbf{x}_0$ at one and the same time t_0.) The problem, therefore, is that of tracing the position vector $\mathbf{x}(\mathbf{x}_0, t)$ as the element drifts within the

well for a large array of $\mathbf{x}_0$-values, and to determine their eventual positions when they end up caught on the boundary wall.

To proceed with such an undertaking, it is first necessary to model the force experienced by a suspended element due to its interaction with the patient sample. This would be a difficult if not insurmountable task, were it not for some crucial features of the motion. It has been pointed out that the incubation period for the patient sample whilst on the outer carousel ring is some 10 - 15 minutes, the time deemed necessary for the reagents to traverse distances of the order of centimetres to reach their final destination on the boundary wall. It is thus clearly the case that within the instrumentation cycle drift velocities are small; and, likewise, drift accelerations are small other than at isolated times when the reagents strike the wall.

To make progress, one may suppose, consistent with the above considerations,

(i) that interactive effects between elements are weak,

(ii) that interfacial tensions are sufficiently large to maintain the general spherical shapes of elements,

and

(iii) that flows in the locality of elements are axially symmetric.

These assumptions are deemed self consistent, appropriate to the information given of the Vitros Immunodiagnostic System , and satisfactory in a first exploratory study. On their bases, the *essential* force on an element due to the continuous phase is an axial drag opposing the relative velocity $\mathbf{U} = \dot{\mathbf{x}}\ (\mathbf{x}_0, t) - \mathbf{v}\ (\mathbf{x},t)$, $\mathbf{v}\ (\mathbf{x},t)$ denoting the velocity field of the patient sample as measured relative to the frame $Oxyz$. If the patient sample were purely viscous then this would be the Stokes drag of amount

$6\pi\varepsilon\eta\,|\mathbf{U}|$, where ε is the radius of the spherical element and η is the viscosity of the continuous phase. Leslie (1961) has made a study of such regimes when the host fluid is elastico-viscous. His findings are that the drag is reduced somewhat by the presence of elasticity and differs in amount from that of the Stokes value by terms $O(|\mathbf{U}|^3)$ when $|\mathbf{U}|$ is small. It is thus reasonable to suppose the drag to be represented, with sufficient approximation, by $-6\pi\varepsilon\eta_0(\dot{\mathbf{x}}\,(\mathbf{x}_0, t) - \mathbf{v}\,(\mathbf{x},t))$, η_0 being the intrinsic viscosity of the patient sample.

6.2 Equation Governing the Motion of the Reagents

The motion that is of interest in the present study is that of the reagents as measured relative to the well whilst in motion on the outer carousel ring, i.e. as measured relative to the frame $Oxyz$ exhibited in Fig. 6.2.1 (and as described in Chapter 3).

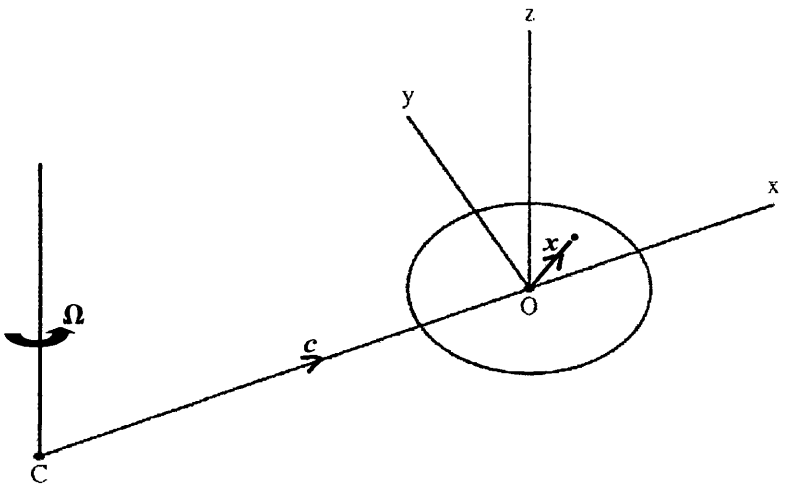

Fig. 6.2.1 The moving frame of reference $Oxyz$, rigidly attached to the well. C denotes the centre of the carousel ring.

In establishing equations which describe in time the drift of a suspended element in position $\mathbf{x} = (x, y, z)$ at time t, one requires a representation for its absolute acceleration $\mathbf{f}_{abs}$. Now the frame $Oxyz$ is rotating with angular velocity $\boldsymbol{\Omega} = (0, 0, \Omega(t))$, and so

$$\begin{aligned} \dot{\mathbf{x}}_{abs} &= \mathbf{v}_0 + \dot{\mathbf{x}} + \boldsymbol{\Omega} \times \mathbf{x} \\ &= \dot{\mathbf{x}} + \boldsymbol{\Omega} \times (\mathbf{x} + \mathbf{c}), \end{aligned} \tag{6.2.1}$$

where $\mathbf{c} = \overrightarrow{CO} = (c, 0, 0)$. In turn

$$\begin{aligned} \mathbf{f}_{abs} &= \mathbf{f}_0 + \ddot{\mathbf{x}} + 2(\boldsymbol{\Omega} \times \dot{\mathbf{x}}) + (\dot{\boldsymbol{\Omega}} \times \mathbf{x}) + \boldsymbol{\Omega} \times (\boldsymbol{\Omega} \times \mathbf{x}) \\ &= \ddot{\mathbf{x}} + 2(\boldsymbol{\Omega} \times \dot{\mathbf{x}}) + \dot{\boldsymbol{\Omega}} \times (\mathbf{x} + \mathbf{c}) + \boldsymbol{\Omega} \times (\boldsymbol{\Omega} \times (\mathbf{x} + \mathbf{c})), \end{aligned} \tag{6.2.2}$$

it being noted that $\dot{\mathbf{c}} = 0$. If $\mathbf{F}$ is the vector sum of the forces acting on the reagent in position $\mathbf{x}$ at time t, then the equation governing its motion is

$$m[\ddot{\mathbf{x}} + 2(\boldsymbol{\Omega} \times \dot{\mathbf{x}}) + \dot{\boldsymbol{\Omega}} \times (\mathbf{x} + \mathbf{c}) + \boldsymbol{\Omega} \times (\boldsymbol{\Omega} \times (\mathbf{x} + \mathbf{c}))] = \mathbf{F}, \tag{6.2.3}$$

where m denotes the mass of the reagent. The vector force $\mathbf{F}$ is comprised of (i) the gravitational force $(0, 0, -mg)$, (ii) the upthrust or buoyancy force $(0, 0, m'g)$, m' being the mass of the sample displaced by the reagent, and (iii) the drag $-6\pi\varepsilon\eta_0(\dot{\mathbf{x}}(\mathbf{x}_0, t) - \mathbf{v}(\mathbf{x}, t))$.

One is now in a position to take advantage of the analyses of the previous Chapters: the velocity $\mathbf{v}$, viz. that of the sample as measured relative to the well, is of the general form

$$v_{(r)} = \frac{1}{r}\frac{\partial \psi}{\partial z}, \quad v_{(\phi)} = r(\omega - \Omega), \quad v_{(z)} = -\frac{1}{r}\frac{\partial \psi}{\partial r}. \tag{6.2.4}$$

Thus the above vector equation of motion may be written in the component form

$$\ddot{x} - 2\Omega\,\dot{y} - \dot{\Omega}\,y - \Omega^2(x+c) = -\tilde{k}\Omega_0[\dot{x} - \frac{x}{r^2}\frac{\partial\psi}{\partial z} + y(\omega - \Omega)], \tag{6.2.5}$$

$$\ddot{y} + 2\Omega\,\dot{x} + \dot{\Omega}\,(x+c) - \Omega^2 y = -\tilde{k}\Omega_0[\dot{y} - \frac{y}{r^2}\frac{\partial\psi}{\partial z} - x(\omega - \Omega)], \tag{6.2.6}$$

$$\ddot{z} = -\tilde{k}\Omega_0(\dot{z} + \frac{1}{r}\frac{\partial\psi}{\partial r}) + (\frac{m'}{m} - 1)g, \tag{6.2.7}$$

where $\tilde{k}$ is the dimensionless parameter $6\pi\varepsilon\eta_0/(m\Omega_0)$, the parameter which characterizes the (main) reaction of the sample under investigation. These equations are to be associated with an array of values of initial conditions, i.e. values of $\mathbf{x}_0$ and associated (realistic) values of $(\dot{\mathbf{x}})_{\mathbf{x}=\mathbf{x}_0}$.

It is all too clear that unless the velocity field $\mathbf{v}(\mathbf{x},t)$ is of a particularly simple type little progress will result in seeking an analytical solution, and that procedures will necessarily have to be numerical. The two basic flow regimes that have been analysed are (i) that resulting from a 'sweep' at constant angular velocity $\boldsymbol{\Omega} = (0, 0, \Omega_0)$, and (ii) that resulting from a'jiggle' at oscillatory angular velocity $\boldsymbol{\Omega} = (0, 0, \mathrm{Re}[\Omega_0 e^{int}])$. The problems relating to the calculation of the drift patterns for these two regimes are now studied.

6.3 The 'Sweep'-Mode at Constant Values of $\boldsymbol{\Omega}$

The analysis undertaken in §3.2.1 shows that when $\boldsymbol{\Omega}$ is constant in value, i.e. when $\boldsymbol{\Omega} = (0, 0, \Omega_0)$, the mixture within the well moves as if it were rigid, i.e. the appropriate solution for the velocity field is $\mathbf{v}(\mathbf{x}, t) = \mathbf{0}$, corresponding to $\psi = 0$, $\overline{\omega} = \Omega_0$. In this event, the equations of motion (6.2.5), (6.2.6) and (6.2.7) reduce to

$$\ddot{x} + \tilde{k}\,\Omega_0\,\dot{x} - 2\Omega_0\,\dot{y} - \Omega_0^2 x = \Omega_0^2 c, \tag{6.3.1}$$

$$\ddot{y} + \tilde{k}\,\Omega_0\,\dot{y} + 2\Omega_0\,\dot{x} - \Omega_0^2 y = 0, \tag{6.3.2}$$

$$\ddot{z} + \tilde{k}\Omega_0\,\dot{z} = (\frac{m'}{m} - 1)g, \tag{6.3.3}$$

i.e. linear differential equations with constant coefficients whose integration is easily effected. It is reasonable to suppose that $m'/m - 1$ is small so that, within the regime looked at, the drift in the z direction is likely to be small. It may therefore be supposed that $z(t) \simeq z_0$. The drift that is relevant here is that in the x, y-plane, i.e. in the plane perpendicular to the axis of rotation, due to a combination of centrifugal actions and sample (inter)actions. This drift in any plane $z = z_0$, is controlled by equations (6.3.1) and (6.3.2).

The homogeneous linear system associated with equations (6.3.1) and (6.3.2) may be solved using matrix methods. By letting

$$\begin{pmatrix} x \\ y \end{pmatrix} = e^{\beta t} \begin{pmatrix} A \\ B \end{pmatrix},$$

one finds that the system has the following matrix form

$$\begin{pmatrix} \beta^2 + \tilde{k}\Omega_0\beta - \Omega_0^2 & -2\Omega_0\beta \\ 2\Omega_0\beta & \beta^2 + \tilde{k}\Omega_0\beta - \Omega_0^2 \end{pmatrix} \begin{pmatrix} A \\ B \end{pmatrix} = 0, \tag{6.3.4}$$

where β, A and B are constants. A necessary and sufficient condition for (6.3.4) to have a nontrivial solution is that β is a solution of the characteristic equation

$$\begin{vmatrix} \beta^2 + \tilde{k}\Omega_0\beta - \Omega_0^2 & -2\Omega_0\beta \\ 2\Omega_0\beta & \beta^2 + \tilde{k}\Omega_0\beta - \Omega_0^2 \end{vmatrix} = 0, \tag{6.3.5}$$

i.e.

$$(\beta^2 + \tilde{k}\Omega_0\beta - \Omega_0^2)^2 = -(2\Omega_0\beta)^2. \tag{6.3.6}$$

The appropriate eigenvalues are β_j $(j = 1, 2, 3, 4)$, where

$$\beta_1 = -\frac{1}{2}\Omega_0(\tilde{k} + 2i) + \frac{1}{2}\Omega_0\sqrt{\tilde{k}^2 + 4i\tilde{k}}, \tag{6.3.7a}$$

$$\beta_2 = -\frac{1}{2}\Omega_0(\tilde{k} + 2i) - \frac{1}{2}\Omega_0\sqrt{\tilde{k}^2 + 4i\tilde{k}}, \tag{6.3.7b}$$

$$\beta_3 = -\frac{1}{2}\Omega_0(\tilde{k} - 2i) + \frac{1}{2}\Omega_0\sqrt{\tilde{k}^2 - 4i\tilde{k}}, \tag{6.3.7c}$$

$$\beta_4 = -\frac{1}{2}\Omega_0(\tilde{k} - 2i) - \frac{1}{2}\Omega_0\sqrt{\tilde{k}^2 - 4i\tilde{k}}. \tag{6.3.7d}$$

Therefore the eigenvectors associated with β_j can be expressed as

$$\begin{pmatrix} A \\ B \end{pmatrix}_j = \begin{pmatrix} 1 \\ (\beta_j^2 + \tilde{k}\Omega_0\beta_j - \Omega_0^2)/2\Omega_0\beta_j \end{pmatrix} E_j, \quad (j = 1, 2, 3, 4). \tag{6.3.8}$$

Here E_j are arbitrary constants. Thus, in any plane $z = z_0$, the drift paths $x = x(t), y = y(t)$ of the reagents are given by the equations

$$x(t) = \sum_{j=1}^{4} E_j e^{\beta_j t} - c, \tag{6.3.9}$$

$$y(t) = \frac{1}{2\Omega_0}\sum_{j=1}^{4}\frac{1}{\beta_j}(\beta_j^2 + \tilde{k}\Omega_0\beta_j - \Omega_0^2)E_j e^{\beta_j t}. \tag{6.3.10}$$

Here $x = -c$, $y = 0$ represent particular solutions of the non-homogeneous equations (6.3.1)-(6.3.2). One has now to associate initial conditions with equations (6.3.1)-(6.3.2), i.e. initial values of $\mathbf{x}_0$ and of $(\dot{\mathbf{x}})_{\mathbf{x}=\mathbf{x}_0}$. The reagents would remain at rest save for the motion of the mixture within the well, and so a realistic initial state would be one in which the reagents reside in the quiescent state $\dot{\mathbf{x}}_{abs} = 0$. For illustration purposes one supposes this to be the case, i.e. one associates with equations (6.3.9)-(6.3.10) the initial conditions

$$\mathbf{x} = \mathbf{x}_0, \ \dot{\mathbf{x}} = -\Omega_0 \times (\mathbf{x}_0 + \mathbf{c}) \ ; \ t = 0. \tag{6.3.11}$$

As the elements migrate within the well, they will from time to time collide with the boundary wall. To allow for the worst possible scenario, perfect reflection of the reagents is allowed at the wall. Hence, if and when an element hits the wall in position $\mathbf{x} = \mathbf{x}_c$ its velocity of rebound is calculated by the formula

$$(\dot{\mathbf{x}})_{\mathbf{x}=\mathbf{x}_c} \rightarrow (\dot{\mathbf{x}})_{\mathbf{x}=\mathbf{x}_c} - 2((\dot{\mathbf{x}})_{\mathbf{x}=\mathbf{x}_c} \cdot \mathbf{n})\mathbf{n}\,[35].$$

The drift or trace paths $\mathbf{x} = \mathbf{x}(\mathbf{x}_0, t)$ when $\mathbf{x}_0 = \mathbf{0}$, i.e. for a reagent starting in the centre of the well, for various values of the (dimensionless) parameter $\tilde{k}\,(= 6\pi\varepsilon\eta_0/(m\Omega_0))$, the parameter characterizing the effect of the patient sample, are exhibited in Figs. 6.3.1-6.3.5. It is seen that for small values of $\tilde{k}$ the elements migrate, without undue hinderance, back and forth across the well before finally settling on the wall. However, as $\tilde{k}$ becomes larger, the elements on reaching the wall find it difficult to push on elsewhere and quickly become entrapped on it.

[35] $(\dot{\mathbf{x}})_{\mathbf{x}=\mathbf{x}_c} \cdot \mathbf{t}$ is continuous but $(\dot{\mathbf{x}})_{\mathbf{x}=\mathbf{x}_c} \cdot \mathbf{n}$ is reversed in direction.

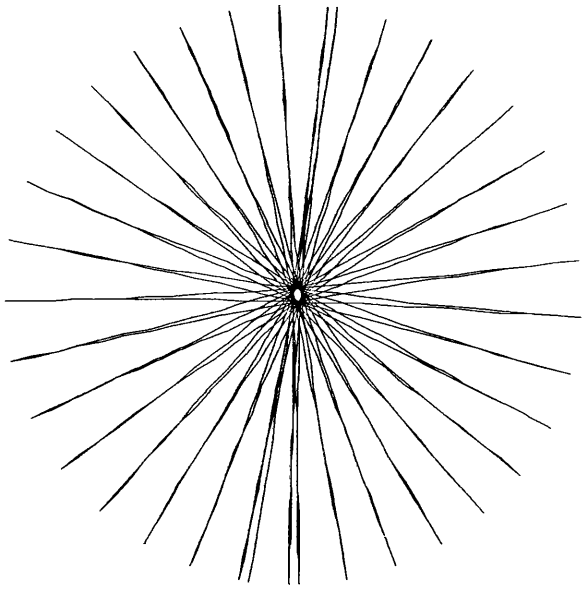

Fig. 6.3.1 An over-view of the trace-path of a reagent with starting position $\mathbf{x_0} = (0,0)$ when $\widetilde{k} = 0$.

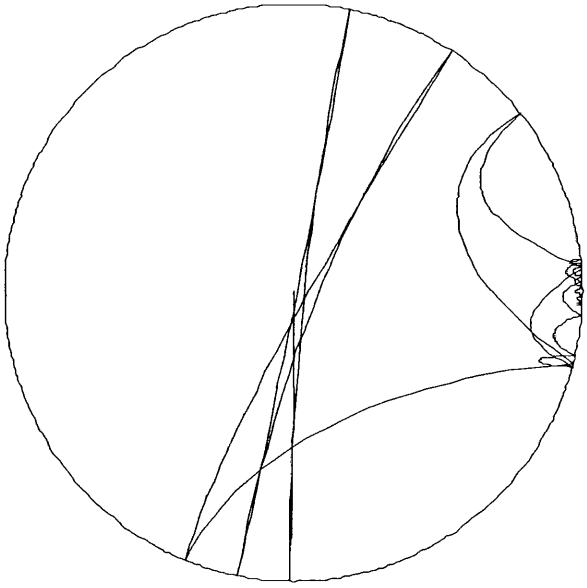

Fig. 6.3.2 An over-view of the trace-path of a reagent with starting position $\mathbf{x_0} = (0,0)$ when $\widetilde{k} = 3$.

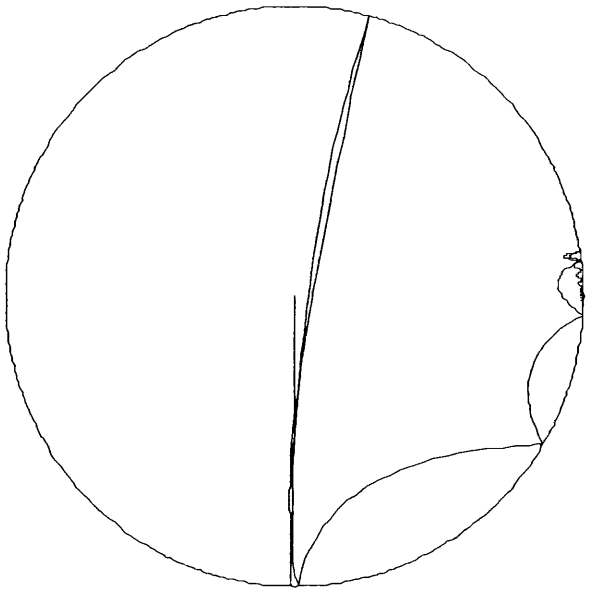

Fig. 6.3.3 An over-view of the trace-path of a reagent with starting position $\mathbf{x_0} = (0,0)$ when $\widetilde{k} = 6$.

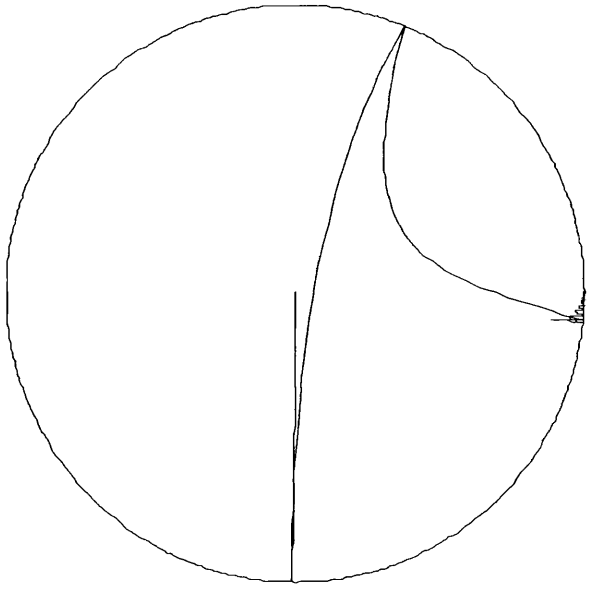

Fig. 6.3.4 An over-view of the trace-path of a reagent with starting position $\mathbf{x_0} = (0,0)$ when $\widetilde{k} = 9$.

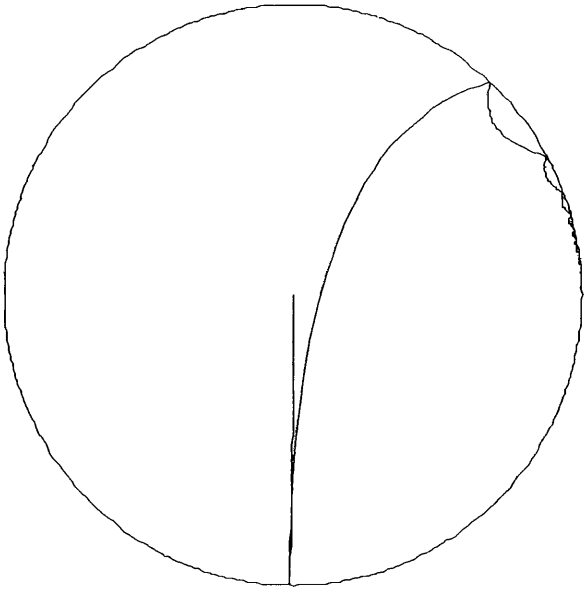

Fig. 6.3.5 An over-view of the trace-path of a reagent with starting position $\mathbf{x}_0 = (0,0)$ when $\widetilde{k} = 12$.

The trace paths for the large array of $\mathbf{x}_0$-values exhibited in Fig. 6.3.6 have been computed for the three cases

$$\text{(i) } \widetilde{k} = \widetilde{k}_1 = 3, \quad \text{(ii) } \widetilde{k} = \widetilde{k}_2 = 6, \quad \text{(iii) } \widetilde{k} = \widetilde{k}_3 = 12.$$

What is found (in each case) is that a guttate band forms on the region of the wall remote from the axis of rotation building up in intensity on either side of the x-axis (i.e. the central line $\overrightarrow{CO}$). The position and extent of this guttate band $\mathbf{A}_i\mathbf{B}_i$ $(i = 1,2,3)$ corresponding to the values $\widetilde{k} = \widetilde{k}_i$ $(i = 1,2,3)$ are exhibited in Figs. 6.3.7-6.3.9. The indication is that the extent of the band increases with increasing $\widetilde{k}$, but the time taken for it to become established on the wall decreases significantly with increasing $\widetilde{k}$.

To illustrate further, it is shown in Figs. 6.3.10-6.3.13 when $\widetilde{k} = \widetilde{k}_3 = 12$ how elements with the different starting positions $(-0.278,0.856)$, $(-0.155,-0.476)$,

$(0.285, 0.093)$, $(0, -0.1)$ all end up being eventually entrapped on the band $\mathbf{A_3B_3}$ of the boundary wall.

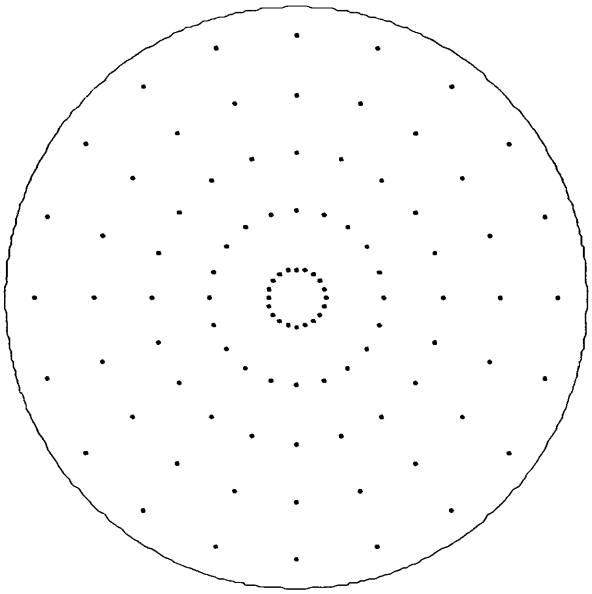

Fig. 6.3.6 Array of $\mathbf{x_0}$-values spreading throughout the plane $z = z_0$.

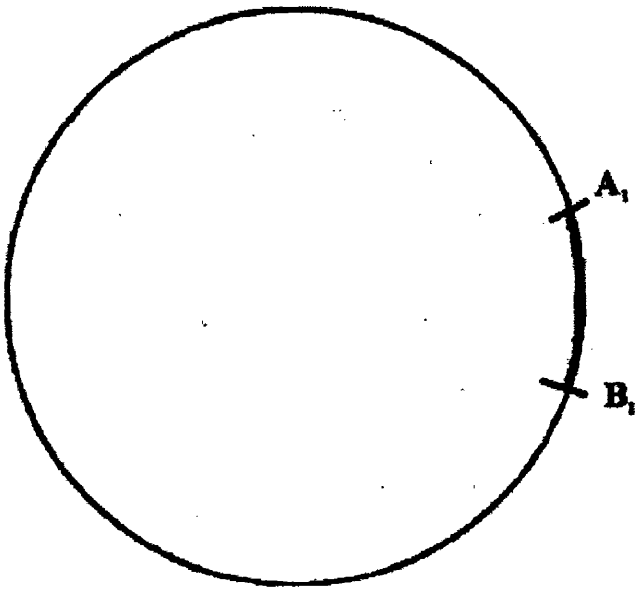

Fig. 6.3.7 The guttate band corresponding to $\widetilde{k} = \widetilde{k}_1 = 3$.

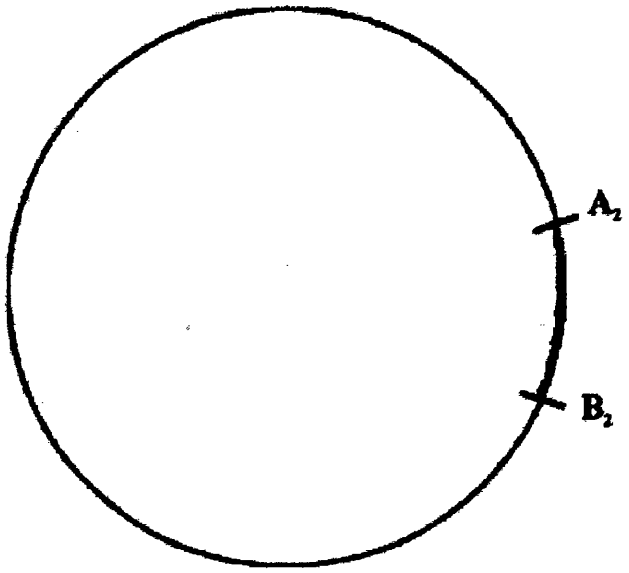

Fig. 6.3.8 The guttate band corresponding to $\widetilde{k} = \widetilde{k}_2 = 6$.

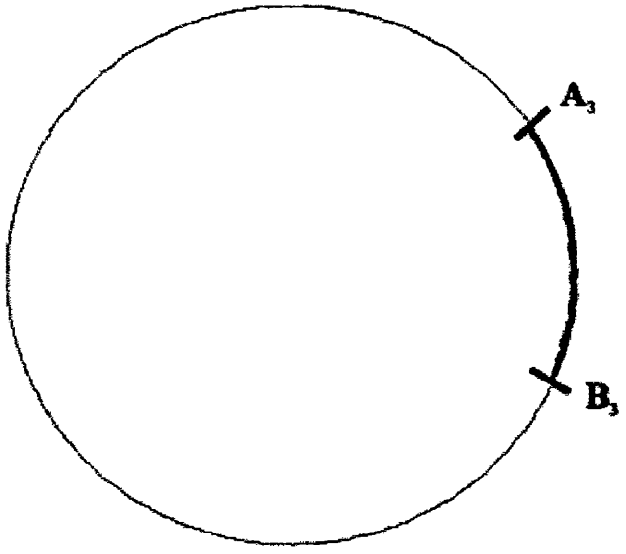

Fig. 6.3.9 The guttate band corresponding to $\widetilde{k} = \widetilde{k}_3 = 12$.

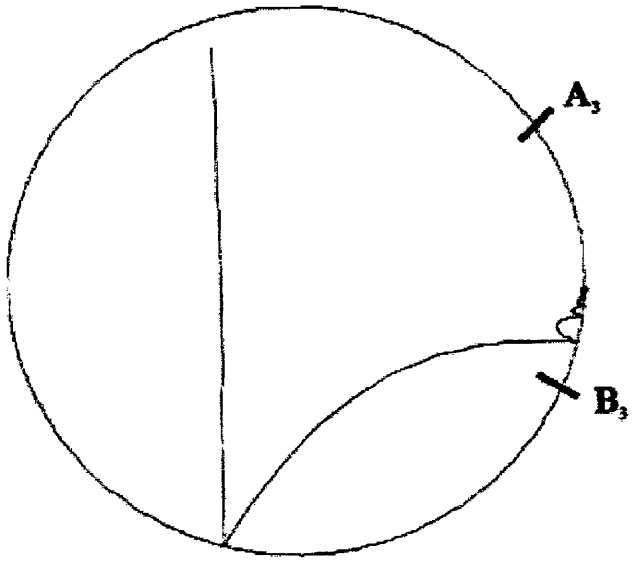

Fig. 6.3.10 An over-view of the trace-path of a reagent with starting position $\mathbf{x}_0 = (-0.278, 0.856)$ when $\widetilde{k} = \widetilde{k}_3 = 12$.

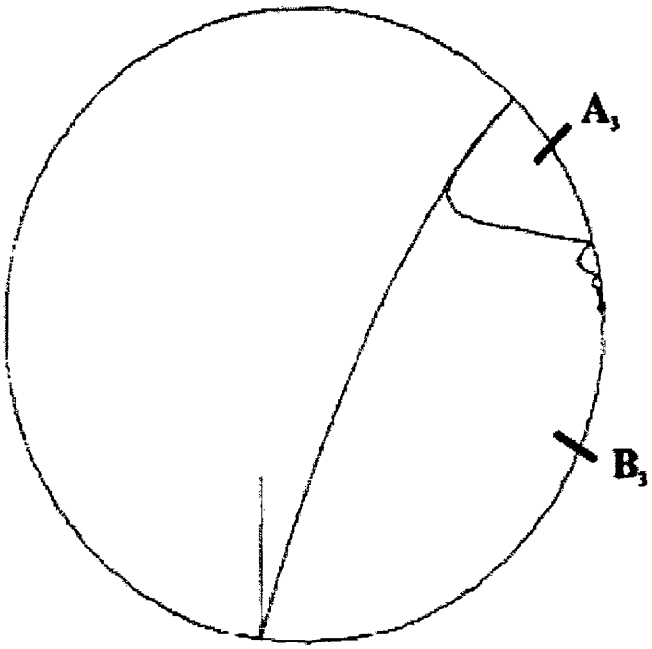

Fig. 6.3.11 An over-view of the trace-path of a reagent with starting position $\mathbf{x}_0 = (-0.155, -0.476)$ when $\widetilde{k} = \widetilde{k}_3 = 12$.

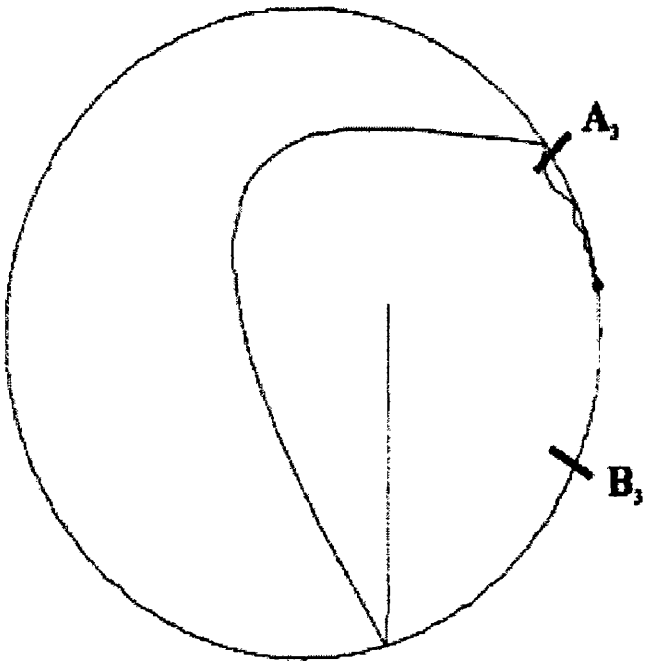

Fig. 6.3.12 An over-view of the trace-path of a reagent with starting position $\mathbf{x}_0 = (0.285, 0.093)$ when $\widetilde{k} = \widetilde{k}_3 = 12$.

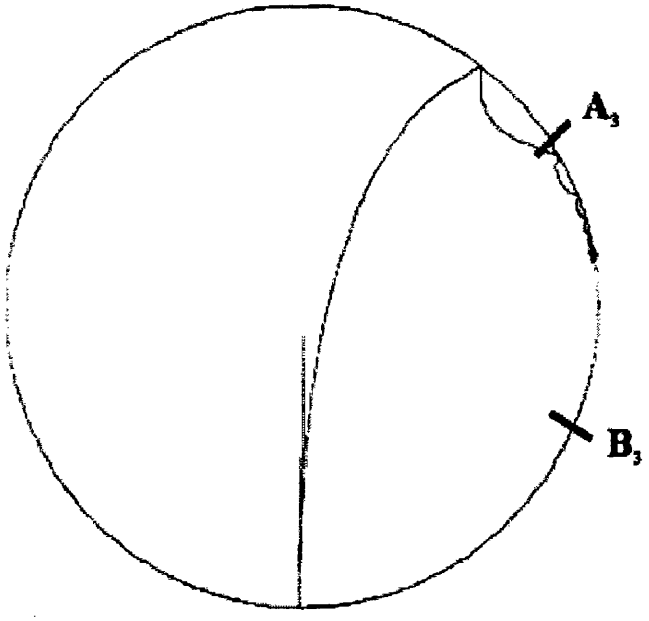

Fig. 6.3.13 An over-view of the trace-path of a reagent with starting position $\mathbf{x}_0 = (0, -0.1)$ when $\widetilde{k} = \widetilde{k}_3 = 12$.

The asymmetry in the boundary activity revealed by the above analyses may not have been appreciated in the instrumentation design. The preferred orientation within the flow will result in a non-uniform coverage of the well boundary wall.

6.4 The 'Jiggle'-Mode at Oscillatory Values of Ω

It is an inescapable fact that when Ω is oscillatory in nature the flow of the mixture within the well, although axially symmetric, is complicated in mathematical structure. This, in turn, results in massively complicated (and analytically intractable) differential equations characterizing the drift of the reagents. To illustrate the difficulties involved one need only consider the simplest case that can be envisaged, viz. that of a deep well when conditions are such that the regime is described by the primary flow, i.e. when the velocity field within the well is described by

$$\psi = 0, \quad \omega - \Omega = \Omega_0[\frac{aJ_1(kr)}{rJ_1(ka)} - 1]\cos nt \quad (r = \sqrt{(x^2 + y^2)}). \tag{6.4.1}$$

In this event, the differential equations that describe the trajectories $\mathbf{x} = \mathbf{x}(\mathbf{x}_0, t)$, in any plane $z(t) = z_0$, reduce to

$$\left.\begin{aligned} \ddot{x} + \tilde{k}\,\Omega_0\,\dot{x} - 2\Omega_0 \cos nt\,\dot{y} - \Omega_0^2 \cos^2 nt\, x + \Omega_0(n \sin nt \\ + \tilde{k}\Omega_0[(aJ_1(kr)/rJ_1(ka)) - 1]\cos nt)\, y = c\Omega_0^2 \cos^2 nt, \\ \ddot{y} + \tilde{k}\,\Omega_0\,\dot{y} + 2\Omega_0 \cos nt\,\dot{x} - \Omega_0^2 \cos^2 nt\, y - \Omega_0(n \sin nt \\ + \tilde{k}\Omega_0[(aJ_1(kr)/rJ_1(ka)) - 1]\cos nt)x = cn\Omega_0 \sin nt. \end{aligned}\right\} \quad \text{(A)}$$

These equations, in contrast with those of the previous section (i.e. those which characterize sweep at constant value of Ω), are neither linear in mathematical form

nor capable of being decoupled. However, when the angular frequency $n/2\pi$ is either *small* or *large,* the flow has a relatively simple structure, what is to all extent and purpose a rigid body rotation. These are seemingly rather special modes of oscillations, but approximations to these are easily realized in practice. So far as one is able to judge, the 'jiggle'-mode is one in which the frequency of oscillation is large. For such a regime, our analysis has shown that, but for a thin layer immediately adjacent to the boundary wall, the flow within the well is equivalent to a rigid body rotation. It is therefore worthwhile to pursue events further when the frequency of oscillation falls within one or other of these two modes to see the type of difficulty that is encountered.

6.4.1 Small Values of n

The earlier study has shown that, with sufficient approximation, the flow within the well is described by

$$\psi = 0, \quad \omega = \Omega_0 \cos nt. \tag{6.4.2}$$

Thus, in any plane $z = z_0$, the drift $\mathbf{x} = (x(t), y(t))$ of the reagents is described by the *linear* differential equations

$$\left.\begin{aligned} &\ddot{x} + \tilde{k}\,\Omega_0\,\dot{x} - 2\Omega_0 \cos nt\,\dot{y} - \Omega_0^2 \cos^2 nt\, x + n\Omega_0 \sin nt\, y = c\Omega_0^2 \cos^2 nt, \\ &\ddot{y} + \tilde{k}\,\Omega_0\,\dot{y} + 2\Omega_0 \cos nt\,\dot{x} - \Omega_0^2 \cos^2 nt\, y - n\Omega_0 \sin nt\, x = cn\Omega_0 \sin nt. \end{aligned}\right\} \quad \text{(B)}$$

6.4.2 Large Values of n

For such values of n, it has been shown that the flow within the well, but for a thin layer immediately adjacent to the boundary wall, is described by

$$\psi = 0, \quad \omega - \Omega = -\Omega_0 \cos nt, \tag{6.4.3}$$

i.e. a rigid body rotation of angular amplitude and frequency as that of the wall but of phase π behind it. Thus, if one were to neglect the boundary layer activity, then, in any plane $z = z_0$, the drift of the reagents is described by the *linear* equations

$$\left.\begin{aligned} &\ddot{x} + \widetilde{k}\,\Omega_0\,\dot{x} - 2\Omega_0 \cos nt\,\dot{y} - \Omega_0^2 \cos^2 nt\, x \\ &\qquad\qquad + \Omega_0 (n \sin nt - \widetilde{k}\,\Omega_0 \cos nt) y = c\Omega_0^2 \cos^2 nt, \\ &\ddot{y} + \widetilde{k}\,\Omega_0\,\dot{y} + 2\Omega_0 \cos nt\,\dot{x} - \Omega_0^2 \cos^2 nt\, y \\ &\qquad\qquad - \Omega_0 (n \sin nt - \widetilde{k}\,\Omega_0 \cos nt)\, x = cn\Omega_0 \sin nt. \end{aligned}\right\} \quad \text{(C)}$$

It is noted that equations (B) and (C) are linear in mathematical form. Nevertheless, they seem too complicated to allow for the construction of analytical solutions, and so, whether one looks at (A), (B) and (C), progress will have to rely on numerical procedures. This challenge is not taken on in the present study.

6.5 References

Leslie, F. M., "The slow flow of a visco-elastic liquid past a sphere", 1961, *Quart. J. Mech. App. Math.*, **14,** 36.

CHAPTER 7
CONCLUDING REMARKS

The present (and final) chapter has three purposes. First, to comment on the significance of the mathematical findings in relation to the Vitros Immunodiagnostic System; second, to indicate a possible programme of further research; and, third, to draw attention to some other factors only touched upon in the main text.

7.1 Mathematical Findings

The design and manufacture of the Vitros Instrument (now widely available in hospitals for the speedy (and reliable) diagnosis of a wide range of illnesses) has neither been guided nor supported by mathematical analysis. The present study is the first attempt to set up a working mathematical model of the hydro-mechanics within the instrumentation cycle. Although the present model may have shortcomings, and is yet to deliver on certain aspects of the cycle of operation, it is anticipated that the broad findings that have hitherto emerged offer opportunities to improve the design and efficiency of the instrument. What is found is that the reagents have preferred orientations within the flow and become entrapped on a preferred site on the boundary wall, and are not uniformly dispersed on the wall surface as previously anticipated. This has to have an important bearing on the optical -photo process- part of the instrumentation cycle. There is as yet no detailed comparison with experiment that one can report upon.

7.2 Further Research

The next move has to be that of investigating equations (B) and (C), and possibly the more complicated equations (A), numerically for a large array of $\mathbf{x}_0$-values subject to the quiescent state $\dot{\mathbf{x}}_{abs} = \mathbf{0}$. Although equations (B), valid for low frequencies of oscillation, are not serious contenders for describing the 'jiggle'-mode, it will, nevertheless, be interesting to see how the associated trace-paths compare with those of descriptions (A) and (C).

The shortfall in all three descriptions (A), (B) and (C) is that, in essence, they give a two-dimensional picture, and fail to account for the secondary flow that is present within the well. A feature of the flow at high frequencies, which characterizes the 'jiggle'-mode, is the boundary layer, or shear layer, which forms at the boundary wall. Outside this layer the flow is approximately that of a rigid body (with the same angular amplitude and frequency as that of the boundary wall but of phase π behind it), a flow insensitive to change in rheological properties of the mixture within the well. It is possible that this structure can be used to obtain simple approximate expressions for the velocity and stress fields, valid at high frequencies, when it may not be possible to obtain a description of events throughout the well valid at all frequencies (i.e. that of obtaining the general solutions of equations (3.2.3a-c) and (3.2.4a-f)).

One approach would be the following. When the (dimensionless) parameter $R_a = \sqrt{(n\rho a^2/\eta_0)}$, the ratio of well characteristic length a to viscous length $\sqrt{(\eta_0/n\rho)}$, is large one anticipates a boundary layer of thickness $O(aR_a^{-1})$ at the wall. One then rescales (suitably) the kinematic and dynamic variables within this boundary

layer and expands them in power series in R_a^{-1}. The solutions so obtained are then matched with the solutions outside the boundary layer, these solutions being likewise developed in power series in the same parameter R_a^{-1}. The approach is the so called method of matched asymptotic expansions. Such an approach is widely used and documented for classical viscous flow (see, for example, Lyne (1970) and Riley (1967)), but less so for elastico-viscous flow. Within the (wider) field of non-Newtonian flow it is (in general) not possible to eliminate the stresses in terms of the velocities. The result is that the dynamic terms, the stresses, need to be analysed side by side with the kinematics terms, the velocities. This makes for difficulties. In developing a boundary-layer theory for elastico-viscous flows, there remains controversy over the assessment of the orders of magnitude of the various dynamic and kinematic terms that appear in the governing equations (see Frater (1970) and Walters (1970) for details). However, James (1975) has had some success in extending the approach to analyse oscillatory flows in curved pipes.

Within the present work one has already first hand experience of the method on having expanded the *exact* expression for the primary and (incipient) secondary flows associated with the hemispherical well in powers of R_a^{-1} (i.e. those results valid when $a\,|k| \gg 1$). No attempt at such a development has, as yet, been instigated.

7.3 Other Factors

Several other hydro-mechanical factors may need to be assessed as (more) experimental results become evident. For example, one cannot be certain if stratification of

density, and possibly of viscosity, affects the process. Again, there may be anomalous flow near the wall; in a solution of high polymeric material, the permitted distribution of molecular orientations very near the wall is restricted by the presence of the wall itself. This may possibly be accounted for by allowing a velocity of slip at the boundary proportional to the skin friction at the wall, a tolerance which may easily be admitted and assessed within the present mathematical development.

It is emphasized that the present study is focussed on the one aspect within the Vitros Immunodiagnostic System in which the sample within the well is transported on the outer carousel ring. No quantitative assessment is attempted of the critical phase in which the sample and reagents are delivered to the well, a robust rheological process (with characteristic time of seconds). Neither is a serious attempt made to shed light on any major spillage of the well content that occurs from time to time, resulting in serious instrument contamination and a breakdown of the testing programme. This aspect is only touched upon in the main text, but it is believed that circumferential vibrations within the carousel seating, along with a change of geometry of the well, may be the cause.

It is with the above few observations that the dissertation is concluded.

7.4 References

Frater, K. R., "On the solution of some boundary-value problems arising in elastico-viscous fluid mechanics", 1970, *Zeitschrift Für Angewandte Mathematik Und Physik,* **21,** 134.

James, P. W., "Unsteady elastico-viscous flow in a curved pipe", 1975, *Rheol. Acta,* **14**, 679.

Lyne, W. H., "Unsteady flow in a curved pipe", 1970, *J. Fluid Mech.,* **45,** 13.

Riley, N., "Oscillatory viscous flows. Review and extension", 1967, *J. Inst. Maths Applies,* **3**, 419.

Walters, K., "On a boundary-layer controversy", 1970, *Journal of Applied Mathematics and Physics (ZAMP),* **21,** 276.

BIBLIOGRAPHY

Brindley, G., and Keene, D. E., "On using a Weissenberg rheogoniometer for oscillatory testing of stiff materials", 1974, *Journal of Physics E: Scientific Instruments*, **7**, 934.

Broadbent, J. M., and Walters, K., "Some suggestions for new rheometer designs II. Interpretation of experimental results", 1971, *Journal of Physics D: Applied Physics*, **4**, 1863.

Einstein, A., 1906, *Ann. Phys. Lpz.*, **19**, 289.

Frater, K. R.,"Flow of an elastico-viscous fluid between torsionally oscillating disks", 1964, *J. Fluid Mech.*, **19**, 175.

Frater, K. R.,"Secondary flow in an elastico-viscous fluid caused by rotational oscillations of sphere. Part 1", 1964, *J. Fluid Mech.*, **20**, 369.

Frater, K. R., "On the solution of some boundary-value problems arising in elastico-viscous fluid mechanics", 1970, *Zeitschrift Für Angewandte Mathematik Und Physik*, **21**, 134.

Fröhlich, H. and Sack, R., "Theory of the rheological properties of dispersions",1946, *Proc. Roy. Soc.* **A**, **185**, 415.

Gijsen, F. J. H., Allanic, E., van de Vosse, F. N. and Janssen, J. D., "The influence of the non-Newtonian properties of blood on the flow in large arteries: unsteady flow in a 90 degrees curved tube", 1999, *Journal of Biomechanics*, **32** (7), 705.

Griffiths, D. F., Jones, D. T. and Walters, K.,"A flow reversal due to edge effects",

1969, *J. Fluid Mech.*, **36**, part 1, 161.

James, P. W., "Unsteady elastico-viscous flow in a curved pipe", 1975, *Rheol. Acta,* **14**, 679.

James, P. W., "A study of time-variant flows of elastico-viscous liquids", PhD Thesis, University of Wales, 1975.

Jones, J. R., "Non-Newtonian effects in axially symmetric oscillatory flows of some elastico-viscous liquids",1970, *Proc. Cambridge Philos. Soc.*, **68**, 731.

Jones, J. R., "A further note on axially symmetric flows of elastico-viscous liquids",1973, *Proc. Cambridge Philos. Soc.*, **73**, 239.

Jones, J. R., and Walters, T. S., "Oscillatory motion of an elastico-viscous liquid contained between two coaxial cylinders", 1965, *Mathematika,* **12**, 246.

Jones, J. R., and Walters, T. S., "Oscillatory motion of an elastico-viscous liquid contained in a cylindrical cup I. Theoretical", 1966, *Brit. J. Appl. Phys.*, **17**, 937.

Leslie, F. M., "The slow flow of a visco-elastic liquid past a sphere", 1961, *Quart. J. Mech. App. Math.*, **14,** 36.

Liepsch, D., Thurston, G. and Lee, M., "Studies of fluids simulating blood-like rheological properties and applications in models of arterial branches", 1991, *Biorheology,* **28** (1-2), 39.

Lyne, W. H., "Unsteady flow in a curved pipe", 1970, *J. Fluid Mech.*, **45,** 13.

Oldroyd, J. G., "On the formulation of rheological equations of state", 1950, *Proc. Roy. Soc.* **A, 200,** 523.

Oldroyd, J. G., "The elastic and viscous properties of emulsions and suspensions", 1953, *Proc. Roy. Soc.* **A, 218,** 122.

Oldroyd, J. G., Strawbridge, D. J., and Toms, B. A., "A coaxial-cylinder elastoviscometer", 1951, *Proc. Phys. Soc.* **B, 64,** 44.

Riley, N., "Oscillatory viscous flows. Review and extension", 1967, *J. Inst. Maths Applies,* **3**, 419.

Roberts, J. E., "Pressure distribution in liquids in laminar shearing motion and comparison with predictions from various theories", 1953, *Proc. II Int. Congr. Rheo. Oxford,* 93.

Roscoe, R., "Viscosity determination by the oscillating vessel method I", 1958, *Proc. Phys. Soc.*, **72,** 576.

Roscoe, R. and Bainbridge, W., "Viscosity determination by the oscillating vessel method II", 1958, *Proc. Phys. Soc.*, **72,** 585.

Rosenblat, S., "Flow between torsionally oscillating disks", 1960, *J. Fluid Mech.,* **8**, 388.

Taylor, G. I., "The viscosity of a fluid containing small drops of another fluid", 1932, *Proc. Roy. Soc.* **A, 138,** 41.

Walters, K., "On a boundary-layer controversy", 1970, *Journal of Applied Mathematics and Physics (ZAMP),* **21,** 276.

Weissenberg, K., "Abnormal substances and abnormal phenomena of flow", 1948, *Proc. Int. Rheological Congr. Holland,* **I**, 29.

Zalosh, R. G. and Nelson, W. G., "Pulsating flow in a curved tube", 1973, *J. Fluid Mech.,* **59**, part 4, 693.